Stretch-Induced Effects on MicroRNA Expression and Exogenous MicroRNA Delivery in Differentiating Skeletal Myoblasts

by

Caroline Rhim

Department of Biomedical Engineering
Duke University

Date:_____
Approved:

_____
Dr. George A. Truskey, Supervisor

_____
Dr. William E. Kraus

_____
Dr. Nenad Bursac

_____
Dr. Kam Leong

_____
Dr. Da-Zhi Wang

Dissertation submitted in partial fulfillment of
the requirements for the degree of Doctor
of Philosophy in the Department of
Biomedical Engineering in the Graduate School
of Duke University

2009

ABSTRACT

Stretch-Induced Effects on MicroRNA Expression and Exogenous MicroRNA Delivery in Differentiating Skeletal Myoblasts

by

Caroline Rhim

Department of Biomedical Engineering
Duke University

Date:_____
Approved:

_____
Dr. George A. Truskey, Supervisor

_____
Dr. William E. Kraus

_____
Dr. Nenad Bursac

_____
Dr. Kam Leong

_____
Dr. Da-Zhi Wang

An abstract of a dissertation submitted in partial fulfillment of the requirements for the degree of Doctor of Philosophy in the Department of Biomedical Engineering in the Graduate School of Duke University

2009

Copyright by
Caroline Rhim
2009

Abstract

The research presented here represents a quest to understand and address limitations in the field of skeletal muscle tissue engineering, with hopes to better understand the factors involved in producing viable, engineered tissues. The driving force behind this research was to address two of the many factors important in muscle cell proliferation and differentiation, toward developing mature and functional bioartificial skeletal muscles (BAMs). Our work focused on understanding the individual effects of mechanical stimulation and microRNAs (miRNAs), as well as the synergistic relationship between the two factors. We hypothesized that (1) myoblast proliferation and differentiation are modulated by mechanical stimulation via temporally regulated miRNAs and that (2) modulating these miRNAs can enhance skeletal muscle function in a 3D tissue-engineered system.

We first established a BAM system using C2C12 mouse myoblasts in a collagen gel, showing that these cells were able to produce mature sarcomeres when cultured under steady, passive tension for up to 36 days. Staining muscle-specific proteins and electron microscopy showed distinct striations and myofiber organization as early as 6 days, post-differentiation. At 33 days, cultures contained collagen fibers and showed localization of paxillin at the fiber termini, suggesting that myotendinous junctions were forming.

We then focused on the effects of mechanical stimulation on C2C12 myoblasts in a simpler 2D system. In particular, miRNA and muscle-specific gene expression were assessed over time and in response to two cyclic stretch regimens using miRNA microarray technology and quantitative real time RT-PCR. Both miRNAs and certain genes, such as Mef2c, had differential responses to the two regimens. Over-expression and inhibition studies of one muscle-specific miRNA, miR-1, abrogated the stretch response, suggesting that a balancing mechanism is in place to avoid large fluctuations in miRNA levels.

Finally, since miRNA modulation quenched the stretch-mediated response in myoblasts, we chose to examine 3D BAM function when miRNA levels were altered to promote differentiation. Using the same collagen gel model established previously, a muscle-specific miRNA, miR-133, known to promote proliferation, was transiently inhibited (anti-miR-133) to encourage differentiation. Forces in the anti-miR-133 BAMs were, on average, 20% higher over the negative control. Further, myofiber diameters were significantly greater, and striations were more organized in the anti-miR-133 BAMs, suggesting that transient, exogenous delivery of miRNAs may be a viable approach to create a more fully differentiated muscle.

Contents

Abstract iv

List of Tables xi

List of Figures xii

Acknowledgements xvi

1. Introduction 1

1.1 Research Overview 1

1.2 Skeletal Muscle Development 5

1.2.1 Skeletal Muscle Structure 5

1.2.2 Skeletal Muscle Gene Transcription 7

1.3 Skeletal Muscle Tissue Engineering 11

1.4 Mechanotransduction 14

1.5 MicroRNAs 18

1.5.1 MicroRNA Biogenesis 18

1.5.2 miRNAs and siRNAs 20

1.5.3 MicroRNA Targets 21

1.5.3 MicroRNAs and Muscle Biology 23

1.5.4 MicroRNAs and Mechanical Stimulation 28

1.5.5 MicroRNA Dysfunction & Possible Therapies 29

1.6 Justification and Significance 30

Chapter 2. Bioartificial Muscle in a 3D Collagen Gel System 33

2.1 Introduction 33

2.2 Methods and Materials 35

2.2.1 Cell Culture & Bioartificial Muscle (BAM) Assembly 35

2.2.2 Histology 36

2.2.3 Live/Dead Assay 37

2.2.4 Staining 37

2.2.5 Electron Microscopy (EM) 38

2.3 Results 39

2.4 Discussion 52

2.5 Conclusions 57

2.6 Chapter Acknowledgements 57

Chapter 3. Preliminary MicroRNA Microarray Analysis of the Effect of Stretch on Myoblasts Exposed to Cyclic Stretch 59

3.1 Introduction 59

3.2 Methods and Materials 61

3.2.1 Cell Culture 61

3.2.2 Mechanical Stimulation 61

3.2.3 MicroRNA Microarray Analysis 62

3.2.4 Quantitative RT-PCR (qRT-PCR) 63

3.3 Results 65

3.3.1 Preliminary Microarray Results with Older Passage Cells 65

3.3.2 Preliminary Microarray Results with Early Passage, Younger Cells 73

3.4 Discussion 80

3.5 Conclusions 84

3.6 Chapter Acknowledgements 85

Chapter 4. Biomechanical Effects on MicroRNA Expression in Skeletal Muscle Differentiation 86

4.1 Introduction 86

4.2 Methods and Materials 89

4.2.1 Cell Culture 89

4.2.2 Mechanical Stimulation 90

4.2.3 Quantitative Real-Time RT-PCR 90

4.2.4 Immunostaining 91

4.2.5 Western Blot Analysis 92

4.2.6 Over-expression and Inhibition of miRNAs 93

4.2.7 Statistical Analysis 94

4.3 Results 95

4.3.1 Effect of Mechanical Stimulation on Myoblast Morphology 95

4.3.2 Effect of Cyclic Stretch on MicroRNA Expression 103

4.3.3 Effect of Cyclic Stretch on miRNA Levels with Over-expression and Inhibition of miR-1 115

4.4 Discussion 121

4.5 Conclusions 132

4.6 Acknowledgements 133

Chapter 5. MicroRNA Delivery to Mediate Bioartificial Muscle Function 134

5.1 Introduction 134
5.2 Methods and Materials 137
5.2.1 Cell Culture & Transient Transfection 137
5.2.2 Bioartificial Muscle (BAM) Assembly 138
5.2.3 Histology 139
5.2.4 Immunostaining & Fiber Diameter Measurements 140
5.2.5 Functional Force Testing 141
5.2.6 Statistical Analysis 142
5.3 Results 143
5.3.1 Function Force Response in Non-Transfected BAMs 143
5.3.2 Transient Transfection in BAMs 144
5.3.3 Over-Expression of miR-1 in BAMs 147
5.3.3 Inhibition of miR-133 in BAMs 149
5.4 Discussion 159
5.5 Conclusions 164
5.6 Acknowledgements 165
6. Conclusions and Future Work 166
6.1 Conclusions 166
6.2 Future Work 171
Appendix A: Oxygen Diffusion through Bioartificial Muscle 173
Appendix B: Primer Sequences for Quantitative Real Time RT-PCR 175
Appendix C: MatLab Code for Force Measurements 176

Appendix D: Copyright Releases 181

References 183

Biography 195

List of Tables

Table 1.1 Comparison of various attributes of miRNAs of siRNAs. 21

Table 1.2 MicroRNAs involved in mammalian skeletal muscle development 27

Table 3.1 Preliminary miRNA microarray data showing miRNA expression in differentiating (passage 6) myoblasts..... 67

Table 3.2 Comparison of preliminary miRNA microarray and qRT-PCR data in older (passage 6) cells. 72

Table 3.3 Preliminary miRNA microarray data showing miRNA expression in differentiating (passage 3) myoblasts..... 75

Table 3.4 Analysis of variance in older and newer passage cells (passage 6 vs. 3). 76

Table 3.5 Comparison of preliminary miRNA microarray and qRT-PCR data using newer (passage 3) cells. 78

Table 4.1 Myogenic fusion index, presented as the percentage of nuclei in striated myotubes 102

List of Figures

Figure 1.1 Skeletal muscle structure and hierarchical organization 6

Figure 1.2 Skeletal myoblast activation in response to muscle injury 8

Figure 1.3 Key signaling pathways involved in mechanotransduction 17

Figure 1.4 Schematic of miRNA biogenesis 19

Figure 2.1 Hematoxylin and eosin (H&E) staining of tissue engineered bioartificial muscle (BAM) at shift day 16 39

Figure 2.2 Hematoxylin and eosin (H&E) staining of BAM at (A) shift day 2 and (B) shift day 30, cultured with 20% horse serum differentiation media 40

Figure 2.3 Live/Dead assay of BAM cultured for 16 days 41

Figure 2.4 Hematoxylin and eosin (H&E) staining of BAMs that were cultured in (A) 2% horse serum DM for two days followed by 8% horse serum for 6 days, (B) 10% horse serum DM for 8 days, and (C) 20% horse serum DM for 8 days 43

Figure 2.5 Rhodamine phalloidin stain for F-actin and Sytox green nuclei stain showing formation of myofibers 45

Figure 2.6 Rhodamine phalloidin stain for F-actin and Sytox green nuclei stain. BAMs cultured for 6 days in (A) 8% horse serum DM, (B) 20% horse serum DM (C) 16 days in 20% horse serum DM, and (D) 30 days in 8% horse serum DM. 46

Figure 2.7 Immunostaning for (A) alpha-actinin on BAMs cultured for 6 days in 20% horse serum DM and (B) myosin on BAMs 47

Figure 2.8 Electron micrograph of BAM cultured for (A) 16 days in 20% horse serum DM. Mature sarcomeres are evident, alongside fused myotubes with stress fibers. (B) BAMs at 16 days in 8% horse serum DM, t-tubules are shown (arrow), and (C) 33 days in 8% horse serum DM. 49

Figure 2.9 Rhodamine phalloidin stain for F-actin and immunostaining for paxillin on BAM cultured for 33 days in 8% horse serum DM. 51

Figure 3.1 Scatter plot of stretch-induced miRNAs with older passage (6) myoblast 66

Figure 3.2 Relative expression of miR-1, 133a, and 206 in myoblasts subjected to a moderate strain regimen for 8 days, post differentiation.....68

Figure 3.3 Relative expression of miR-125b in myoblasts subjected to a moderate strain regimen for 8 days, post differentiation. 69

Figure 3.4 Relative expression of (A) miR-214 and (B) miR-140, which were assessed via qRT-PCR after initial results of the first miRNA microarray study 71

Figure 3.5 Scatter plot of miRNA microarray data with lower passage (3) myoblasts....74

Figure 3.6 Relative expression of (A) miR-422b and (B) miR-31, which were assessed via qRT-PCR.....77

Figure 4.1 Rhodamine phalloidin stain for F-actin and Sytox green nuclear stain of differentiating myoblasts subjected to equibiaxial stretch.....97

Figure 4.2 Alpha-actinin immunostaining with a Sytox Green nuclei counterstain of differentiating myoblasts subjected to a moderate strain (10%) regimen.....99

Figure 4.3 Alpha-actinin immunostaining with a Sytox Green nuclei counterstain of differentiating myoblasts subjected to a high strain (17%) regimen 101

Figure 4.4 Temporal regulation of muscle specific miRNAs demonstrates a marked increase as muscle differentiation proceeds.....104

Figure 4.5 Effect of cyclic stretch on miRNA levels (miR-1, miR-133a, miR-206) at various time points measured by quantitative RT-PCR (qRT-PCR).....106

Figure 4.6 Ratio of miR-133 to miR-1 expression levels, presented in myoblasts subjected to the (A) moderate strain regimen and a (B) high strain regimen.....109

Figure 4.7 Gene expression analysis in myoblasts subjected to moderate and high strain regimens via quantitative RT-PCR for (A) MyoD, (B) Myogenin, (C) HDAC4, and (D) SRF. 111

Figure 4.8 Gene expression analysis via quantitative RT-PCR for Mef2c.....113

Figure 4.9 Western blot analysis for HDAC4 showing a decreasing trend in HDAC4 protein expression in myoblasts exposed to a moderate strain regimen.....114

Figure 4.10 Average temporal effect of miR-1 over-expression demonstrating a marked increase in mature miR-1 expression in the transiently transfected myoblasts over the negative controls 116

Figure 4.11 The effect of cyclic stretch with a moderate strain regimen combined with miR-1 over-expression..... 118

Figure 4.12 Western blot analysis of HDAC4 showing effect of cyclic stretch with a moderate strain regimen and miR-1 inhibition 120

Figure 4.13 Schematic of miRNA regulation through mechanical stimulation 131

Figure 5.1 Functional force transducer setup..... 142

Figure 5.2 Representative functional force measurements showing peaks at various frequencies (0Hz – 5 Hz) for BAMs cultured with non-transfected myoblasts 144

Figure 5.3 Transient transfection of Cy-3 labeled pre-miR and anti-miR negative controls in differentiating myoblasts 24 hours after transfection 145

Figure 5.4 Transient transfection of Cy3-labeled pre-miR and anti-miR negative controls in BAMs 36 hours after transfection (shift day 0)..... 146

Figure 5.5 Representative H&E staining of longitudinal sections of negative control and pre-miR-1 BAMs..... 147

Figure 5.6 Immunostaining for alpha-actinin in negative control and pre-miR-1 BAMs 148

Figure 5.7 Functional force measurements at a stimulation frequency of 5 Hz for BAMs cultured with negative control and pre-miR-1 myoblasts 149

Figure 5.8 Representative H&E staining of negative control and anti-miR-133 BAMs..151

Figure 5.9 Immunostaining for myosin (MF20) in BAMs containing myoblasts transfected with either control sequence or anti-miR-133 152

Figure 5.10 Immunostaining for myosin (MF20) in BAMs cultured with negative control-transfected or anti-miR-133 myoblasts..... 153

Figure 5.11 Immunostaining for alpha-actinin in BAMs cultured with negative control-transfected or anti-miR-133 myoblasts for 6 days in DM 154

Figure 5.12 Average fiber diameter of non-transfected, negative control, and anti-miR-133 BAMs 155

Figure 5.13 Functional force measurements at a stimulation frequency of 5 Hz for BAMs cultured with negative control and anti-miR-133a myoblasts. 156

Figure 5.14 Bar graph showing ratio of peak (A) force and (B) stress of anti-miR-133 BAMs over negative control BAMs cultured for 6-8 days in DM 157

Acknowledgements

As with any given journey, I truly believe that making it through only comes with not one, but many communities behind the cause. First, I would like to thank my advisor, Dr. George Truskey, most for his mentorship and deep hope in and for me to experience the joys of science. His attention to this project and encouragement to persevere were unwavering, and I attribute the successes to his guidance. I would also like to acknowledge Dr. William Kraus, my co-advisor, whose support and many thought-provoking conversations, gave me confidence as a scientist. I am thankful for his ability to see the big picture, encouraging me to do the same. I also have been the recipient of much support from my committee members – Dr. Kam Leong, who encouraged me to stay focused and embrace academia, Dr. Nenad Bursac, who always found interest in my work and excited me to keep pursuing this project, and Dr. Da-Zhi Wang, who, despite being a leader in the field of miRNAs, always had time to explain the small details. For my community of mentors, I am incredibly lucky to have such examples to follow.

Graduate school would not have been the same without my colleagues and fellow laborers. A special thanks to members of the Truskey lab: Melissa Brown, Steve Wallace, and Cindy Cheng. We have had many brainstorming sessions and late night chats about science and everything in between. We have had more fun in lab than I

could have imagined with our special snack times and lab races; these moments will continue to make me smile. A special thank you to Shannon, Juliana, and Rebecca for constant support and encouragement from day one. I am grateful for your companionship through this journey and know you will continue to succeed wherever you go.

And of course, to my friends and family near and far. You have never stopped investing in me, even through my intense curiosity and crazy ideas. To Lydia, for being my first best surprise in graduate school. To Yee, my fellow sister in life, thank you for hoping more for me than I could for myself. I especially thank my family for providing me with meaningful life lessons. To Dad for taking my curiosity as is and encouraging me to think beyond the surface, and to Mom, for teaching me how to seek a selfless life by sharing an authentic love for others. For Mo and Joonhyung, we have been partners since the day you were born and I have been blessed to be the recipient of your care. Finally, to my husband Jason. Thank you for sharing your amazing faith and steadfast spirit with me. I could not have imagined a more perfect life partner than you. And above all, to God, through whom all things are possible.

1. Introduction

1.1 Research Overview

The research presented here represents a quest to understand and address the limitations in the field of skeletal muscle tissue engineering and our hope to better understand the factors involved in producing viable, engineered muscle tissue. Progress to date has demonstrated mature myofiber formation *in vitro* with some functionality exhibited as spontaneous twitch forces and excitability to electrical stimulation. However, a fully differentiated construct of aligned, bundled myofibers has yet to be achieved outside the body. Researchers have attempted to create more functional tissue by utilizing known effectors of skeletal muscle development, such as cell type, mechanical and electrical stimulation, matrix configuration, and surface morphology [18, 39, 40, 64, 82, 124, 183], but there still remains a large gap between engineered and native muscle.

The major goal of this research was to engineer a tissue construct which functions more closely to native tissue by focusing on two known effectors of downstream muscle development: mechanical stimulation and gene regulation via microRNAs (miRNAs), as well as the link between the two. With this goal in mind, the major objectives of this project were to demonstrate that (1) myoblast proliferation and differentiation is modulated by mechanical stimulation via temporally regulated

miRNAs and that (2) using these miRNAs can modulate skeletal muscle function in a 3D tissue-engineered system.

We first approached these hypotheses in a simplified 2D system, using the commercially available Flexercell™ system to cyclically stretch silastic-bottomed six-well plates. MiRNA microarray technology was then used to scan a wide range of miRNAs for a stretch-induced response four days after the onset of the stimuli. Subsequent quantitative real time RT-PCR (qRT-PCR) methods were used to quantify select miRNA and mRNA expression during skeletal myoblast differentiation with and without cyclic stretch. Western blotting and immunostaining were used to determine the qualitative effects of stretch.

MiRNA mediation was employed through transient transfection of miRNA-specific mimics (for over-expression) or anti-sense miRNA molecules (for inhibition). Based on results from the 2D studies, we found that the stretch-mediated effect was lessened when miRNAs were modulated, presumably because the balance of the master regulatory protocol was offset in the cell, and the threshold for miRNA target expression was changed by the altered levels of the miRNAs themselves. Given the importance of miRNAs in key cellular processes, we hypothesized that modulating these tiny regulators independent of stretch would be a sufficient approach to enhance

differentiation *in vitro*; and therefore, we chose to focus exclusively on modulating miRNAs in the more complex 3D studies.

In **Chapter 2**, we explored the viability of bioartificial skeletal muscle (BAM) constructs from a C2C12 mouse myoblast cell line and demonstrated that a collagen gel system provided a suitable matrix for skeletal muscle differentiation and maturation. Histological and immunostaining methods were utilized to show myoblast fusion and myofiber development. Electron microscopy provided further conclusive evidence of mature myofiber formation, similar to that found in native muscle. However, non-uniform myofiber formation and distribution were among some of the limitations observed in our model.

In **Chapter 3**, we began to address these limitations in producing a mature muscle structure *in vitro* by exploring the role of miRNAs in the stretch-induced response of skeletal myoblasts. Using a Flexercell system, differentiating myoblasts were subjected to a 'moderate strain' cyclic stretch at a frequency of 0.5Hz and 10% strain for 1 hour followed by 5 hours of rest for a total of 4 days. MiRNA microarray analysis was done to compare unstretched to stretched samples of newer and older passage cells. Subsequent qRT-PCR techniques provided temporal profiles of several stretch-sensitive miRNAs.

In **Chapter 4**, we extended our examination of miRNA expression in differentiating myoblasts subjected to two different stretch regimens by creating temporal profiles using qRT-PCR. A 'high strain' cyclic stretch regimen consisting of a 17% strain at 1Hz for 1 hour with 23 hours of rest was used in addition to the moderate strain regimen used in Chapter 3. Gene expression and western blotting were employed to study the effect of stretch at the transcriptional (mRNA) and translational (protein) levels. Fusion and structural organization were assessed using immunostaining. Further, over-expression and inhibition of a muscle-specific miRNA, miR-1, was combined with stretch to observe downstream effects on miRNA regulation.

In **Chapter 5**, we address our second hypothesis by using miRNA mediation to modulate BAM function. Based on previous work in the field, miR-1 was shown to promote differentiation while miR-133 promotes proliferation. In order to enhance differentiation in the 3D system, we either transiently over-expressed miR-1 or inhibited miR-133a (for arguably the same effect). A custom force transducer apparatus was used to measure spontaneous force output and excitability at various electrical stimulation frequencies.

In **Chapter 6**, we summarize our main results and present conclusions that are extrapolated from our research findings. We also look toward the future by addressing subsequent studies and translational implications of modulating miRNAs *in vitro*.

1.2 Skeletal Muscle Development

1.2.1 Skeletal Muscle Structure

The skeletal muscle system is built on a hierarchy of parallel filament organization that spans the length scale from nanometers (myofilaments) to centimeters (whole muscle). Figure 1.1 illustrates the structure of skeletal muscle and dissects the organization at each level [94]. Bundles of myofilaments (nm) form myofibrils (μm) which form muscle fibers (μm x 100) that form muscle fascicles (mm), which ultimately form whole muscle (cm) [94]. At the smallest scale, myofilaments combine to form units responsible for muscle contraction, known as sarcomeres. The sarcomere consists of thick filaments of myosin and thin filaments of actin, which interdigitate to form areas of overlap known as the A-band, I-band, and Z-band, which lengthen and shorten as the myosin and actin filaments slide past each other during contraction (as in the 'sliding filament theory'). These areas of overlap also give the skeletal muscle a striated appearance [94].

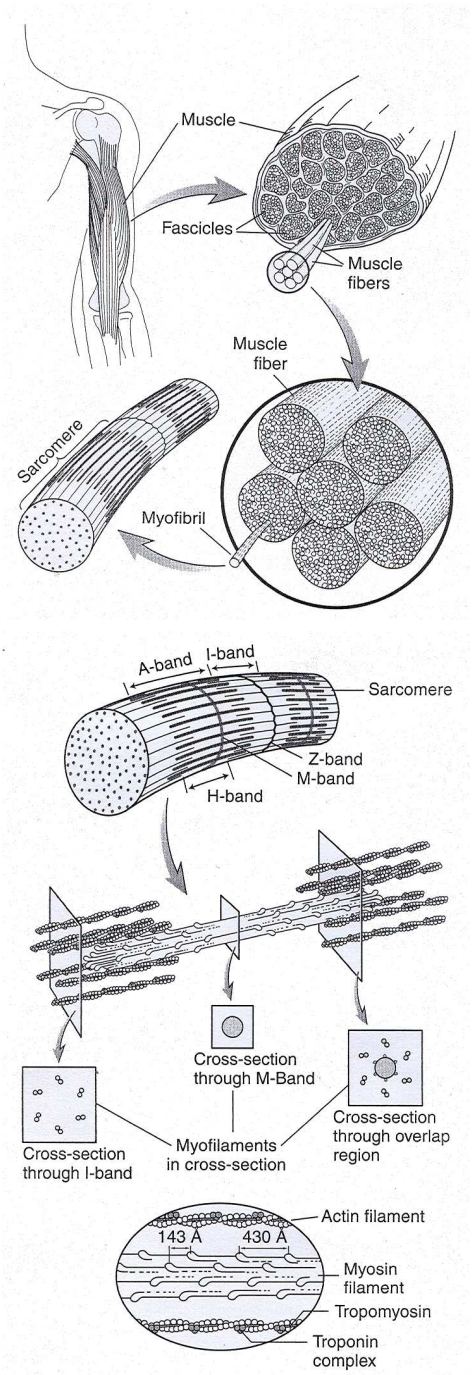

Figure 1.1 Skeletal muscle structure and hierarchical organization. Image reproduced with permission from Lippincott Williams & Wilkins [94].

On the cellular level, skeletal muscle of adults is composed of multinucleated myofibers that have no regenerative capacity. However, a population of mononucleated muscle precursor cells, or satellite cells, resides between the basal lamina and the sarcolemma of each fiber [54]. Upon external stimuli, such as muscle injury, these precursor cells, also known as myoblasts, are activated, undergo proliferation, and eventually begin to differentiate as the mononuclear myoblasts fuse together into multinucleated myotubes [179].

1.2.2 Skeletal Muscle Gene Transcription

Skeletal muscle differentiation involves a complex sequence of signaling and gene regulation events that lead the myoblast satellite cell into a fusion sequence resulting in a differentiated, multinucleated myotube. The muscle lineage is mainly controlled by myogenic regulatory factors (MRFs), which are categorized as basic helix-loop-helix (bHLH) transcription factors. The four major players are: MyoD, Myf5, myogenin, and MRF4, and each has the capacity to attain a skeletal muscle phenotype when expressed in non-muscle cells [47, 61, 174]. Figure 1.2 shows a schematic of myoblast fusion and maturation and the key MRFs involved at the various stages [61].

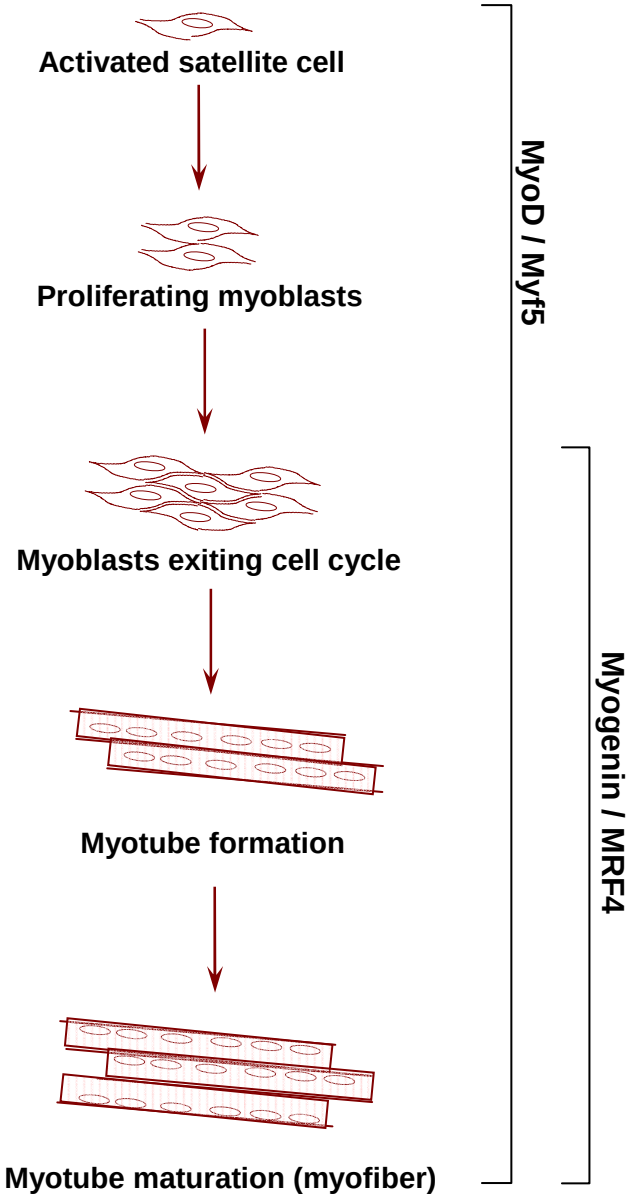

Figure 1.2 Skeletal myoblast activation in response to muscle injury. Adapted from [61].

MyoD and Myf5 are key components in muscle specification and widely thought to be redundant [32, 38, 138]. Myoblasts, the proliferating precursors to mature muscle myofibers, already have induced MyoD and Myf5 upregulation [32]. As the myoblasts exit the cell cycle and begin to enter the terminal differentiation stage, myogenin and MRF4 are up-regulated to promote muscle differentiation. Myogenin is specifically involved in the fusion and formation of myofibers, or myotubes, while MRF4 plays a significant role in further muscle maturation [38, 170]. All MRFs work together throughout the entire process of mature muscle formation. For example, even during the latter stages of muscle differentiation, MyoD is still involved in myoblast fusion and down-regulating proliferation signals [72]. Muscle-specific genes, such as muscle creatine kinase (MCK) and myosin heavy chain (MHC), are up-regulated in sequence in the stages following myoblast fusion and myotube maturation [32]. While *in vitro* injury induces satellite cell proliferation and differentiation, differentiation is induced *in vitro* by switching from a high fetal serum growth media to a low adult serum or differentiation media and requires a sufficient supply of insulin-like growth factor-1 [187].

Another complementary group of transcription factors, known as the myocyte enhancer factor-2 (Mef2), work cooperatively with the MRFs to induce muscle differentiation [42, 191]. The Mef2 family consists of 4 distinct genes: Mef2a, -b, -c, and -

d, which encode for proteins that work together to promote differentiation at various stages in development [121, 122, 188]. While this family of transcription factors is necessary, along with the MRFs, to proceed with the differentiation pathway, it is not sufficient alone to form functional tissue [110]. Although present in other tissues, such as brain and neural crest, the Mef2 family of proteins is predominantly associated with cardiac, skeletal, and smooth muscles [47]. Expression of Mef2c is the first to appear in the embryonic somite myotome (E9.0) and is followed by Mef2a and Mef2d, although the roles of the latter are not as clearly elucidated [47]. Ectopic expression of Mef2a was found to work with MyoD to initiate skeletal myogenesis [66]. But, studies have focused primarily on Mef2c as deletion of this member of the Mef2 family has resulted in sarcomere disorganization due to M line deterioration [122] and embryonic death due to vascular malformation [153]. Additionally, a control region of the Mef2c gene is a direct target for both bHLH and MEF2 myogenic factors [172]. The activation of the Mef2 transcription factors occur when repression by histone deacetylases (HDAC) is inhibited, oftentimes via the calcium/calmodulin-dependent protein kinase (CaMK) pathway [107]. Activation of CaMK signaling was found to block HDAC4 from translocating into the nucleus, thereby preventing inhibition of myogenic differentiation [109].

1.3 Skeletal Muscle Tissue Engineering

The field of tissue engineering has expanded rapidly over the last few decades, and while it started primarily as a biomaterials and cell interaction project, has now incorporated nanoscale to microscale approaches to enhance differentiation *in vitro*. In early models of tissue-engineered skeletal muscle, either mixed co-cultures of myoblasts and tendon fibroblasts or a pure population of myoblasts were used [116, 148]. The C2C12 myoblast cell line derived from C3H normal adult mouse as well as satellite cells isolated from neo-natal rats and human muscle tissue were common cell sources [40, 124, 183]. Cells were seeded into a variety of different 3D matrix scaffolds, such as collagen and fibrin gels, synthetic polymers, and decellularized muscle [18, 63, 90, 169].

Utilizing a collagen gel matrix, a C2C12 model system for skeletal muscle differentiation was investigated in our lab for three dimensional tissue engineering. Immunofluorescence demonstrated that mature striated muscle fibers were formed from a stable mammalian cell line, as early as the sixth day in differentiation conditions and were maintained for up to 33 days. Electron microscopy provided conclusive evidence that mature sarcomeres had formed as early as 16 days post shifting to differentiation media. By shift day 33, the beginning stages of myotendinous junction formation and newly synthesized collagen I fibers were evident [133]. A similar model system using

C2C12 myoblasts in a fibrin gel was recently optimized by focusing on regulating fibrinolysis *in vitro* [68].

But, beyond assessing ultrastructural elements, the ultimate functional output of a given construct is of utmost importance. Functional force and excitability measurements have shown that tissue engineered skeletal muscle can produce spontaneous twitch forces and tetany, both measurable responses to electrical stimulation, but at levels far below that of native muscle [41, 184]. Similar to the collagen gel system, fibrin gels were seeded with primary rat myoblasts that were able to generate maximal twitch force and tetanus in the range of several hundred μN, and also responded to hormonal treatments, such as IGF [63]. The same group, Huang *et al*., found that myoblasts isolated from rat soleus muscle (slow twitch) produced fibrin gel constructs that were 30% slower to contract and relax than those cultured with myoblasts from fast tibialis anterior rat muscle [64].

Further, contracted monolayers of cells, or myooids, cultured with C2C12 myoblasts and10T1/2 fibroblasts and neonatal rat myoblasts had higher baseline force outputs than myooids cultured with adult rat myoblasts [40]. But, another similar study with adult and neonatal rat myoblasts found that adult myooids exhibited higher specific forces than those cultured from the neonatal myoblasts (up to 40 days in culture), as neonatal myooids had a large fibroblast shell that was not considered viable

muscle area [74]. Building on that same model, a nerve-muscle construct was engineered with co-cultures of rat myotubes and embryonic rat spinal cord [87]. Both twitch and tetanus forces were higher in the nerve co-culture myooids over the myooids cultured with myoblasts alone [87].

Recent studies have also begun to show how surface morphology affects muscle function. One study isolated satellite cells from neonatal rats, which were then seeded on a matrix of parallel, type I collagen fibrils. Thicker matrices of aligned, collagen-based constructs were made using a layering process. Developed forces were on also in the range of several hundred μN, which also had corresponding responses to increasing electrical stimulation frequencies [183]. Another group employed the use of micropatterned features with fibrin gels to create both unaligned and aligned constructs. The twitch and tetanus forces were significantly higher in the aligned constructs, but still on the order of several hundred μN [82]. Micromolded features were also used to create different pore sizes and control myoblast alignment in fibrin gel-based tissue engineered skeletal muscle [16].

Furthermore, mechanical stimulation has been applied to 3D constructs in an effort to produce more native-like muscle, both in morphology and function. When a slow cyclic stretch and relaxation regimen was applied, construct elasticity was increased 2- to 3-fold, and myofiber area also increased by 40% [125]. While these

studies have shown some increase, at least in more organized morphology and myotube formation, a fully functional construct has yet to be produced, and there remains a large gap between native muscle and muscles created *in vitro*.

1.4 Mechanotransduction

Muscle adaptation to various mechanical stimuli can affect nearly all its components, such as fiber diameter, length, and distribution, muscle architecture, mitochondrial distribution, and myosin heavy chain profile [94]. Correspondingly, mechanical stretch of skeletal myoblasts *in vitro* results in protein synthesis and cellular hypertrophy [167, 168]. Studying these effects outside of the *in vivo* environment requires tight control of several key variables such as stretch frequency, strain and strain rate, and rest duration, which are critical in determining this cellular response. Additionally, changes to one or more of these factors may lead to vastly different responses both *in vivo* and *in vitro*. The effect of strain on muscle injury has been characterized to some degree to suggest that a 10-20% strain is within a physiologic range while strains greater than this lead to injury [23]. Translated to a 2D system, studies examining ~10% strains at moderate frequencies (0.5 Hz) and longer rest periods have been shown to enhance myoblast differentiation [192].

In contrast, a 17%-strain applied over a 1-hour stretch cycle at 1Hz followed by a 23 hour rest period inhibited myogenesis as the myoblasts were directed toward a more proliferative response [79]. The regulation of the proliferative cycle was enhanced by mechanical stimulation via focal adhesion kinase (FAK), Rac-1, and NF-κB, which induced cyclin dependent kinase (cdk2) [79]. When primary myoblasts from Balb/c mice were stretched 25% at 0.5Hz for 5 hours in a uniaxial stretch device, BrdU incorporation increased about 30% after 24 hours and cell number increased 40% after 48 hours, relative to unstretched controls, and myogenin levels were also decreased [119]. Exposure of primary rat hind limb cultured satellite cells to 25% equibiaxial stretch at 12-s intervals for 12 to 36 hours led to increased BrdU incorporation after 12 hours. Antibody blocking of hepatocyte growth factor inhibited stretch-induced BrdU incorporation [150]. These higher levels of strain are towards the upper limit of strains encountered physiologically [23] and may induce an injury response involving the release of growth factors [154], and TNF-α at high strains may explain the shift in response to stretch. Low levels of TNF-α stimulate p38 production, but high levels inhibit differentiation [35].

Another study confirmed these results by showing that a low frequency, low strain cyclic stretch regimen (0.05Hz, 3% strain for up to 72 hours) was able to inhibit the anti-myogenic activity of TNF-α [31]. Higher strains, up to 18%, were found to up-

regulate proinflammatory genes, such as Nos2, which is induced by TNF-α, but application of any type of cyclic stretch abrogated the effect of these proinflammatory cytokines [31]. Similarly, static stretch at strains of 8-9% induced p38 MAPK signaling, which promotes myogenesis by Mef2c, myogenin, p21, and myosin heavy chain (MHC) [190]. While few major studies have demonstrated that Mef2 and HDAC4 are affected by mechanical stimulation directly, key players in mechano-sensitive pathways, such as calcium/calmodulin [131] and MAPK signal transduction pathways [73], are associated with both proteins [107, 109, 193, 195].

A summary of several key factors associated with skeletal muscle mechanotransduction is shown in Figure 1.3. The many compensatory mechanisms the cell possesses to mediate key processes enables cells to adjust its internal protocols in response to different mechanical stimuli. This short list of pathways includes validated targets for miRNAs. For example, cell division cycle 42 (cdc42) and RhoA are known targets of miR-133 with a role in cardiac hypertrophy [27]. Additionally, SRF is a target of miR-133 in skeletal muscle as well [34]. The intersection of these mechanisms is one question this research proposal addresses.

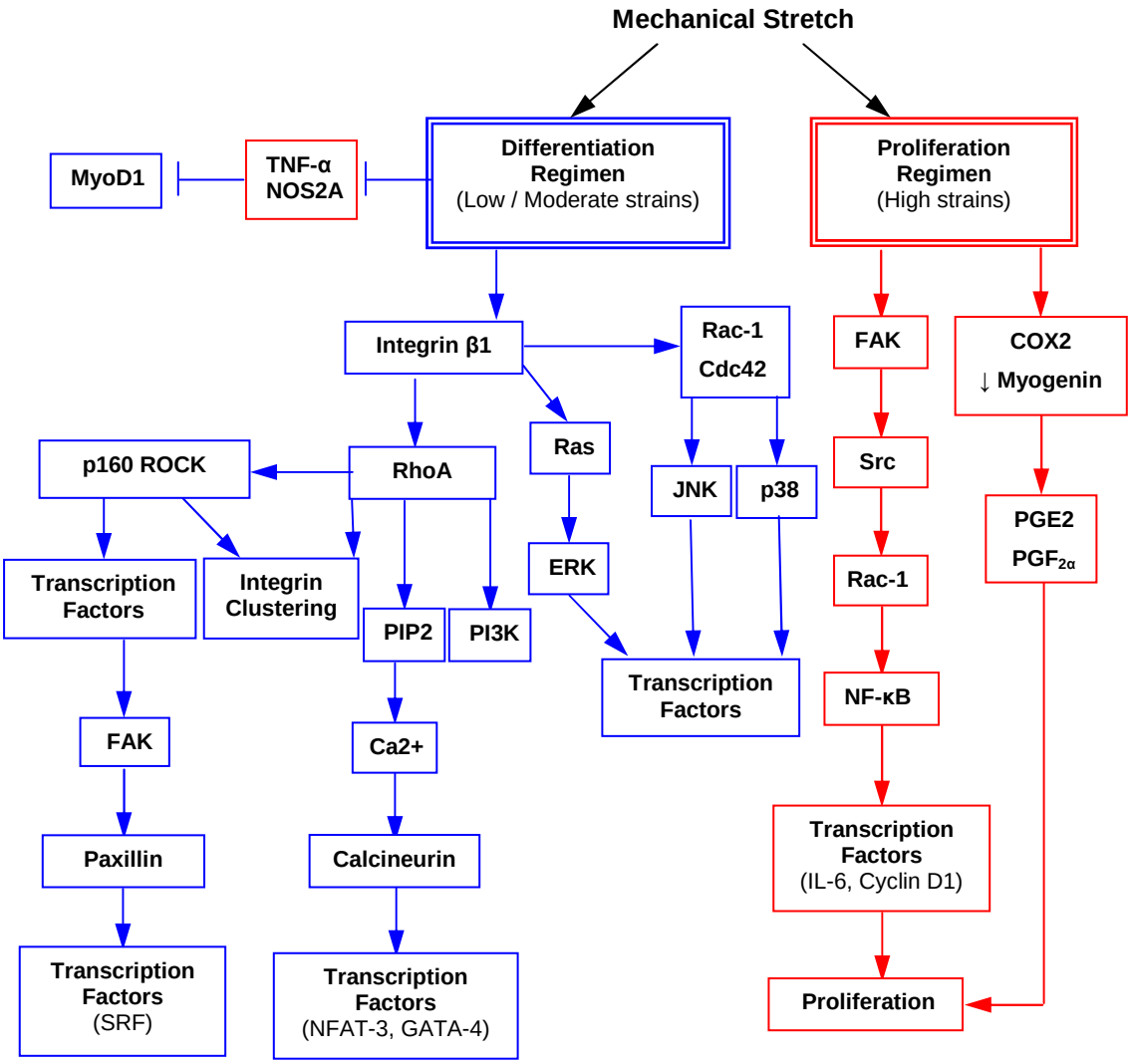

Figure 1.3 Key signaling pathways involved in mechanotransduction. Stretch regimens with low or moderate strains promote myoblast differentiation. A summary of integrin-mediated signaling through Integrin β1 is shown above in blue [28]. The regulation of the proliferative cycle in red was enhanced by mechanical stimulation via FAK, Rac-1, and NF-κB, which induced cdk2 [79]. A similar inflammatory response involving COX2 was observed when a cyclic, uniaxial strain of 25% was applied for 5 hours at a frequency of 0.5Hz [118]. A 3% strain applied at a frequency of 0.05Hz up for to 72h inhibited effects of TNF-α and inflammatory cytokine NOS2A, thereby promoting differentiation [31].

1.5 MicroRNAs

1.5.1 MicroRNA Biogenesis

Since their discovery in the *C. elegans* genome in the mid-1990s [89], microRNAs (miRNAs) have been the subject of great interest and much of their regulatory function still remains to be elucidated. MiRNAs are short, non-coding RNAs, ~ 20-22 nucleotides in length, involved in post-transcriptional gene regulation [3, 9]. Many miRNAs act as repressive elements to proteins that are themselves repressors. Found either in the introns of pre-mRNAs or part of separate segments of the genome, these non-coding RNAs start with sizable precursor hairpin structures that are known as primary, or pri-miRNAs. A schematic of miRNA biogenesis is illustrated in Figure 1.4.

Drosha, a nuclear endonuclease, cleaves the tail-end of the pri-miRNAs to form precursor, or pre-miRNA intermediates with an approximate size of 60-70 nucleotides. After transport out of the nucleus with the aid of Ran-GTP and Exportin-5, pre-miRNAs are further cleaved by another endonuclease, Dicer, to form a double stranded miRNA complex. This transient complex is unwound by a helicase, and the mature, single-stranded miRNA is released, often after preferential incorporation into a RNA-induced silencing complex (RISC) [65]. The RISC targets sequences within the genome that are complementary, or nearly complementary, to that of the incorporated miRNA and either cleaves the mRNA target or represses translation [9, 157]. While most pre-miRNAs may

be transported out of the nucleus, there is some evidence that not all of these precursors are processed by Dicer. Different post-transcriptional mechanisms can also control which miRNAs become mature, usually in a tissue-specific manner [115].

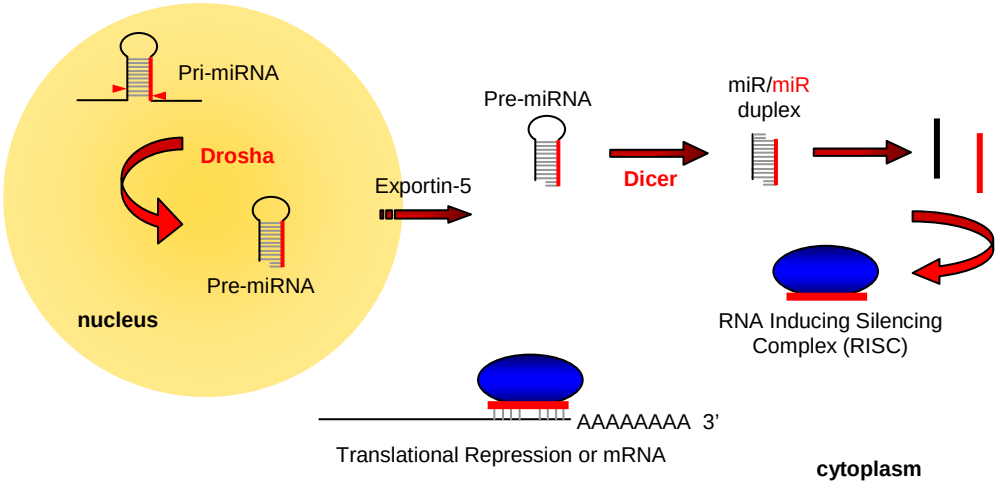

Figure 1.4 Schematic of miRNA biogenesis. The precursor hairpin structures known as pri-miRNAs are cleaved by Drosha, a nuclear endonuclease, to form pre-miRNA intermediates with an approximate size of 60-70 nucleotides. With the aid of Ran-GTP and Exportin-5, the pre-miRNA structure is shuttled out of the nucleus and further cleaved by the endonuclease Dicer. Now a double stranded miRNA complex, which is transient in nature, is unwound by a helicase thereby releasing the mature, single-stranded miRNA. This mature miRNA associates with a RNA-induced silencing complex (RISC) and through perfect or nearly perfect complementarity to its target mRNA, the miRNA represses translation.

1.5.2 miRNAs and siRNAs

With the 2006 Nobel Prize awarded for the discovery and work in the field of non-coding RNAs, RNA interference (RNAi) has been at the forefront of uncovering gene regulation mechanisms. MicroRNAs are often confused with siRNAs, as much of the processing components of both are dependent on the same proteins and protein complexes. While the downstream impact of inhibiting protein synthesis is the same for both miRNAs and siRNAs, their modes of regulation and how they are regulated are distinctly different.

While miRNAs are highly conserved, endogenous regulators, siRNAs are not conserved for the most part and often exogenous or can be endogenous as well. By this nature, miRNAs are encoded by genes and in many cases, are transcribed from the same cluster while siRNAs are not encoded by genes and characteristically consist of separate elements with repeated units [4, 53, 136]. Both utilize the RNase III endonuclease, Dicer, in the final stages of processing which results in a ~20-22 nucleotide single-stranded RNA, while some pre-processing components differ. miRNAs contain a seed sequence that binds imperfectly to its mRNA target to eventually repress translation or in some cases (usually in plants) cause mRNA cleavage [4, 53, 136]. siRNAs are an exact match of their targets, which results in mRNA cleavage or chromatin modification or silencing [137]. A comparison of these two regulatory molecules is summarized in Table 1.1 [137].

Table 1.1 Comparison of various attributes of miRNAs of siRNAs.

Element	miRNA	siRNA
Species conservation	Yes	No
Synthesis	Endogenous	Endogenous or exogenous (viral infection)
Encoded by nuclear genes	Yes	No
Clustering	Families of miRNA clusters, also individuals	Individual units, often with repeated DNA sequences
Hairpin structure	Yes	No
Processing machinery	RNA polymerase II, Drosha, Dicer	Dicer
Nucleic Length	~20-22 bases	~20-22 bases
Complementarity	Imperfect match, 7-8 bp 'seed' sequence utilized	Exact match
Modes of action	Translational repression, some mRNA cleavage	mRNA cleavage, chromatin modification and silencing

1.5.3 MicroRNA Targets

Conserved in most related species, miRNAs are a critical regulatory mechanism for gene regulation [9, 76]. To date, over 400 miRNAs have been found in the human species alone, and it has been postulated that one-third of all human genes are regulated by miRNAs [10, 45, 85, 127]. Additionally, miRNAs are thought to represent 1-5% of the genome of humans, *C. elegans*, and *D. melanogaster* [9, 20]. Not all of the target sequences of the miRNAs are known, but new database and genome searches have given rise to

predicted targets [9, 10, 96]. Although elevated before miRNAs are specifically expressed in a given tissue, studies have shown that the targets of these miRNAs decrease as the miRNAs accumulate, which further supports the idea that miRNAs function as repressors of their targets [52].

While the mature miRNA is approximately 20-22 nucleotides long, the key portion that dominates in binding to its target consists of 6-8 nucleotides at the 5′ end and is often referred to as the 'seed' sequence; the 3′ end of the miRNA also plays a compensatory role that aids in target binding [21, 43]. Further, flanking adenosines adjacent to the seed sequence provide another criteria by which miRNAs find their targets [93]. While there is nearly perfect complementarity of miRNAs and their targets in plants [134], animal genomes display both near perfect and only partial complementarity [14]. Additionally, nearly half of target mRNA regions, usually in the 3′ UTR, have matches for two or more miRNAs, with some having site complementarity to 12 miRNAs [146]. These factors contribute to numerous permutations of possible miRNA-target binding events. Therefore, the prediction of miRNA targets has proven to be quite complex. There have been numerous algorithms developed to predict these targets via sequence complementarity, target site conservation in various species, miRNA-mRNA thermodynamic stability, and number of binding sites [14, 103]. While

the rate for false positives is still high, these prediction tools, taken in combination, provide a good basis for validating a miRNA target.

1.5.3 MicroRNAs and Muscle Biology

New discovery tools, such as oligonucleotide chips, miRNA microarrays, and multiplexed RT-PCR kits have enabled us to globally scan for miRNAs isolated from organ-specific tissue, in a normal or diseased state [11, 15, 85, 96]. Spatial and temporal regulation of miRNAs has been observed in specialized tissues, such as miR-124 in brain, miR-1 in muscle, and miR-233 in bone marrow [33, 95, 143]. Recent studies have shown that miRNAs play a crucial role in regulating cardiac and skeletal muscle development. MicroRNA-1 (miR-1) is abundant only in cardiac and skeletal muscle and comprises nearly 50% of miRNAs found in the murine heart [81]. Zhao *et al*. showed that miR-1 genes are downstream targets of muscle specific factors, such as serum response factor (SRF), MyoD, and Mef2 [194], further suggesting feedback loops present in miRNA regulation. A transcription factor, Hand2, is a miR-1 target and thought to enhance cardiac differentiation by modulating cell proliferation. Over-expression of miR-1 decreased proliferation of cardiomyocytes [22, 194] and cardiac differentiation in *D. melanogaster* [80]. Additionally, murine C2C12 cells also have the ability to differentiate toward the osteoblastic and adipogenic lineages [55, 56], but miR-1

modulated myogenic differentiation pathways and did not have an effect on fate determination [114].

In addition to miR-1, miR-181 was linked with myoblast differentiation (C2C12 myoblasts) via repressing the homeobox protein, Hox-A11, ultimately shedding light on the differentiation mechanism of myoblasts [113]. MiR-181 is up-regulated during differentiation, which further down-regulates homeobox protein, Hox-A11. This, in turn, up-regulates overall MyoD expression and other downstream, myogenic elements such as myogenin, myosin heavy chain (MHC) and muscle creatine kinase (MCK) [113]. Furthermore, miR-181 was found in the B-lymphoid bone-marrow cells of a mouse and modulated lineage differentiation of the B-cell [33].

Several major studies that involved global scanning with microarrays pinpointed three miRNAs that are involved in myogenesis: miR-1, miR-133, and miR-206 [11, 81, 143, 176]. Subsequent studies have examined downstream targets and functional effects of these miRNAs. Chen *et al*. showed that miR-1 and miR-133 promote skeletal muscle differentiation and proliferation, respectively [34]. Specifically, miR-1 targets histone deacetylase 4 (HDAC4), which is a transcriptional repressor of Mef2, a critical component for myoblast differentiation [101]. Similarly, miR-133 down-regulates SRF, which blocks myoblast proliferation. This group further showed that miR-1 and miR-133 are separated by 9.3 kilobases on mouse chromosome 2 and 2.5 kilobases on mouse

chromosome 18 [34]. Although the miR-1 and miR-133 genes are transcribed together and controlled at the primary step, the mechanism by which they regulate protein output follow two different pathways that work in a complementary manner in the muscle maturation process. Both knockdown (via antisense oligonucleotide probes) and over-expression studies confirmed that miR-1 plays a critical role in myogenesis while miR-133 alone promoted proliferation and partially inhibited myoblast differentiation [34, 173].

MyoD and myogenin bind to upstream regions of miR-1, miR-133, and miR-206, thereby regulating their expression [130]. Although some have postulated that miR-1 and miR-133 follow two independent pathways [34], both Chen *et al*. and Rao *et al*. found that MyoD regulates the expression of miR-1 and miR-133 [34, 130]. Further, MyoD and myogenin can bind upstream of miR133a-2 on chromosome 2 and upstream from miR-133a-1 and both upstream and downstream from miR-1 on chromosome 18 [130]. For example, MyoD and Mef2c, which are correlated to myoblast differentiation, are predicted targets for miR-133, a miRNA that is thought to promote proliferation [130]. Similarly, a newly validated target of miR-133 was nPTB, a key component to alterative splicing that leads to undifferentiated patterns if uninhibited [19].

Exclusive to skeletal muscle [106], differentiation has been further enhanced by miR-206, and was found to hinder withdrawal from the cell cycle and subsequent fusion

and differentiation. miR-206 acts by down-regulating DNA polymerase α (Pola1), which leads to cell cycle arrest and eventual cell differentiation [69]. Further, miR-206 expression was elevated in newly formed myotubes and showed a temporal increase with myoblast differentiation [189]. Expression of miR-206 also varied within different muscle groups. A recent study found there were differences in miR-206 expression levels in soleus and plantaris muscle of mice where expression in the soleus muscle was 7 times than in the plantaris [104]. In rat myogenic cells, miR-206 was enriched in the nucleolus and cytoplasm with 28S rRNA [120].

Two newly characterized miRNAs, miR-24 and miR-26a, are also involved in the myogenic differentiation process. Skeletal muscle differentiation was enhanced by negative regulation of miR-24 through TGF-β1 and Smad3 [147]. Another study shows, using C2C12 myoblasts, that miR-26a directly targets *Enhancer of Zeste homolog* 2 (Ezh2), a repressor of muscle differentiation [178]. A summary of miRNAs involved in the development of mammalian skeletal muscle is compiled in Table 1.2 [26, 49].

Table 1.2 MicroRNAs involved in mammalian skeletal muscle development

miRNA	Validated Targets	Upstream Regulators	Downstream Functional Effect	Refs.
miR-1	HDAC4	MyoD, Mef2, SRF	Myogenesis (Differentiation), Hypertrophy	[34, 97, 104, 130]
miR-133	SRF, nPTB	MyoD, Mef2, SRF	Myogenesis (Proliferation), Alternative splicing, Hypertrophy	[19, 34, 97, 104, 130]
miR-206	Pola1, Utrn, Fstl1	MyoD	Myogenesis (Differentiation)	[19, 69, 135, 149]
miR-181	HOXA11	unknown	Myogenesis (Differentiation)	[113]
miR-24	Unknown	TGF-β1 + Smad3	Myogenesis (Differentiation)	[147]
miR-26	Ezh2	Unknown	Myogenesis (Differentiation)	[178]

***Table Abbreviations**: Histone deacetylase 4 9HDAC4), serum response factor (SRF), polypyrimidine tract biding protein (PTB), DNA polymerase α (Pola), Utrophin (Utrn), Follastatin 1 (Fstl1), Homeobox protein A11 (HOXA11), Enhancer of Zeste homolog 2 (Ezh2), Myocyte enhancer factor 2 (Mef2), Transforming growth factor β1 (TGF-β1), SMAD family member 3 (Smad3)*

Both blocking and over-expression studies have demonstrated the critical effect these RNAs have on downstream protein targets. Additionally, validated targets for key muscle-specific miRNAs (both skeletal and cardiac), such as serum response factor (SRF), RhoA, and cdc42, are also crucial in signaling pathways associated with mechanical stimulation [27, 34].

1.5.4 MicroRNAs and Mechanical Stimulation

The effect of mechanical stimulation on miRNA levels and function has not been extensively explored in mammalian cell and tissue development. One study showed that cyclic stretch upregulated miR-146a, which thereby affected levels of its target, Numb, and inhibited myogenesis [78]. Another study in *Arabidopsis* has named miRNAs that might be regulated as a result of mechanical stress caused by xylem development [99]. While current research linking the two is limited, both mechanical stimulation and miRNA regulation are known effectors of various tissues, such as cardiac and skeletal muscle, and it is known that mechanical stimulation has a significant effect on cell growth, proliferation, and differentiation [168].

Even though the dynamic changes in miRNA regulation have not been widely explored, the levels of miRNA in diseased or stressed states have been studied. A recent study in human and mouse systems found that levels of miR-1 and miR-133 decreased with cardiac hypertrophy. Furthermore, over-expression of these two miRNAs *in vitro* prevented entry into the hypertrophic state [27]. It was found that miR-133 inhibits remodeling [27] while deletion of miR-208 prevents hypertrophic remodeling [159]. Others have also found that miR-1 is downregulated in a cardiac hypertrophy environment [140]. Induction of cardiac hypertrophy also caused an up-regulation of a number of miRNAs including miR-21 and miR-195 [158].

In skeletal muscle, the effects of hypertrophy through *in vivo* injury to rat soleus and plantaris muscle were explored on miR-1 and miR-133a regulation, where a decrease was demonstrated following 7 days of functional overload. Levels of miR-206 did not change [104]. A different response in miRNA processing was observed in old and young human subjects to an anabolic stimulus [44]. Levels of the pri-miR-1 and pri-miR-133 were increased in older subjects while there were no differences in the mature levels of these miRNAs; miR-206 was also unchanged with age. Further miRNA expression was more easily altered in the younger subjects, suggesting that aging has direct affects on miRNA regulation [44]. Recently, miR-181, 1, and 107 expression were all upregulated in the quadriceps muscles of C57BI/6J mice in response to a single bout of exercise (90-minute set), whereas miR-23 expression decreased, and miR-133 expression remained the same compared to the sedentary control [139]. Further, similar to other studies [5, 180], peroxisome proliferator-activated receptor gamma coactivator 1 (PGC-1α) mRNA and protein expression were increased with this exercise regimen.

1.5.5 MicroRNA Dysfunction & Possible Therapies

In the past year, miRNA regulation has been implicated in diseases such as cardiac ailments, cancer, and muscular dystrophies. Since then, the focus has been shifted to exploring the possibility of using these small RNAs for therapeutic purposes

[60, 145, 160, 161]. Specifically, in the case of muscular dystrophies, specific miRNAs can be targeted for a particular type, such as Duchenne's muscular dystrophy (DMD). In this case, miR-362, 299-5p, and 487b were found to be upregulated exclusively in DMD over the ten other dystrophies explored [48]. Similarly, miR-155 and miR-146b expression could be measured in patients with nemaline myopathy (NM) [48].

With miRNAs either up- or down-regulated in certain disease states, blocking or additional delivery of specific miRNAs is being explored. The use of locked nucleic acids (LNA) and antagomiRs focuses on inhibiting miRNA function and may be a way to exogenously modulate miRNAs that are upregulated in these disease states [75, 77, 171, 175]. There continue to be challenges related to stable inhibition or up-regulation of miRNAs *in vivo*, especially in a tissue-specific manner; however, current work suggests that this is a possibility and business opportunities are arising at a rapid pace [102].

1.6 Justification and Significance

Muscular diseases are often incurable and lead to debilitating outcomes. Treating these issues on a broad scale through regenerative medicine is the ultimate goal of this project. From a skeletal muscle perspective, tissue engineering provides a two-fold purpose which is to one, create a viable construct for implantation and two, establish an *in vitro* model system for non-invasive tests of various biochemical and

mechanical treatments. However, despite recent advances in the field of skeletal muscle tissue engineering, the limited ability of myoblasts to fully differentiate *in vitro* remains a hurdle. Mechanical stimulation is one effector of muscle development and growth, and although this type of stimulation can promote differentiation, mature muscle fibers have not been produced *in vitro* [124].

Concurrently, from the gene regulation standpoint, controlling the molecular machinery of the cell may prove to be an effective method to modify cellular behavior for a given situation. Recently, non-coding RNAs, particularly miRNAs, have proven to have an immense impact on cellular function via translational inhibition. Because these miRNAs can modulate specific functions of differentiated skeletal muscle, they represent a promising target for manipulation. The proposed research examines miRNA expression in skeletal myoblast proliferation and differentiation in response to different mechanical stimuli, and the results provide important new information on the manner by which miRNAs regulate the myoblast response to these mechanical signals. Further, we implement exogenous miRNA delivery to modulate cellular function, or force output in this case, to address shortcomings in the field of skeletal muscle tissue engineering. By completing this study, we have begun to understand the adaptive mechanisms of skeletal muscle satellite cells to mechanical stimulation, the importance of miRNAs in skeletal muscle development, and the genetic controls that link the biomechanical cues

observed outside the cell membrane to transcriptional level control in the nucleus in 2D and 3D myoblast models.

Chapter 2. Bioartificial Muscle in a 3D Collagen Gel System

Adapted, with permission, from:
Rhim C, Lowell DA, Reedy MC, Slentz DH, Zhang SJ, Kraus WE, Truskey GA, "Morphology and Ultrastructure of Differentiating Three-Dimensional Mammalian Skeletal Muscle in a Collagen Gel", Muscle and Nerve, 36:71-80, 2007.

2.1 Introduction

Somatic cell therapies involving the use of committed skeletal muscle satellite cells, or myoblasts, have evolved over the past decades and have ranged from relatively simple somatic cell transfer to the use of tissue-engineered organ replacements. Due to the non-regenerative nature of the mature myocardium, degenerating heart muscle tissue irreversibly loses function, but there is some evidence supporting the use of skeletal muscle tissue to restore contractile function to failing myocardium [1, 46, 67, 112, 151]. However, certain gap junction proteins, such as connexin43 (Cx43), that are pivotal for electrical propagation in cardiac cells, are absent in skeletal myoblasts. Researchers are investigating the incorporation of these proteins into the myoblast cellular machinery and have met some success [1].

Both skeletal myoblasts and whole muscle grafts have been explored as a treatment to replace injured and necrotic myocardium and restore cardiac function [1, 2, 67, 112, 151]. Myoblast transfer also has been used as a method of providing functional dystrophin in individuals with Duchenne Muscular Dystrophy (DMD) through the

fusion of donor myoblasts containing normal dystrophin with existing myofibers lacking dystrophin protein [126]. While satellite cells represent an attractive option for a number of muscle-related tissue engineering applications, there are others in which the use of mature skeletal muscle organoids would be preferable, in which instances, mature muscle organoids would have to be produced *in vitro,* while having the advantage of being preconditioned to specific mechanical and energetically stressful environments.

Synthesis of tissue engineered skeletal muscle constructs *in vitro* primarily has used either mixed co-cultures of myoblasts and tendon fibroblasts or a pure population of myoblasts [116, 148]. The matrix scaffolds into which cells were seeded have also ranged from collagen and fibrin gels to synthetic polymers to decellularized muscle [18, 63, 169]. Many of these conditions produce some features of mature muscle; however, very few have replicated *in vitro,* many features of mature, mammalian muscle in three-dimensional culture.

The goal of the current study was to establish conditions that would produce mature sarcomeres in a mammalian-derived skeletal muscle construct developed from an established murine cell line (C2C12). Adapted from the protocol of Vandenburgh [165], bioartificial muscles (BAMs) were created using C2C12 cells in a Matrigel/collagen gel system. We evaluated the effects of collagen, cell density, and serum concentration on histologic, histochemical, and functional parameters indicative of mature muscle. Striated muscle fibers were formed as early as 6 days post-differentiation and

maintained for as long as 33 days. The presence of distinct skeletal muscle ultrastructure was observed by fluorescence staining and verified via electron microscopy, thereby demonstrating a 3D tissue culture system for muscle regeneration *in vitro*.

2.2 Methods and Materials

2.2.1 Cell Culture & Bioartificial Muscle (BAM) Assembly

C2C12 myoblasts from normal adult C3H mouse muscle were obtained from American Type Culture Collection (ATCC) (Rockville, MD) and used at passages 4 to 6 [182]. Cells were cultured at 37°C, 5% CO_2 in a growth medium (GM) that consisted of high glucose DMEM (Gibco, Grand Island, NY) with 8% fetal bovine serum (Hyclone Laboratories, Logan, UT), 8% bovine calf serum (Hyclone Laboratories, Logan, UT), 0.5% chick embryo extract (Accurate Chemicals, Westbury, NY), and 0.1% gentamicin (Gibco, Grand Island, NY). Before confluence was reached, the myoblast cultures were trypsinized in a 0.05% trypsin/EDTA solution (Gibco, Grand Island, NY) and centrifuged at 1000 rpm for 5 minutes.

The cell pellet was then resuspended in a Matrigel solution (BD Biosciences, Bedford, MA) and added to a chilled solution of GM yielding final concentrations of 1.4mg/ml type I rat tail collagen (BD Biosciences, Bedford, MA) and 3mM NaOH to a

final 3:1 ratio of collagen to Matrigel. One to five million cells were suspended within this collagen gel mixture to give each BAM a total volume of 0.4ml.

As previously described [124, 165], BAM troughs were made using silicone tubing (Nalgene, Rochester, NY), split longitudinally with tiny sections of silicone sheets (Nalgene, Rochester, NY) and glued to the open ends of the tubing with RTV silicone adhesive (GE, Waterford, NY). Small stainless steel minutien pins (Fine Science Tools, Foster City, CA) held Velcro tabs at the ends of the mold to act as attachment sites for the collagen/matrigel construct, and over time, to maintain passive tension. The assembled molds were glued onto the bottom of a standard tissue culture dish and gas sterilized with EtO.

After 1 hour at 37°C, warm GM was added to the dishes over the gelled Matrigel construct. The BAMs were cultured for 2 days in GM and then the media was shifted to one that promoted differentiation. This differentiation media (DM) consisted of high glucose DMEM (Gibco, Grand Island, NY), 8-20% horse serum (HS, Hyclone Laboratories, Logan, UT), and 0.1% gentamicin (Gibco, Grand Island, NY). Cultures remained in DM for 6 to 36 days (shift day, SD 6 to 36).

2.2.2 Histology

The BAMs were fixed for 2 hours in 10% neutral buffered formalin at 4°C, then rinsed and stored in phosphate buffered solution (PBS) for histochemistry. All

histochemistry procedures were performed in the Pathology Laboratory, Duke Medical Center. Briefly, the samples were dehydrated in a graded series of ethanol solutions and embedded in paraffin for sectioning. Specimens were cut into 5μm sections in both the longitudinal and cross-sectional directions and stained using hematoxylin and eosin (H&E).

2.2.3 Live/Dead Assay

Cell viability was determined with a live/dead assay kit (Molecular Probes, Eugene, OR). Media from the culture wells was carefully removed and rinsed once with Dulbecco's PBS. The samples were incubated with ethidium homodimer (4μM) and calcein AM (2μM) for 1 hour at 37°C and rinsed once more with Dulbecco's PBS. The samples were then observed via confocal microscopy.

2.2.4 Staining

The BAMs were fixed for 2 hours in 10% neutral buffered formalin at 4°C, rinsed in PBS, then permeabilized with 1% nonidet P-40 (NP-40) for 4 hours at 37°C. Afterwards, the samples were thoroughly rinsed and stored in PBS. The permeabilized BAMs were incubated for 1 hour with rhodamine-phalloidin (Molecular Probes, Eugene, OR), 25U/ml, to stain for F-actin filaments, and an additional 30 minutes with Sytox Green, (Molecular Probes, Eugene, OR), 1μM, was used for nuclei staining.

For immunohistochemical staining, the samples were fixed and permeabilized in the same manner as described above. Primary antibodies, alpha-actinin (Sigma, St. Louis, MO) and myosin MF20 (Developmental Studies Hybridoma Bank, Iowa City, IA), were diluted 1:800 and 1:50, respectively, in a 1% BSA solution and incubated with the BAMs overnight at 4°C. After thorough rinsing with PBS, the construct was incubated at 37°C with a secondary FITC goat anti-mouse antibody (Zymed, S. San Francisco, CA) for 4 hours. A monoclonal anti-paxillin antibody (Zymed, S. San Francisco, CA) was diluted 1:100 in 10% goat serum, incubated for 1-2 hours at 37°C, and rinsed with PBS. The BAM was incubated with a secondary goat anti-mouse antibody, Alexa Fluor 488 (Molecular Probes, Eugene, OR), for 1 hour at 37°C. Samples were then viewed via confocal microscopy.

2.2.5 Electron Microscopy (EM)

BAMs were fixed with 3% formaldehyde / 3% glutaraldehyde in 0.1M sodium cacodylate buffer (pH 7.35) (Tousimis, Rockville, MD) for 2 hours at room temperature, post-fixed for 2 hours in 1% osmium tetroxide in 100mM KPO_4 buffer with 10mM $MgCl_2$ (pH 6.1), ice cold, block stained in aqueous 2% uranyl acetate for 2 hours, cold, dehydrated through a 50-100% ethanol series and embedded in Araldite resin. Thin (30-60nm) longitudinal and cross sections were stained with 2%$KMnO_4$ followed by Sato Lead [132].

2.3 Results

Three-dimensional cultures of differentiating C2C12 cells in collagen gels were sustained for over 1 month. Although cells were distributed uniformly throughout the construct at the start of culture, cells began to migrate to the outer layer of the construct by shift day 6, as evidenced by polarized myoblasts and corresponding migration tracks through the collagen gel. Hematoxylin and eosin (H&E) staining and electron microscopy showed few cells in the BAM center, but confirmed the presence of multinucleated myotubes on the periphery of a the BAM by shift day 6 (Figure 2.1).

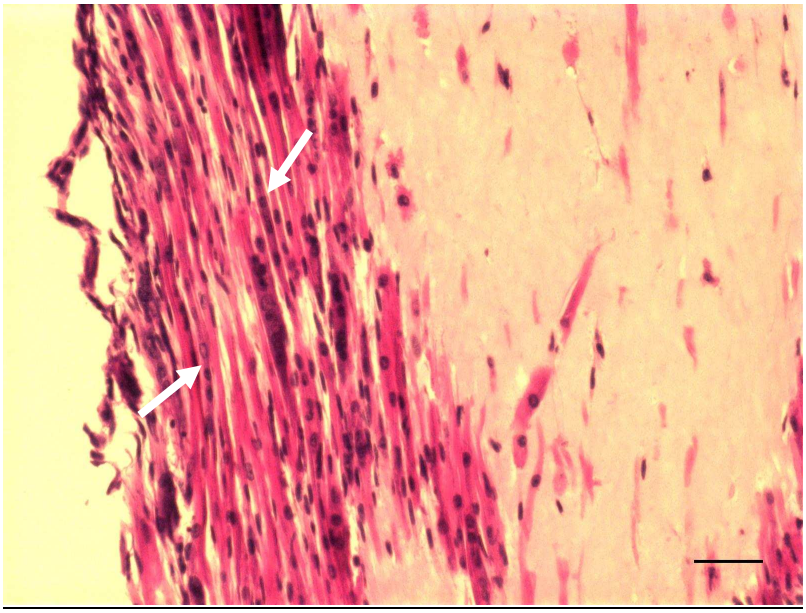

Figure 2.1 Hematoxylin and eosin (H&E) staining of tissue engineered bioartificial muscle (BAM) at shift day 16. A longitudinal section of (BAM) reveals multinucleated fused myotubes that are shown by the arrows. Image was captured at 20X, scale bar is 50μm.

Both mononucleated myoblasts and multinucleated myotubes were visible in the periphery; however, of the cells found within the central region of the construct, most were unfused myoblasts. There was no migration of cells to the periphery when the BAM was maintained in growth media. An early H&E stain at shift day 2 shows a fairly even distribution of cells while at day 30, a thick "shell" of cells has formed around the periphery while few cells remain in the center (Figure 2.2). There was limited debris in this central portion of the construct.

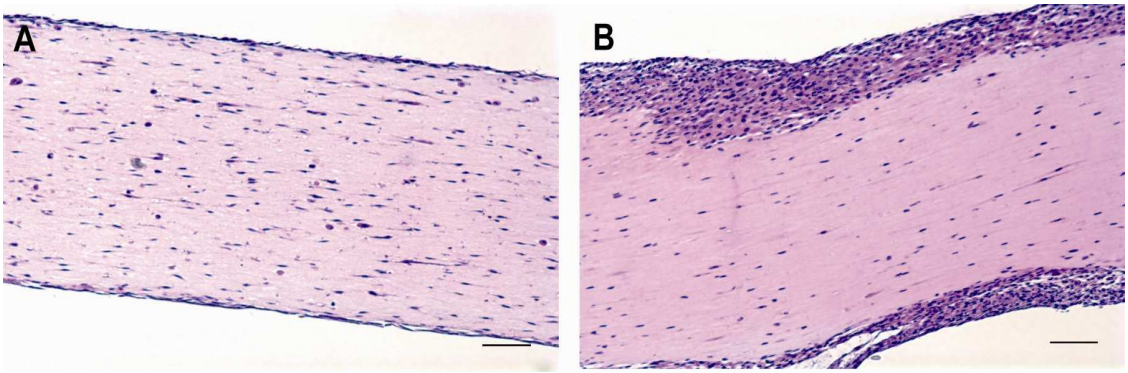

Figure 2.2 Hematoxylin and eosin (H&E) staining of BAM at (A) shift day 2 and (B) shift day 30, cultured with 20% horse serum differentiation media. Fairly even cellular distribution was noted at 2 days while at 30 days, the lack of much cellular debris, and a thick "shell" of cells on the periphery suggests that myoblasts may have migrated toward the outer edges of the construct. The image was captured at 10X, scale bar is 100μm.

The live/dead assay (BAMs cultured in 8% horse serum DM for 16 days; Figure 2.3) revealed some dead, perhaps apoptotic, cells toward the center of the BAM. The dead cells appeared to be mononuclear and rounded. Cell migration from the center of

the BAM, leaving only a few dead cells behind, reflected probable diffusion limitations of nutrients toward the center of the construct. Multinucleated fibers were abundant on the surface of the BAM, and overall, no fibers took up the ethidium homodimer dye, which signified that cell death had not occurred within the outer myotube layers.

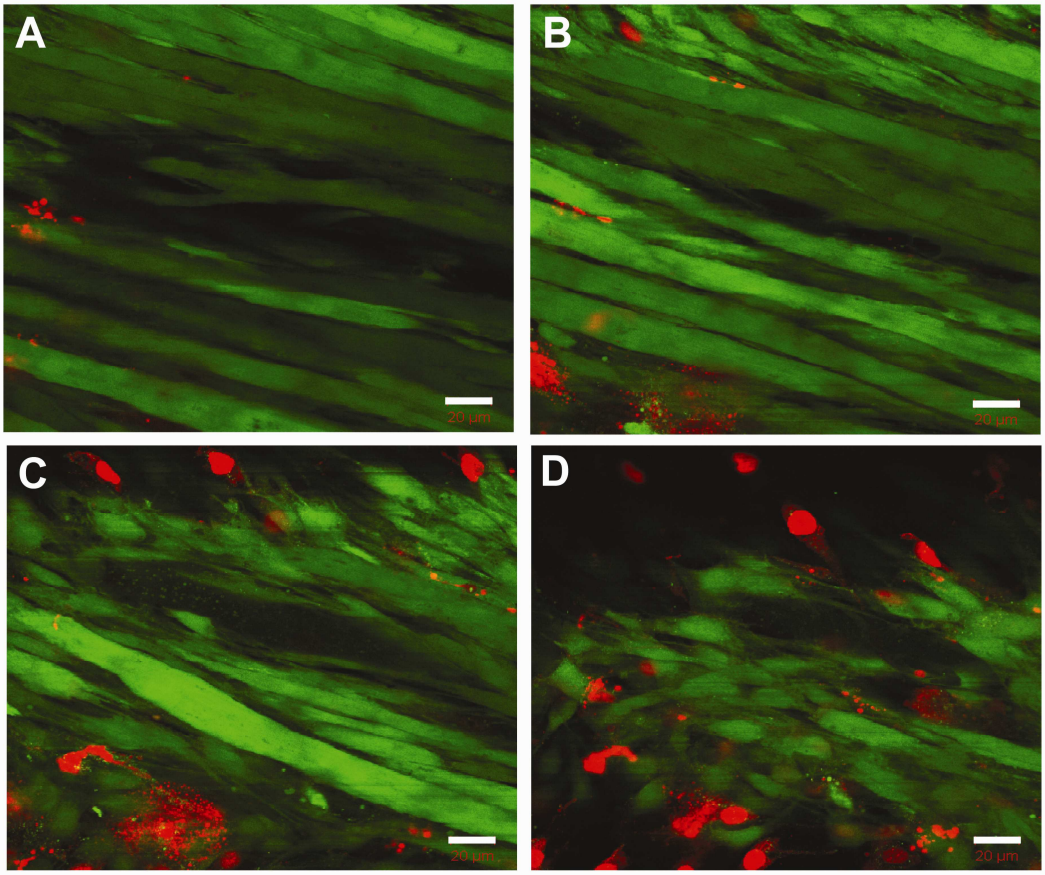

Figure 2.3 Live/Dead assay of BAM cultured for 16 days. Live cells are stained green and dead cells red. (A – D) Bioartificial muscle cultured for 16 days in 8% horse serum DM, shown in increasing order of depth from the surface. Scale bars are 20µm.

Additionally, polarized myoblasts, sometimes in short chains of two or three, were seen along "paths" of lower density in the gel. In two cases, the lead cell in the

chain had reached the periphery and appeared to be bending to move along the inner surface of the cells at the periphery, followed by the trailing myoblasts (image not shown). Therefore, these results, along with the absence of much debris in the center of the BAM, suggest that myoblasts are migrating from the center to the periphery of the BAM, where all proliferation and fusion occur.

In this study, viable multinucleated fibers were observed over a range of culture conditions. High initial cell concentrations (greater than $3x10^6$ cells per BAM) and collagen concentration (1.4 – 4.2 mg/ml) were generally found to lead to poor myoblast fusion within the BAM. Serum concentration at the onset of differentiation (in DM) had some effects on spontaneous contraction: higher serum concentrations generally produced less noticeable contraction; however, fusion and the presence of a non-uniform "shell" of cells on the periphery, as shown in Figure 2.4, were demonstrated despite varying serum concentrations between 2% and 20%.

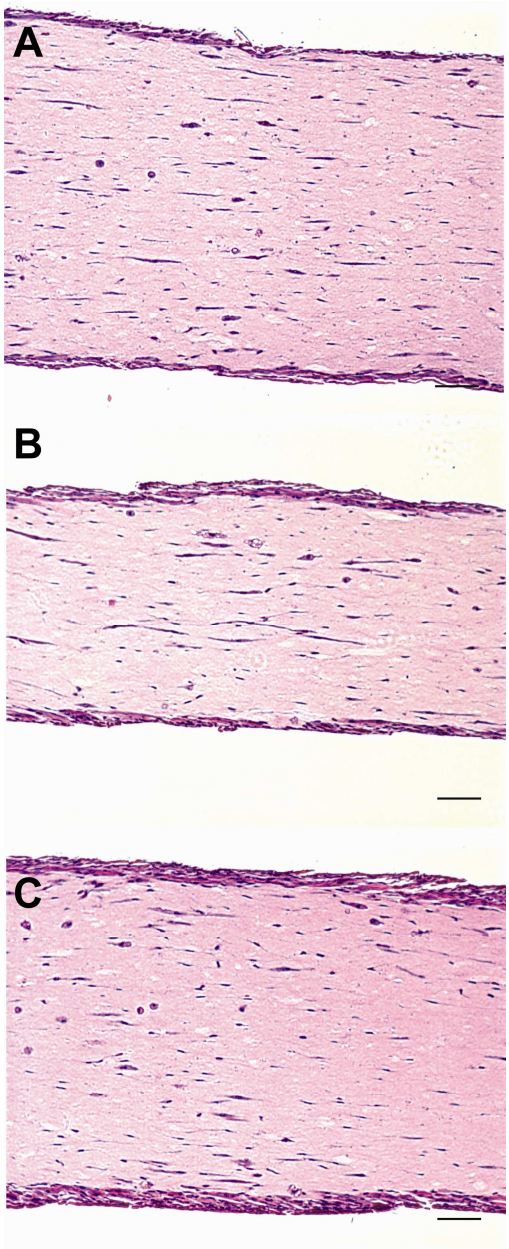

Figure 2.4 Hematoxylin and eosin (H&E) staining of BAMs that were cultured in (A) 2% horse serum DM for two days followed by 8% horse serum for 6 days, (B) 10% horse serum DM for 8 days, and (C) 20% horse serum DM for 8 days. In all cases, the majority of the myoblasts and fused myotubes were congregated in the periphery, and often the thickest layer of cells most evident in the BAMs shifted with 20% horse serum DM. Images were captured at 10X, scale bar is 100μm.

Spontaneous contraction is a marker of functional health of the cellular syncitium that myocytes form. These contractions were most visible when myoblasts were differentiated in 8-10% horse serum and least visible at 20% horse serum. This phenomenon was consistent throughout the culture time, up to 33 days. However, the frequency and strength of contractions were not necessarily indicative of the differentiation and maturation of the engineered muscle. Staining for F-actin with rhodamine phalloidin and nuclei staining with Sytox green demonstrated clear fusion in the BAMs that were cultured for 16 days in high serum DM (20% horse serum) even though contractile activity appeared reduced (Figure 2.5).

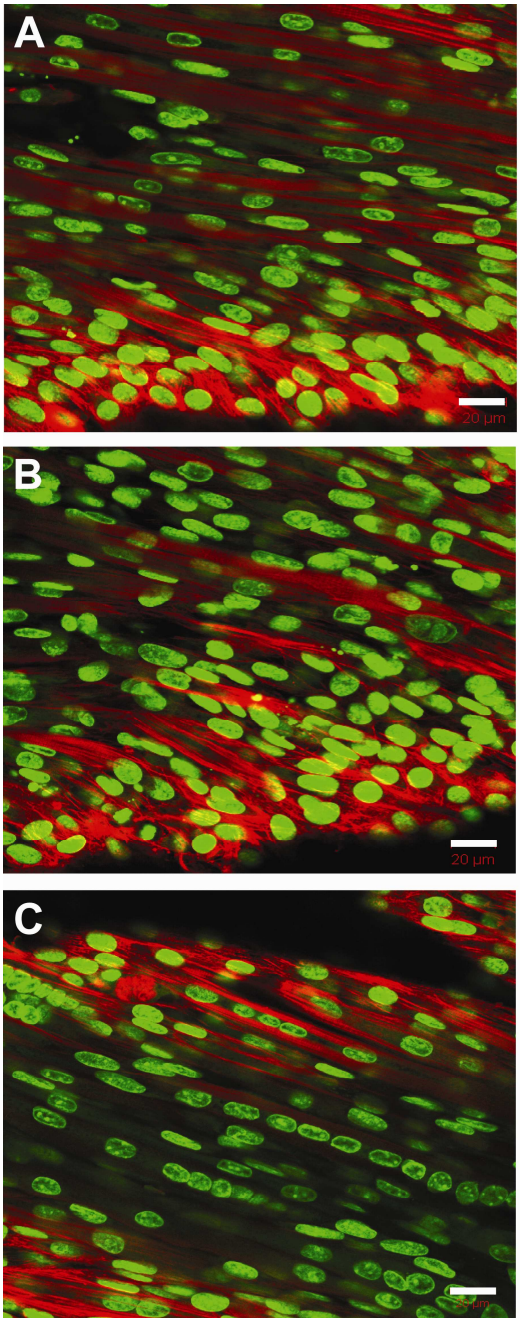

Figure 2.5 Rhodamine phalloidin stain for F-actin and Sytox green nuclei stain showing formation of myofibers. BAMs were cultured for 2 days in standard growth media, then (A) 2 days in DM with 2% horse serum, the 14 days in 8% horse serum, (B) 16 days in 10% horse serum DM, (C) 16 days in 20% horse serum DM, with this showing a particularly distinct example of fusion. Scale bars are 20µm.

Fluorescence staining for F-actin demonstrated that striations, which are strongly associated with mature sarcomeres, were visible as early as 6 days after shifting media and were prominent out to shift day 30 (Figure 2.6).

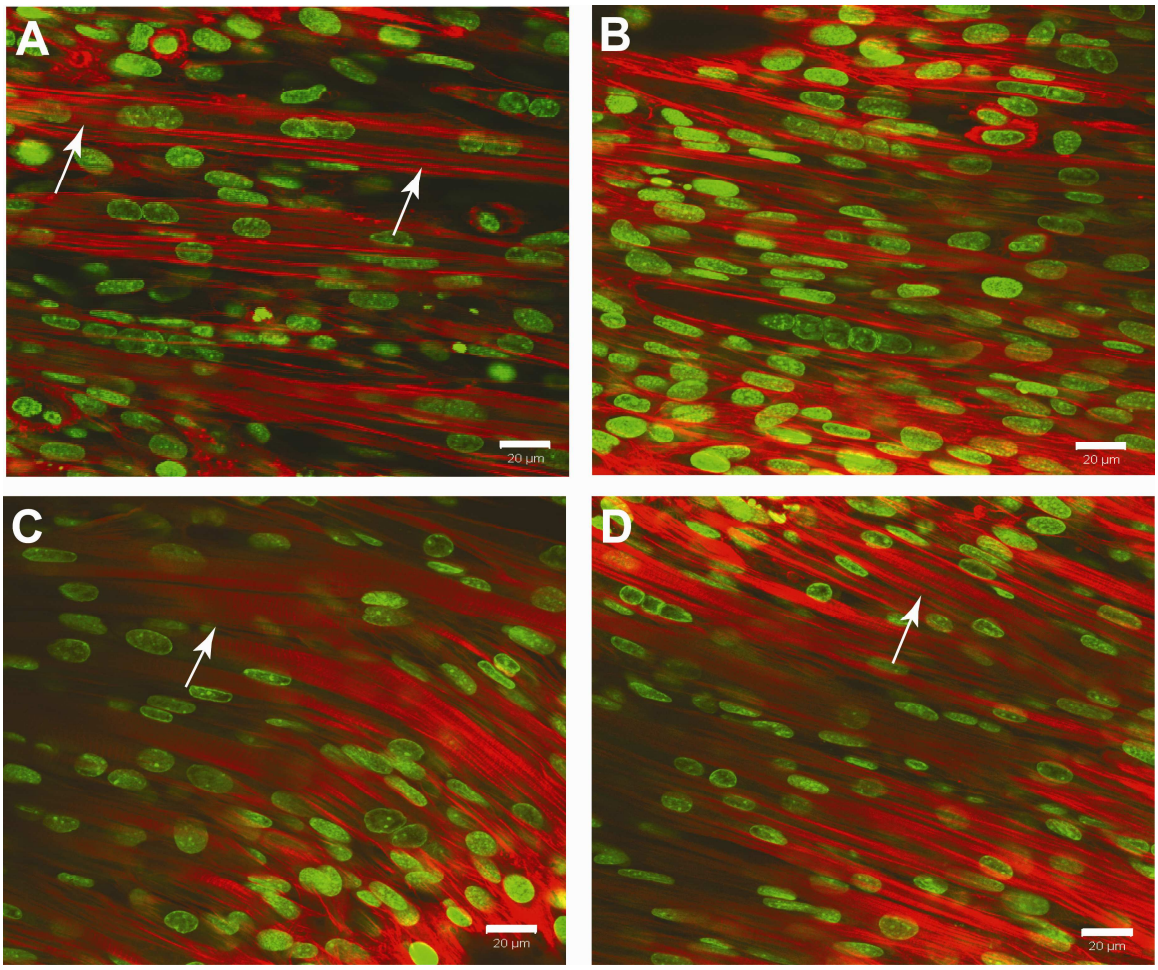

Figure 2.6 Rhodamine phalloidin stain for F-actin and Sytox green nuclei stain. BAMs cultured for 6 days in (A) 8% horse serum DM, (B) 20% horse serum DM (C) 16 days in 20% horse serum DM, and (D) 30 days in 8% horse serum DM. Scale bars are 20µm.

Immunostaining for alpha-actinin and myosin on BAMs cultured for 8 to 16 days in 8% HORSE SERUM DM confirmed these observations (Figure 2.7).

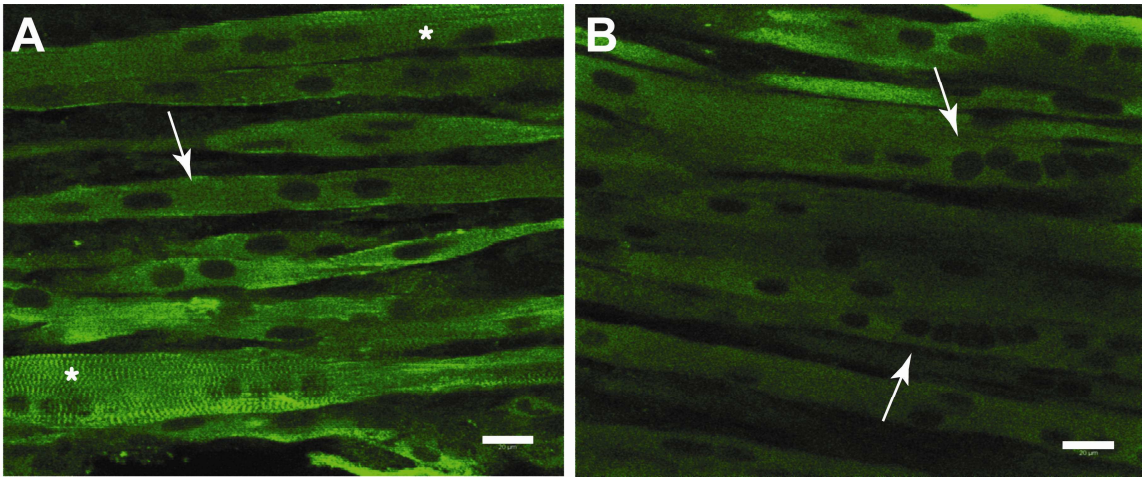

Figure 2.7 Immunostaning for (A) alpha-actinin on BAMs cultured for 6 days in 20% horse serum DM and (B) myosin on BAMs cultured for 8 days in 8% horse serum DM. Arrows show multinucleated fibers while the asterisks show striations in the myofibers. Scale bars are 20μm.

We used electron microscopy (EM) to evaluate the subcellular details of myocyte differentiation in the BAM constructs. For these experiments and comparison of serum conditions in particular, one BAM was shifted in 8% horse serum DM for 16 days, one in 20% horse serum DM for 16 days, and one shifted in 8% horse serum DM for 33 days. Myoblasts found at the core of the construct under all of these conditions were viable, although sparse. Cells at various stages of differentiation were evident in each BAM, regardless of time in culture. Generally, the BAMs consisted of a mixture of very mature sarcomeric myofibrils, myotubes with non-periodic stress fibers, and unfused myoblasts (Figure 8a).

Actin and myosin filaments and Z-bands were clearly visible in the sarcomeric areas, whereas non-periodic dense bodies were dispersed within areas populated with stress fibers. In the 16-day BAM, cultured in 20% horse serum, the vast majority of the nuclei were centrally located, signifying less mature differentiation, despite myoblast fusion detected via fluorescence staining. The few peripherally located nuclei may have been contributed by myoblasts that had just fused with an existing myotube. In contrast, the 16-day BAM cultured under 8% horse serum, presented some distinctly peripheral nuclei, in addition to well ordered sarcomeres. The formation of sarcoplasmic reticulum, and even some t-tubules were evident (Figure 8b), which suggests a greater degree of differentiation when using 8% horse serum levels in the differentiation media.

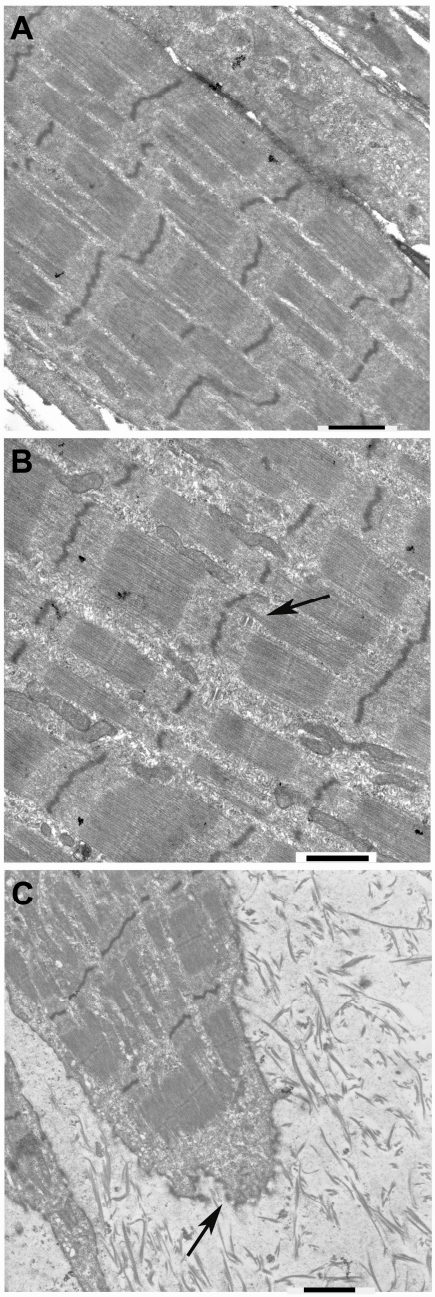

Figure 2.8 Electron micrograph of BAM cultured for (A) 16 days in 20% horse serum DM. Mature sarcomeres are evident, alongside fused myotubes with stress fibers. (B) BAMs at 16 days in 8% horse serum DM, t-tubules are shown (arrow), and (C) 33 days in 8% horse serum DM. Mature sarcomeres are evident near the suggested formation of a myotendinous junction (MTJ, arrow). Collagen I fibrils are dispersed at the end of the MTJ. Scale bars are 1μm.

The termini of BAMs cultured for 33 to 36 days in DM with 8% horse serum, exhibited features of what seemed to be a newly forming myotendinous junction (MTJ). Electron microscopy of one BAM (Figure 8c) showed numerous collagen fibers contacting the angled ends of multi-nucleated myotubes that suggested nascent MTJ formation, although the dense membrane coat characteristic of mature junctions was not observed. The terminal, invaginated ends of the myofibril were clearly visible, and collagen I fibers showed the 64nm periodic banding pattern characteristic of mature myofibrils. Presumably, the mammalian C2C12 myoblasts and/or multinucleated myotubes were synthesizing these collagen I fibrils at the site of the MTJ without the aid of fibroblasts. Immunostaining with paxillin, a focal adhesion protein enriched in the MTJ region [86, 156], showed some localization of the focal adhesion protein at fiber ends (Figure 2.9). This paxillin localization was visible in at least three separate constructs.

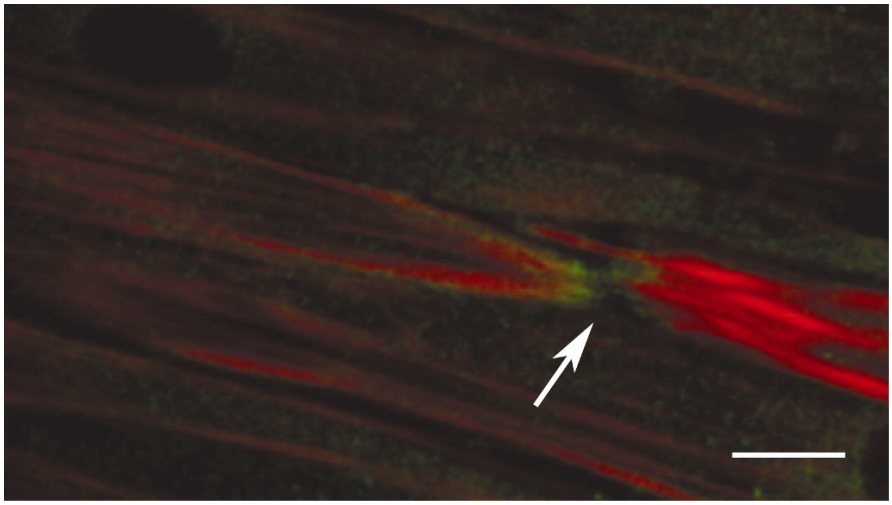

Figure 2.9 Rhodamine phalloidin stain for F-actin (red) and immunostaining for paxillin (green) on bioartificial muscle cultured for 33 days in 8% horse serum DM. Paxillin, a focal adhesion protein, is localized at the end of a myofiber, suggesting further organization and maturation of the myotube. Scale bar is 10μm.

2.4 Discussion

We chose to study the C2C12 murine system because it is a well established model for skeletal muscle differentiation [111]. Our constructs remained viable and functional for up to 36 days and had generated highly organized sarcomeric structures. Since the gestation period for a mouse is only 20 days, investigating cultures for up to 30 days is arguably enough time to examine muscle differentiation, as it normally would occur *in utero*.

In our study, fluorescence staining for F-actin and immunostaining for myosin and alpha-actinin verified a striated assembly of muscle components and continuous fibers as early as the sixth day under differentiation conditions. Others culture satellite cells of neonatal rat hind limb in an aligned collagen gel system to produce parallel, striated fibers visible with phalloidin staining [183]. Vandenburgh and colleagues created constructs from both primary avian skeletal myocytes [166] and more recently, human primary cultures in a collagen-Matrigel mixture (HBAMs) [124]. Differentiation for 8 to 16 days produce parallel "postmitotic myofibers," and immunostaining for localized sarcomeric tropomyosin verify the presence of muscle-specific proteins.

Despite these similarities to native muscle, many tissue-engineered constructs do not have morphology and ultrastructure that replicate mature muscle tissue. In numerous cases, the sarcomeric striations characteristic of mature muscle fibers are not clearly evident, implying that the culture conditions often do not support the

development of organized, mature muscle structures in artificial skeletal muscle organoids, or myooids [39]. Even with mechanical stimulation, myofiber diameter is still below the 10-100μm diameters found in adult skeletal muscle fibers, and only about 10% of the total area is occupied by myofibers [124]. A centrifugal cell packing method in collagen gel has been used to form a dense, hybrid muscle from a murine skeletal myoblast cell line (C2C12) [117]. Under these conditions, viable multinucleated myotubes are visible throughout the construct along with a few necrotic cells four days after the onset of differentiation [117].

Additional differences between engineered and native muscle were evident in myoblast distribution throughout the BAM constructs in our experiments. Histochemical and EM analysis revealed probable myoblast migration in most of the BAM cultures, possibly induced by poor diffusion of nutrients, mainly oxygen, through the collagen gel to the cells in the middle of the construct. Previous studies demonstrate the permeability limitations through collagen gels [128]. With thicknesses of the construct spanning 700-800μm, the myoblasts presumably maintained viability by moving to the outer shell of the BAM. This behavior was noticeable as early as shift day 6. Based on the assumption that oxygen diffusion was the limiting factor through a defined outer layer of metabolically active cells, approximations showed that the oxygen consumption rate here (approximately 10^{-8} mol/cm^3/s) is slightly lower than that found *in vivo* (10^{-7} mol/cm^3/s). Boundary conditions and calculations are shown in appendix A.

There were several observations that were unexpected and provide insight into the capacity of developing muscle to form and manipulate their environment *in vitro*. The beginning stage of what appears to be myotendinous junction (MTJ) formation with a pure myoblast population was a surprising finding. This may have been a response to the passive forces exerted in the gel during cellular differentiation and maturation, much like that which exists *in utero* between muscle and bone during fetal development. Previous data on muscle-like structures, including the MTJ, were reported in a quail myoblast and chick-leg fibroblast co-culture model [148]. EM examinations show evidence of well-differentiated fibers with discernable Z lines, organized sarcomeres, and basal lamina around the muscle fibers when collagen gel constructs of quail skeletal myoblasts and fibroblasts are allowed to differentiate for up to four weeks [148]. In addition to EM assessments, immunostaining for proteins specific to the MTJ, such as talin and paxillin, have been utilized [86, 156]. Particularly, a recent study demonstrated that co-cultures of rat tendon and muscle led to functional MTJ *in vitro*, and showed a localization of paxillin at the muscle-tendon interface [86]. While MTJ and other differentiated structures are established with avian myotubes and mixed mammalian systems, this demonstration of mature myofiber formation is significant with regards to three-dimensional (3D) cultures of a pure, mammalian myoblast cell line.

Interestingly, this pure population of cells has led to collagen I fibril and pre-mature MTJ formation *in vitro*. Although fibroblasts are known for synthesizing

collagen, previous studies on a murine skeletal muscle cell line (G8-1) demonstrate that extracellular matrix proteins, such as collagen (types I, III, and IV), laminin, and fibronectin, can be synthesized by a pure myoblast-myotube population [12, 129]. Since the C2C12 cells are a pure myoblast population, the collagen I fibrils confirm the ability of pure myogenic cells to synthesize collagen I fibrils.

The use of fibroblasts, especially in co-culture with myoblasts, is widely believed to provide an excellent substrate for myoblast differentiation because extracellular matrix proteins secreted by fibroblasts provide resident myoblasts with adhesion molecules and other important differentiation cues, such as substrate compliance [50]. Reports on the generation of artificial myooids include comparisons of constructs engineered with primary myoblast cell cultures versus those obtained from an established cell line. In one experiment, primary rat myooids from co-cultures [39] are compared with those created from a co-culture of myoblast (C2C12) and fibroblast ($10T_{1/2}$) cell lines [40]. C2C12 cells alone are not sufficient in making viable myooids under this system, and no evidence of mature sarcomeric structure formation was reported [40]. However, our results indicate that fibroblasts were not required for creating a mature sarcomeric structure, and C2C12 cells were capable of creating a fully functional artificial tissue.

While collagen gels have been the most popular extracellular matrix choice, fibrin gels and even decellularized tissues have been used by several groups [18, 63]. In

rat myoblasts, cultured with neuronal slices and suspended in a fibrin gel, multinucleated myofibers are identified by phase contrast microscopy, but myocyte cellular ultrastructure was not otherwise investigated [6]. Primary rat myoblasts, fibrinogen, and thrombin are also used to form a cell sheet that ultimately contracted around two silk sutures into a solid tissue structure [63]. Biochemical and force experiments confirmed active physiologic function, and immunostaining for myosin heavy chain and EM examination confirm the presence of arrays of contractile proteins in addition to some sarcomere-like structures. However, these structures are poorly organized and the Z-lines are not aligned [63]. On the contrary, in a model using decellularized mouse extensor muscle as a scaffold for C2C12 cells [18], transmission EM show hexagonal arrays of myosin and actin filaments, as well as the presence of multinucleated cells.

While mature fibers have been observed in 3D myooids in avian co-cultures or cultures in existing muscle scaffolds, the current demonstration of skeletal muscle maturation, particularly from a pure myoblast cell line, suggests that mature muscle can be produced in 3D mammalian cultures. In order to further develop these constructs for tissue engineering, we need to ensure that a majority of the myoblasts present differentiate into myotubes in addition to obtaining uniform cell distributions throughout the 3D cultures.

2.5 Conclusions

A C2C12 model system for skeletal muscle differentiation was investigated for three dimensional tissue engineering. Fluorescence and immunostaining demonstrated that very mature striated muscle fibers were formed from a stable mammalian cell line, as early as the sixth day in differentiation conditions (shift day). Viable and mature cultures were maintained for 6 up to 36 days post differentiation. EM provided conclusive evidence that mature sarcomeres had formed as early as shift day 16. By shift day 33, the beginning stages of myotendinous junction formation and newly synthesized collagen I fibers were also evident via EM and immunostaining evaluation. Although this level of differentiation has previously been shown in an avian model, the present study represents an important advancement in demonstrating mature muscle synthesis in a three dimensional mammalian myoblast cell line. This culture model produced a three-dimensional mature muscle that can be used to evaluate the effects of various mechanical and biochemical cues on muscle development and maturation, often active in clinical muscular and cardiac disorders.

2.6 Chapter Acknowledgements

The authors thank Milton Campbell for his assistance and Duke Medical Center Pathology for help with immunohistochemistry. The MF-20 mouse monoclonal antibody developed by Donald A. Fischman, M.D. was obtained from the

Developmental Studies Hybridoma Bank developed under the auspices of the NICHD and maintained by The University of Iowa, Department of Biological Sciences, Iowa City, IA 52242. We also acknowledge funding from the National Institutes of Health (NIH) grant R01-EB2408 and grant R037-AR14317 for MCR.

Chapter 3. Preliminary MicroRNA Microarray Analysis of the Effect of Stretch on Myoblasts Exposed to Cyclic Stretch

3.1 Introduction

As the presence of miRNAs came to light in the early 1990s [89], miRNA profiling has been at the forefront of new discovery methods. Tools such as the miRNA microarray, oligonucleotide chips, and multiplexed RT-PCR kits have cleared a way to globally scan for miRNAs in a given tissue or condition [11, 15, 85, 96]. Spatial and temporal regulation of miRNAs has been observed in specialized tissues, such as miR-124 in brain, miR-1 in muscle, and miR-233 in bone marrow [33, 95, 143]. Profiling of these small RNAs has also crossed over a wide range of species, which started with *C. elegans* and *Drosophila*, but also has focused on human, mouse, and rat genomes [83, 96, 152].

Additionally, global miRNA scanning has proved to be instrumental in comparing normal to diseased tissue. With miRNA involvement in key cellular processes, such as proliferation, differential miRNA profiles have been implicated in various types of cancer [24, 25]. Similar to aberrant miRNA regulation found in cancers, miRNA expression patterns were changed in primary muscular disorders compared to normal muscle tissue. In that study, 185 miRNAs were altered in 10 different muscular

dystrophies, demonstrating the need for miRNA profiling as a first step to pinpoint key miRNAs involved in critical cellular pathways [48]. As key targets of muscle-specific miRNAs, such as serum response factor, RhoA, and cdc42, have been linked to pathways modulated by mechanical stretch [27, 28, 34], we postulated that there were miRNAs affected by cyclic stretch.

The studies in this chapter present preliminary data that was used to canvas the effect of cyclic mechanical stretch on miRNA regulation in differentiating skeletal myoblasts. We utilized a mechanical stretch regimen, which consisted of a 'moderate strain' cyclic stretch at 0.5Hz, 10% strain for 1-hour with a 5-hour rest period, which has been shown to enhance differentiation [192]. The microarray studies were completed to identify miRNAs that were either up- or downregulated by a stretch regimen known to enhance myoblast differentiation. We also aimed to find novel, stretch-induced miRNAs through miRNA microarray analysis and verify its expression patterns during the differentiation process *in vitro* with quantitative RT-PCR (qRT-PCR).

3.2 Methods and Materials

3.2.1 Cell Culture

Murine C2C12 myoblasts (ATCC, Rockville, MD), a subclone derived from a cell line that originated from normal adult C3H mouse leg muscle [17], were grown on a 6-well tissue culture plate (Flexcell International, Hillsborough, NC) coated with 100μg/ml growth factor reduced Matrigel® (GFR Matrigel, BD Biosciences, Bedford, MA). The cells were fed daily with growth medium (GM) containing high glucose Dulbecco's modified Eagles' medium (DMEM; Gibco/Invitrogen, Carlsbad, CA), 8% new born calf serum (HyClone Laboratories, Logan, UT), 8% fetal bovine serum (HyClone), 0.5% chicken embryo extract (Accurate Chemicals, Westbury, NY), and 0.1% gentamicin (Gibco/Invitrogen) at 37 ºC and 5% CO_2 until the cells reached 85-90% confluency. To promote differentiation of myoblasts to fuse into myotubes, the growth medium was shifted to differentiation medium (DM), consisting of DMEM supplemented with 8% horse serum (HyClone) and 0.1% gentamicin (Gibco/Invitrogen).

3.2.2 Mechanical Stimulation

Mechanical stretch was applied using a FT-4000T Flexercell Unit (Flexcell International). After culturing the C2C12 myoblasts on silastic membrane 6-well plates (Flexcell International) and allowing them to reach 85-90% confluency, cyclic equibiaxial stretch was started, along with shifting media from the high fetal serum

GM to the low adult serum DM. A 'moderate strain' regimen that consisted of a cyclic stretch at 0.5Hz, 10% strain for 1-hour with a 5-hour rest period was used. Each regimen was sustained for 4 days, after which total RNA (including miRNAs) was used for subsequent microarray studies. Controls were maintained under static conditions in the same bioflex plates and DM for 4 days. Either the unstretched sample or a separate total RNA isolated from mouse embryo (10-12 days) was used as the common reference for these preliminary studies.

3.2.3 MicroRNA Microarray Analysis

Total RNA was isolated using the mirVana miRNA isolation kit (Ambion), which ensured that the short miRNAs were preserved. A concentrated sample of total RNA (10μg/μl) was processed by the Duke University Microarray Facility using the mirVana miRNA labeling kit and miRNA probe set (miRNA-AI, both Ambion and Invitrogen sets), which was used to end label and purify small RNA probes and markers. Briefly, the miRNAs were appended to have 3' amine-modified tails. One time point, shift day 4 was chosen as a critical time point (arguably at the myogenic switch point of our system).

Three separate microarray studies were completed. In the first microarray experiment, cells of passage six were cultured under static conditions and the extracted total RNA (including miRNAs) were labeled with a Cy3 dye. Total RNA

from the stretched cells were Cy5-labeled. In the second and third microarray experiments, the unstretched and stretched miRNA samples were Cy5-labeled while miRNAs from normal mouse embryo (10-12 days) tissue (Ambion First Choice Total RNA) were labeled with a Cy3 dye. The fluorescence intensities of these two dyes reflect the levels of a given miRNA, which is tracked by the hybridization location. The results from the first were presented as output ratios of Cy5:Cy3 fluorescence, signifying the stretched to unstretched miRNA ratios. In the second and third studies, the Cy5:Cy3 ratios were obtained separately for both the unstretched control and stretched RNA samples; then, these ratios were compared to each other. This method filters noise more efficiently, but manual filtering of all three microarray studies was sufficient to give reliable results. Each microarray chip consisted of over 662 probes, with a majority from human, mouse, and rat species (Ambion, Invitrogen). RNA purity analysis was completed using the NanoDrop ND-1000 spectrophotometer (NanoDrop, Wilmington, DE) and the Agilent Bioanalyzer (Agilent, San Jose, CA).

3.2.4 Quantitative RT-PCR (qRT-PCR)

Total RNA was isolated and purified using the mirVana miRNA Isolation Kit (Ambion). RNA concentration and RNA quality was measured and assessed using the NanoDrop ND-1000 spectrophotometer (NanoDrop, Wilmington, DE). cDNA was prepared using the microRNA reverse transcriptase kit (ABI, Applied Biosystems,

Foster City, CA) with a MyCycler (Bio-Rad) thermal cycler per manufacturer instructions. The TaqMan Universal PCR Master Mix (ABI) was combined with the cDNA samples and the resulting solutions were placed in the 7300HT Real-Time PCR Detection System (ABI) using standard kit protocols. The $2^{-\Delta\Delta C_T}$ method was used to analyze the real-time gene expression data [98]. The appropriate hairpin primers were included in the TaqMan miRNA RT-PCR assays that were purchased for each miRNA of interest (ABI). A small nucleolar RNA (RNU6B, ABI) was used as the endogenous control and RNA isolated from mouse embryo (10-12 days old) was used as a calibrator.

3.3 Results

3.3.1 Preliminary Microarray Results with Older Passage Cells

Although an extensive miRNA microarray study was not performed, there was evidence of miRNA modulation following the 'moderate strain' regimen in each of the three experiments performed. Figure 3.1 shows a scatter plot of various miRNAs that were present in differentiating myoblasts (passage 6) at shift day 4. The plot depicts the ratio of miRNA expression from stretched myoblasts over its unstretched control. These results include only points that were from mouse and human probes (as they are identical in most cases) and do suggest that the majority of the miRNA probes showed no difference with stretch (ratio close to 1). Distinctly high or low ratios were oftentimes found with a stretch response of the same miRNA originating from different chromosomal loci (e.g. miR-133a, miR-133b).

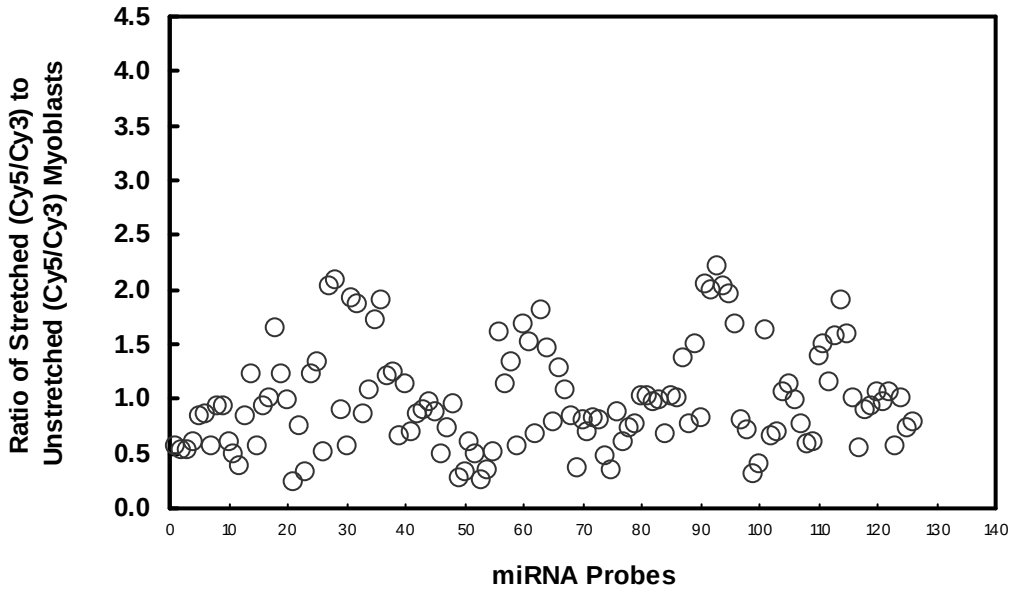

Figure 3.1 Scatter plot of stretch-induced miRNAs with older passage (6) myoblasts, presented as a ratio of Cy5 to Cy3 dye fluorescence. A ratio of 1 signifies the same levels of miRNA expression in stretched versus unstretched myoblasts.

Table 3.1 below shows the results of the first microarray study, listing those miRNAs that had at least a two-fold upregulation or downregulation in response to stretch. For this study, C2C12 cells at passage 6 were used. miR-133a and 133b as well as miR-125b were upregulated two-fold while both miR-214 and miR-140 were downregulated with stretch. Several other miRNAs were upregulated with stretch (less than a 2-fold difference); however, we chose to focus on the most prominent set for the first scan.

Table 3.1 Preliminary miRNA microarray data showing miRNA expression in differentiating (passage 6) myoblasts after 4 days of 10% cyclic stretch at 0.5Hz for 1 hour followed by 5 hour rest (relative to unstretched control), n=1.

miRNA	Fold-Difference
miR-133a	2.1
miR-125b	2.0
miR-133b	2.0
miR-214	0.5
miR-140	0.35

Based on this initial screen, temporal responses of the miRNAs listed in Table 3.1, in addition to several key miRNAs from published literature, were examined via qRT-PCR. Specifically, the expression of key, muscle specific miRNAs – miR-1, miR-133, and miR-206 – were quantified. Figure 3.2 shows the relative expression of miR-1, 133a, and 206 in passage 6 myoblasts subjected to a moderate strain regimen for 8 days, post differentiation. While there was a slight effect of stretch in miR-1 and miR-133a, a linear regression of the data showed no statistical difference between stretched and unstretched samples. There was no effect of stretch in miR-206 regulation. The data are shown as the mean ± SEM of 4 independent experiments.

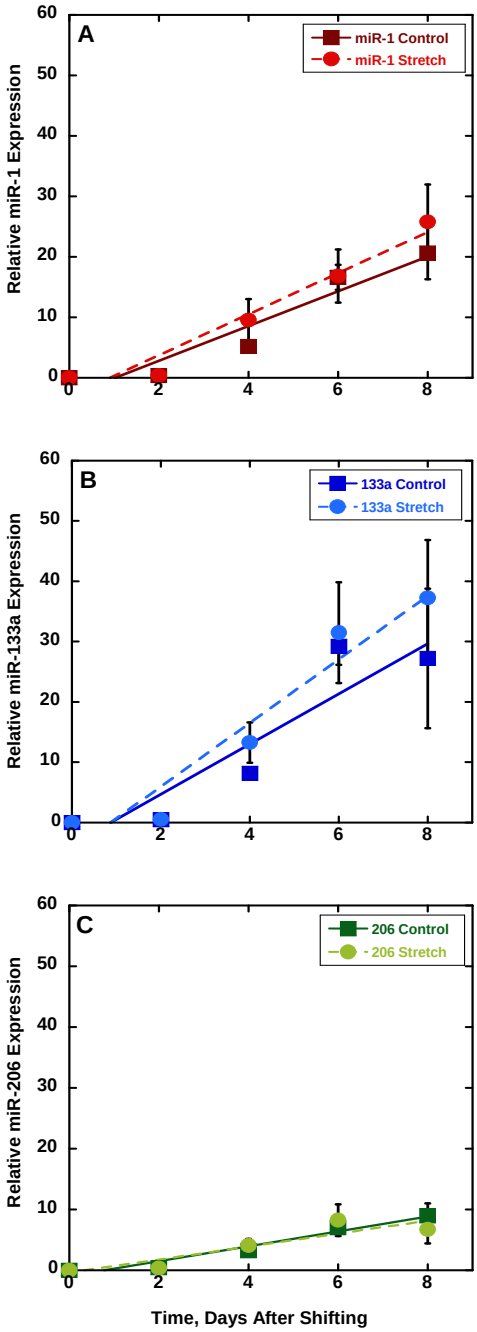

Figure 3.2 Relative expression of miR-1, 133a, and 206 in myoblasts subjected to a moderate strain regimen for 8 days, post differentiation. While there was a suggestive effect of stretch in miR-1 and miR-133a, a linear regression shows no statistical difference between stretched and unstretched samples. There was no effect of stretch in miR-206 regulation. Passage 6 myoblasts, mean ± SEM, n=4.

Based on the microarray data, miR-125b was also upregulated with stretch. We examined its expression over the course of 8 days, post-differentiation; however, we did not find significant correlation with stretch, as shown below in Figure 3.3. While miR-1, 133a, and 206 followed a linear trend over time, miR-125b seemed to increase until shift day 6 and then decrease, both in unstretched controls and stretched samples. Further, the level by which miR-125b increased after shifting is much less than observed with the miRNAs shown in Figure 3.2.

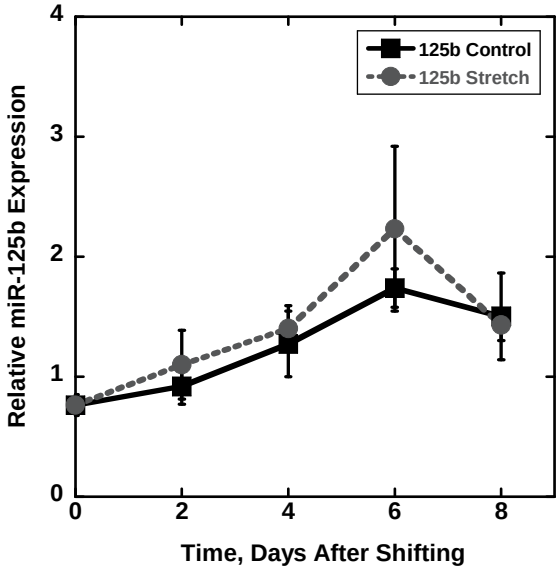

Figure 3.3 Relative expression of miR-125b in myoblasts subjected to a moderate strain regimen for 8 days, post differentiation. There was no significant effect of stretch on miR-125b. Passage 6 myoblasts, mean ± SEM, n=4.

In our initial scan, miR-214 and miR-140 were downregulated with stretch. Further examination with qRT-PCR found a decreasing trend with stretch, but none with significance (Figure 3.4).

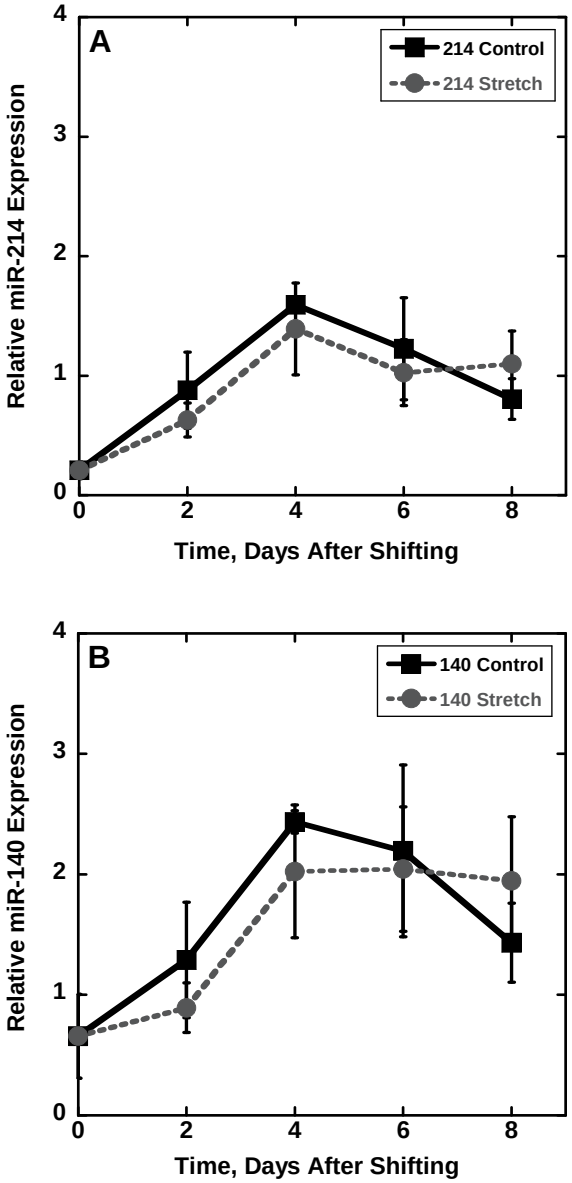

Figure 3.4 Relative expression of (A) miR-214 and (B) miR-140, which were assessed via qRT-PCR after initial results of the first miRNA microarray study. Based on the microarray study, both miR-214 and miR-140 were downregulated with stretch at shift day 4. Subsequent qRT-PCR studies showed a downregulation trend of the miRNAs with stretch, but deviations in response were substantial. Passage 6 myoblasts, mean ± SEM, n=4.

Table 3.2 compiles results from the first microarray study as well as data from subsequent qRT-PCR studies, all from the older (passage 6) myoblasts. While there was some consistency in the results from both analysis techniques, as in the upregulation at shift day 4 with miR-133a and ratio near 1 (within error) for miR-206, there were more inconsistencies in the results. Particularly, whereas miR-214 and miR-140 showed a down-regulation with stretch via microarray analysis, qRT-PCR showed a near opposite effect.

Table 3.2 Comparison of preliminary miRNA microarray and qRT-PCR data in older passage cells, showing miRNA expression in differentiating myoblasts after 4 days of 10% cyclic stretch at 0.5Hz for 1 hour followed by 5 hour rest (relative to unstretched control), passage 6 myoblasts, n=1 for microarray, mean ± SEM, n=4 for qRT-PCR data.

miRNA	Fold-Difference (Microarray)	Fold-Difference (qRT-PCR)
miR-133a	2.1	1.9 ± 0.7
miR-125b	2.0	1.2 ± 0.3
miR-133b	2.0	n/a
miR-214	0.5	1.2 ± 0.4
miR-140	0.35	1.4 ± 0.5
miR-1	n/a	2.1 ± 1.0
miR-206	1.1	1.4 ± 0.5

Although the initial microarray scan showed promise in finding miRNAs affected by cyclic stretch, subsequent miRNA-specific qRT-PCR experiments did not show significant differences. From this, we chose to replicate the miRNA microarray scan (in

duplicate) with a new lot of younger cells (passage 3). While the morphological integrity and growth capacity of the C2C12 cell line is quite robust even after 8 or more passages, gene regulation (and miRNA regulation) may be altered after so many population doublings.

3.3.2 Preliminary Microarray Results with Early Passage, Younger Cells

The two subsequent microarray studies, presented as a scatter plot in Figure 3.5 and summarized in Table 3.3, showed an approximate 1.5-fold difference in several miRNAs when myoblasts were stretched. There were slight differences in several of the ratios, but only elevated ratios of stretched to unstretched miRNAs found in *both* sets of microarray data were considered. In addition to notable increases in the levels of miR-206 and miR-133a above the control levels, new miRNAs – miR-422b, and miR-31 – were consistently higher in myoblasts that were mechanically stretched relative to those that remained unstretched. Only miR-133a upregulation with stretch overlapped with previous results. Whereas miR-214 was downregulated two-fold in the first microarray scan with the older cells, it was increased with moderate strain in the current set of microarray experiments. It is important to note that in these two microarray studies, a separate outside control (pure RNA isolated from mouse embryo, day 10-12 tissue) was utilized. This modification did not have an effect on the relative change in miRNAs levels compared to the unstretched controls.

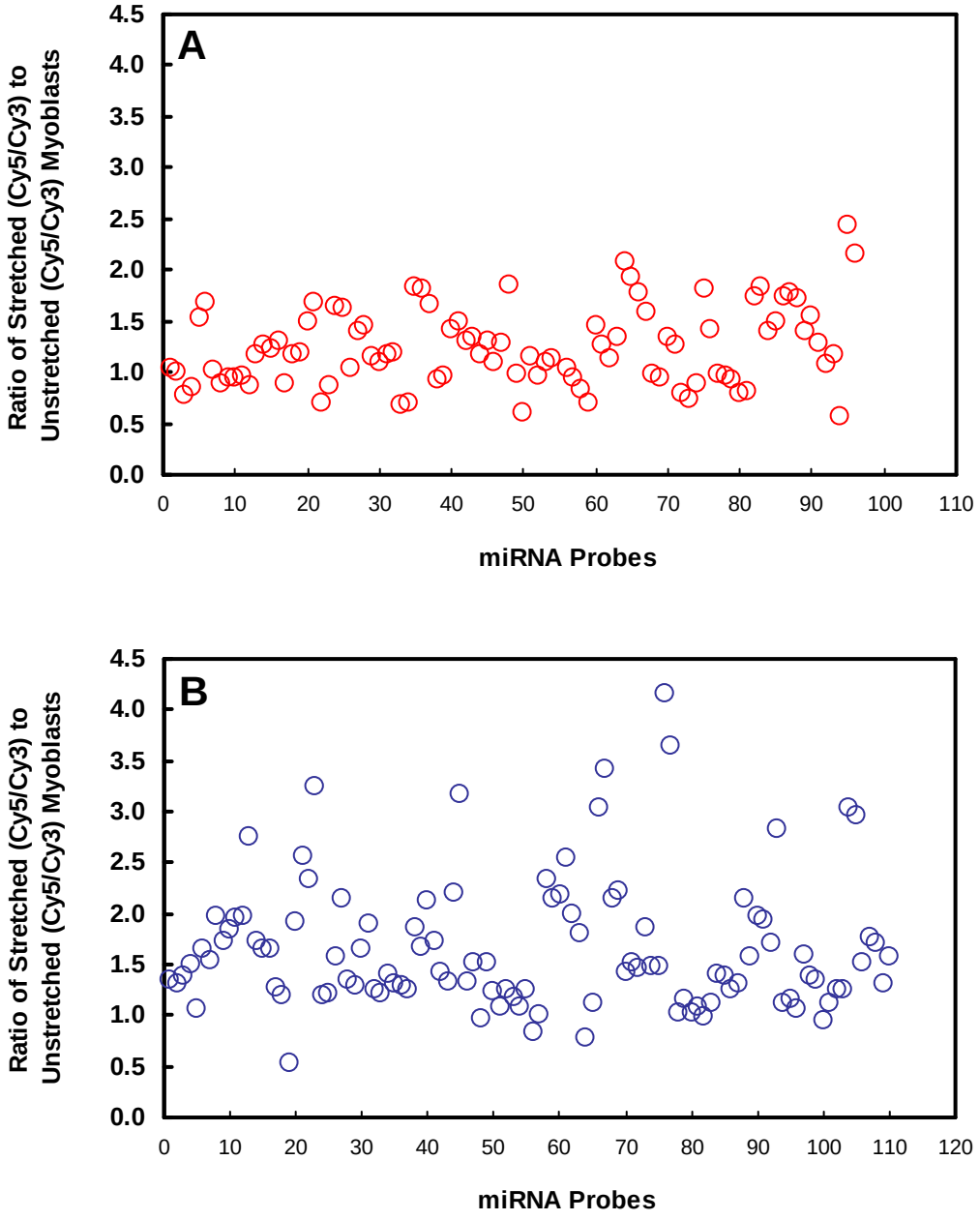

Figure 3.5 Scatter plot of miRNA microarray data with lower passage (3) myoblasts. The plots are presented as the ratio of miRNA expression in myoblasts stretched with moderate strain regimen over the unstretched control in (A) the second and (B) third microarray experiments.

Table 3.3 Preliminary miRNA microarray data showing miRNA expression in differentiating (passage 3) myoblasts after 4 days of 10% cyclic stretch at 0.5Hz for 1 hour followed by 5 hour rest (relative to unstretched control), n=2.

miRNA	Fold-Difference
miR-206	1.45-1.50
miR-133a	1.40-1.45
miR-422b	1.40-1.50
miR-31	1.40-1.60
miR-214	1.35-1.65
miR-23b	1.20

Similar to the qRT-PCR studies done following the first microarray study, we examined the temporal profile of three key, muscle-specific miRNAs – miR-1, 133a, and 206 – with stretch. The results of those studies are presented in detail in chapter 4; but in summary, a significant effect of cyclic stretch with a moderate strain regimen was observed in these three miRNAs using lower passage cells.

Table 3.4 presents the mean values of the coefficient of variation (CV) in both older, passage 6 and newer, passage 3 myoblasts. The variation was most apparent in the stretch samples and is included in the table for illustration. Although there is a smaller CV in the newer cells, a t-test, averaging CV over the three time points, showed that there was only a significant difference of cell passage in miR-206 expression with stretch ($p=0.001$). The difference of cell passage in miR-1 with stretch was modestly significant ($p=0.09$), and was not significant with miR-133a ($p=0.26$). On the contrary, the CVs for the unstretched controls were larger for the new cells, but there were no

significant differences between the CVs of the unstretched controls and stretched samples within a given group (old or new).

Table 3.4 Analysis of variance in older and newer passage cells (passage 6 vs. 3). The coefficients of variation (CV) for miR-1, miR-133a, and miR-206 in qRT-PCR data were averaged from shift day 2 to shift day 6 for unstretched and stretched myoblasts.

miRNA	Control Average CV (Old)	Stretch Average CV (Old)	Control Average CV (New)	Stretch Average CV (New)
miR-1	0.48	0.82	0.61	0.54
miR-133a	0.46	0.74	0.59	0.57
miR-206	0.34	0.67**	0.42	0.41**

**miR-206 expression with stretch in old versus new cells (p=0.001)

In addition to the three muscle-specific miRNAs, miR-422b and 31 were examined with qRT-PCR (Figure 3.6). miR-422b did not present a significant effect with stretch, but did show significant upregulation in levels over time. On the other hand, miR-31 did not have a much different temporal profile with upregulation after 2 days post-differentiation and a subsequent downregulation on days following. However, there was no effect of stretch on miR-31 levels.

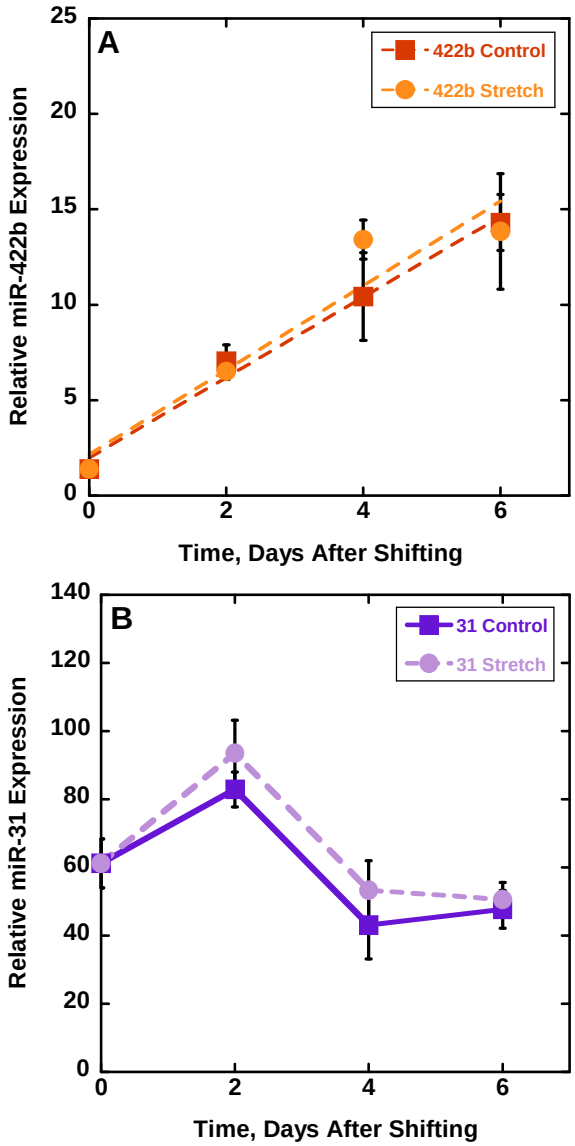

Figure 3.6 Relative expression of (A) miR-422b and (B) miR-31, which were assessed via qRT-PCR after results of the second set of miRNA microarray studies. Based on the microarray study, both miR-422b and miR-31 were upregulated with stretch at shift day 4. However, subsequent qRT-PCR studies showed no significant effect of stretch. Passage 3 myoblasts, mean ± SEM, n=5 (for miR-422b) and n=7 (for miR-31).

While miR-214 and miR-23b showed some promise, they were not included in the immediate round of qRT-PCR experiments because of a minimal difference between stretched and unstretched conditions at shift day 4.

Table 3.5 compiles results from the second and third microarray study as well as data from subsequent qRT-PCR studies, all from the younger (passage 3) myoblasts. Other than miR-1, which did not appear on any of the microarrays, all of the microarray and qRT-PCR data correlated fairly well in the second round (sets 2 and 3) of microarray experiments.

Table 3.5 Comparison of preliminary miRNA microarray and qRT-PCR data using passage 3 cells showing miRNA expression in differentiating myoblasts after 4 days of 10% cyclic stretch at 0.5Hz for 1 hour followed by 5 hour rest (relative to unstretched control), n=2 for microarray, mean ± SEM, n=5 – 8 for qRT-PCR data.

miRNA	Fold-Difference (Microarray)	Fold-Difference (qRT-PCR)
miR-206	1.45-1.50	2.0 ± 0.5
miR-133a	1.40-1.45	1.9 ± 0.3
miR-422b	1.40-1.50	1.9 ± 0.8
miR-31	1.40-1.60	1.7 ± 0.4
miR-214	1.35-1.65	n/a
miR-23b	1.20	n/a
miR-1	n/a	2.3 ± 0.8

While the preliminary round of microarray experiments showed some promise in finding novel stretch-sensitive miRNAs, we chose to first focus on the three muscle-specific miRNAs. The microarray experiments using separate Cy3-labeled controls led to more robust results due to separate chips used for canceling background or erroneous signals and is the preferred method of analysis.

3.4 Discussion

Taken together, these results show that miRNA profiles differed between older and younger passage cells. There was some decrease in the variation of the stretch response in miR-1 and miR-133a, but none that was attributable directly to cell passage number whereas there was significant decrease in variation in miR-206 expression in stretched, younger passage cells (Table 3.4). Hence, there was a particular interest in the response of miR-206 to cyclic stretch (Figure 3.2). While older cells did not produce a significant response of miR-206 expression with stretch, newer passage cells did show a significant response with a moderate strain regimen (full data presented in Chapter 4). Further, there was greater consistency between the qRT-PCR data and the microarray results with the younger, or lower passage, cells. Recent findings have connected miRNA regulation with skeletal muscle development, and in a study with dystrophin-deficient (*mdx*) mouse and dog models, miR-206 expression was found to be significantly increased in developing and newly formed myofibers, suggesting that upregulation of this miRNA is tied to muscle formation [189].

The change in the stretch response in miR-206, which is highly expressed only in skeletal muscle, is not a surprising finding as it has been well-documented that the integrity of various cellular functions is altered with age [8, 142]. Side-by-side studies show decreased MyoD expression with primary myoblasts from aged mice as well as late passage (>300 population doublings) C2C12 cells [62]. MyoD has also been shown

to directly activate miR-206 expression in this same skeletal muscle cell line via follistatin-like 1 (Fstl1) and utrophin (Utrn) genes [135]. This phenomenon perhaps gives insight into different miRNA profiles that occur between normal skeletal muscle and tissues afflicted with various muscular diseases and altered states associated with the effects of ageing.

Prior to differentiation, miR-1, miR-133a and miR-206 levels were very low in proliferating myoblasts. Levels of these miRNAs increased with onset of differentiation in both stretched and unstretched samples, as well as in older and early passage cells. Results were consistent with previous time course studies, and both miR-1 and miR-133a had parallel responses which were consistent with the similar regulation of these two miRNAs [34], [130], [57].

From the preliminary miRNA microarray data, different miRNAs also responded to stretch for older and early passage cells. Although the microarray studies were not extensive, the results implied that there are stretch-induced miRNAs that coincide with current trends in literature. For example, miR-125b is a miRNA that is associated with limb development in the mouse [141] that increased with myoblast differentiation in our system (Figure 3.3). Two miRNAs found to initially be downregulated with stretch, miR-140 and miR-214, exhibited a different trend than miR-1, 133a, or 206, with peak expression occurring at shift day 4 (Figure 3.4, Table 3.2). Previous work shows that miR-140 plays a key role in chondrocyte

differentiation by repressing histone deacetylase (HDAC) expression [155], also a target of miR-1 and miR-206, and at early times, may be working in conjunction with miR-1 to repress HDACs. Interestingly, inhibiting miR-214 decreased cell apoptosis in HeLa cells [36]. Where stretch generally decreased miR-214 expression, there was no significant difference in miR-214 levels between stretched and unstretched samples. These results suggest that mechanical stimulation may activate other regulatory mechanisms involving miRNAs in addition to the ones currently known.

The mismatch in results from the first microarray and following qRT-PCR studies (Table 3.2) may also shed light on the experimental setup and the need to use a separate endogenous control to correctly filter out background signals. Additionally, the use of older cells seems to have an effect as well. The CVs were averaged over three time points (shift day 2, 4, and 6) to find that the variation in the control samples were less than with the newer cells, which is most likely due to the timing of the myogenic switch, which may have been more unpredictable in the newer cells (or perhaps slower or more steady in the older cells). However, in the stretched samples, the variation was significantly higher in the older cells, specifically with miR-206. We predict that the stretch response is more variable in the older cells, which can shed more light on the mismatch of the microarray data and the results from qRT-PCR.

The second and third microarray sets did correlate quite well with the qRT-PCR data (Table 3.5). A recent study showed that miR-422b is expressed during C2C12

differentiation [177], by gradually increasing over 4 days, post-differentiation. Our results also confirmed the upregulation of miR-422b as myogenesis proceeded (Figure 3.6a). On the other hand, miR-31 has not been associated with skeletal muscle maturation to date. This particular miRNA has been identified in colorectal cancers [7, 88, 144] as well as primary myelofibrosis granulocytes [7, 59] and normal human fibroblasts [84]. In contrast to the linearly increasing trends observed with muscle-specific miRNAs, miR-31 levels were elevated at early time points and decreased after shift day 2 (Figure 3.6b); however, no time course studies have been done in muscle cells for comparison. Targets of miR-31 involve repressors of growth promoters and muscle specific proteins, suggesting that miR-31 may play a role in the early proliferative response but is downregulated as differentiation progresses. While miR-31 would be an interesting miRNA to explore, we did not find solid evidence that it is stretch-induced and chose not to focus on this miRNA for subsequent studies.

Surprisingly, miR-1 was not detected on any of the microarray studies, but was consistently and significantly upregulated by shift day 4 when quantified through qRT-PCR. Although the microarrays contained the most recently validated miRNAs with replicates, perhaps another probe set is needed to ensure all miRNAs are correctly identified. Additionally, one major assumption in all miRNA analyses is that miRNA enrichment in a given total RNA sample is the same for each sample. We assume that miRNAs comprise about 0.01% of the total isolated RNA across all experimental

samples, and although there is no direct evidence to conclude otherwise, it is still an assumption that must be addressed in the future [70]. Despite general trends that are fairly consistent with the current literature, we did not find significant evidence of novel, stretch-induced miRNAs at this time and therefore chose to focus on three, well-validated miRNAs – miR-1, miR-133, and miR-206 – which did show evidence of responding to cyclic stretch with a new lot of early passage, younger myoblasts.

3.5 Conclusions

Initial miRNA microarray studies presented possible candidates for stretch-induced miRNAs, such as miR-125b, 422b, and 31. However, after subsequent qRT-PCR studies, no significant effects of stretch were observed with these miRNAs. One round of experiments was done using an older lot of cells (passage 6), where expression of key muscle-specific miRNA, miR-206, was unchanged with stretch. Stretch did seem to elevate expression of miR-1 and miR-133 over time in the older, passage 6 cells, but a significant difference was not attained. In contrast, the use of a newer lot of cells (passage 3) produced less variability and significant upregulation of miR-1, miR-133a, and miR-206 with a moderate strain cyclic stretch, with a marked difference in miR-206. Although the initial aim of the study was to examine novel, stretch-sensitive miRNAs, we chose to focus on the three key muscle-specific miRNAs to show a link between stretch and miRNA regulation. These results are discussed in detail in chapter 4.

3.6 Chapter Acknowledgements

We would like to acknowledge the Duke Microarray Facility for miRNA microarray probing. We especially thank the team of Laura-Leigh Rowlette, Zhengzheng Wei, and Holly Dressman for their assistance. We are also grateful to Chris Miller from Applied Biosystems for his guidance with qRT-PCR and miRNA assay setup.

Chapter 4. Biomechanical Effects on MicroRNA Expression in Skeletal Muscle Differentiation

4.1 Introduction

In many cases, mechanical stretch of skeletal myoblasts results in increased protein synthesis and cellular hypertrophy [167, 168]. Like the *in vivo* response, cellular hypertrophy *in vitro* occurs when cells are stressed at low frequencies (<0.5Hz) and high intensities (>15% strain) while a high frequency (>1Hz) and low intensity (<5% strain) regimen causes an increase in metabolic activity, without major changes to muscle morphology [168]. However, the ranges for these parameters vary greatly with experimental design, and stimulation variables such as frequency, strain rate, and rest duration are critical in determining the downstream cellular response.

The normal range for muscle strain is quite narrow (10-20%), and strain beyond this point leads to muscle injury [23]. In our lab, studies examining ~10% strains at moderate frequencies (0.5 Hz) and longer rest periods have been shown to enhance myoblast differentiation [192]. In contrast, a 17%-strain applied over a 1-hour stretch cycle at 1 Hz followed by a 23 hour rest period inhibited myogenesis as the myoblasts were directed toward a more proliferative response through increased gene expression of various factors, including cyclin D1 [79]. While few major studies have demonstrated that pro-myogenic factor, myocyte enhancer factor 2 (Mef2), and its repressor, histone

deacetylase 4 (HDAC4), are affected by mechanical stimulation directly, key mechano-sensitive pathways, such as calcium/calmodulin [131] and MAPK signal transduction pathways [73], are associated with both proteins [107, 109, 193, 195].

Recently, microRNAs (or miRNAs), or short non-coding segments of RNA, ~20-22 nucleotides in length, have been shown to regulate expression of genes that influence proliferation or differentiation in skeletal muscle. These miRNAs act by targeting mRNAs which encode key proteins involved in these processes [34, 69, 130]. Several major studies that involved global scanning with microarrays pinpointed three miRNAs that are involved in myogenesis: miR-1, miR-133, and miR-206 [11, 81, 143, 176]. Subsequent studies have examined downstream targets and functional effects of these miRNAs. In particular, Chen *et al*. showed that miR-1 and miR-133 promote skeletal muscle differentiation and proliferation, respectively [34]. Specifically, miR-1 targets HDAC4, which is a transcriptional repressor of Mef2, and Mef2 is critical for myoblast differentiation [101]. Similarly, miR-133 down-regulates serum response factor (SRF), which blocks myoblast proliferation.

Although the miR-1 and miR-133 genes are transcribed together and controlled at transcription, they regulate protein expression of two different pathways that work in a complementary manner in the muscle maturation process. Both knockdown (via antisense oligonucleotide probes) and over-expression studies confirmed that miR-1

plays a critical role in myogenesis while miR-133 alone promoted proliferation and partially inhibited myoblast differentiation [34, 173].

The effect of mechanical stimulation on miRNA levels and function has not been extensively explored in mammalian cell and tissue development. One study showed that cyclic stretch (0.17Hz, 5% strain for 48 hours) upregulated miR-146a, which thereby affected levels of its target, Numb, and inhibited myogenesis [78]. Another study in *Arabidopsis* has identified miRNAs that might be regulated as a result of mechanical stress caused by xylem development [99]. Others have shown downregulation of miR-1 and 133 with muscle hypertrophy models [104]. While current research linking mechanical stimulation and miRNA regulation is limited, both are known effectors of various tissues, such as cardiac and skeletal muscle, and it is known that mechanical stimulation has a significant effect on cell growth, proliferation, and differentiation [168]. Additionally, validated targets for key muscle-specific miRNAs (both skeletal and cardiac), such as SRF, RhoA, and cdc42, are also crucial in signaling pathways associated with mechanical stimulation [27, 28, 34].

This study aimed to link mechanotransduction with miRNA regulation and function. By analyzing miRNA regulation with two different stretch regimens – moderate (10%) and high (17%) strains, we showed that key muscle-specific miRNAs were differentially regulated with stretch. Because miRNAs can modulate specific

functions of differentiated skeletal muscle they represent a promising target for manipulation and may be enhanced by mechanical stimulation.

4.2 Methods and Materials

4.2.1 Cell Culture

Murine C2C12 myoblasts (ATCC, Rockville, MD), a subclone derived from a cell line that originated from normal adult C3H mouse leg muscle [17], were grown on a 6-well tissue culture plate (Flexcell International, Hillsborough, NC) coated with 100μg/ml growth factor reduced Matrigel® (GFR Matrigel, BD Biosciences, Bedford, MA). The cells were fed daily with growth medium (GM) containing high glucose Dulbecco's modified Eagles' medium (DMEM; Gibco/Invitrogen, Carlsbad, CA), 8% new born calf serum (HyClone Laboratories, Logan, UT), 8% fetal bovine serum (HyClone), 0.5% chicken embryo extract (Accurate Chemicals, Westbury, NY), and 0.1% gentamicin (Gibco/Invitrogen) at 37 ºC and 5% CO_2 until the cells reached 85-90% confluency. To promote differentiation of myoblasts to fuse into myotubes, the growth medium was shifted to differentiation medium (DM), consisting of DMEM supplemented with 8% horse serum (HyClone) and 0.1% gentamicin (Gibco/Invitrogen).

4.2.2 Mechanical Stimulation

Mechanical stretch was applied using a FT-4000T Flexercell Unit (Flexcell International). After culturing the C2C12 myoblasts on silastic membrane 6-well plates (Flexcell International) for approximately 2 days and allowing them to reach 85-90% confluency, the GM was changed to DM and one of two mechanical regimens was started. The moderate strain regimen consisted of a cyclic stretch at 0.5Hz, 10% strain for 1-hour with a 5-hour rest period [192]. The high strain regimen consisted of a cyclic stretch at 1Hz, 17% strain for 1-hour with a 23-hour rest period [79]. Each regimen was sustained for up to 6 days.

4.2.3 Quantitative Real-Time RT-PCR

Total RNA was isolated and purified using the mirVana miRNA Isolation Kit (Ambion). RNA concentration and RNA quality were measured and assessed using the NanoDrop ND-1000 spectrophotometer (NanoDrop, Wilmington, DE). cDNA was prepared using the microRNA reverse transcriptase kit (ABI, Applied Biosystems, Foster City, CA) with a MyCycler (Bio-Rad) thermal cycler per manufacturer instructions. The TaqMan Universal PCR Master Mix (Applied Biosystems) was combined with the cDNA samples and the resulting solutions were placed in the 7300HT Real-Time PCR Detection System (ABI) using standard kit protocols. The

$2^{-\Delta\Delta C_T}$ method was used to analyze the real-time gene expression data [98]. The appropriate hairpin primers were included in the TaqMan miRNA RT-PCR assays that were purchased for each miRNA of interest. A small nucleolar RNA (RNU6B, ABI) was used as the endogenous control, and RNA isolated from mouse embryo (10-12 days old) was used as a calibrator. For the muscle-specific genes of interest, SYBR green chemistry was used and melt curve analyses were done for each reaction to ensure that the desired amplification was completed. Oligonucleotide primers were obtained from HS Kim (UNC) and IDT Technologies. Primer sequences are listed in Appendix B.

4.2.4 Immunostaining

Skeletal myoblast cultures were fixed with 3.7% formaldehyde for 15 minutes at room temperature and permeabilized in 0.5% Triton-X (Sigma) in PBS for 15 minutes. Cells were then incubated with 10% goat serum in PBS for 30 minutes at 37°C to block non-specific binding and immunostained in PBS for 1 hour with specific antibodies (alpha-actinin, Sigma, St. Louis, MO). The primary antibody was detected with a secondary mouse anti-IgG conjugated with Alexa Fluor 546-labeled secondary antibody (Invitrogen). Sytox Green (Invitrogen) was added after the secondary incubation as a counter stain for nuclei. Rhodamine phalloidin (Sigma, St. Louis, MO) was used to stain for F-actin in a dilution of 1:100.

4.2.5 Western Blot Analysis

Cultured C2C12 cells were lysed in a 1:10 solution of Cell-Lytic M and protease/phosphatase inhibitor (Sigma) for approximately 30 min on ice. Nuclear and insoluble debris are removed by centrifuging for 5 min at 10000 rpm. Protein concentrations were determined by the BCA assay (Pierce/Thermo Scientific, Rockford, IL) and at least 20μg of solubilized total protein were loaded in each lane of a 10% (w/v) Tris-HCl polyacrylamide gel (Bio-Rad, Hercules, CA). Transfer of the protein to a PVDF membrane (BioRad) was completed overnight, and the membrane was blocked with 5% nonfat dry milk in TBST (Tris - buffered saline with 0.1% Tween 20) for 1 hour at room temperature. The membranes were then incubated with the primary antibodies overnight at 4°C in a 1% nonfat dry milk-TBST solution. Primary antibodies were obtained from the following resources: GAPDH (Abcam, Cambridge, MA), PCNA, alpha-actinin, HDAC4 (Santa Cruz Biotechnology, SCBT, Santa Cruz, CA). After rinsing with TBST, the membranes were incubated with a horseradish peroxidase-conjugated IgG anti-mouse or anti-rabbit antibody (SCBT) for 1 hour at room temperature. Proteins were detected by ECL SuperSignal West (Pierce/Thermo Scientific) on blue X-ray films. Developed films were scanned and subjected to densitometry measurement using NIH Image J (Version 1.62) and expressed as intensity in arbitrary units. At least three independent experiments were used for each condition.

4.2.6 Over-expression and Inhibition of miRNAs

For the over-expression studies, Pre-miR precursor molecules specific for the mature miR-1 sequence (Ambion) were transfected with siPORT NeoFX transfection agent (Ambion) into myoblasts per manufacturer instructions. A Cy-3 labeled, non-targeting negative control (Pre-miR Negative Control #1, Ambion) was used to obtain transfection efficiencies. Briefly, the transfection agent was diluted in Opti-MEM I (Gibco) and mixed with 50nM of the Pre-miR-1 precursors or with the same concentration of the negative control. After incubating for 10 minutes at room temperature, the mixture was then dispensed into the appropriate wells. The cell suspension was added to the wells, and cultured in normal conditions for 24 hours, with antibiotic-free GM. The GM was then replaced with fresh DM, at which point cell viability and morphology were assessed, and if normal, the moderate strain regimen was started. Proper transfection was verified using qRT-PCR to verify that the miRNA was expressed in the mature form at higher levels. For inhibition of miR-1, the same transfection procedures outlined above were used with Anti-miR-1 oligonucleotides (Ambion) and the corresponding Anti-miR negative control (Ambion). Inhibition of miR-1 was assessed via Western blot analysis of its target, HDAC4.

4.2.7 Statistical Analysis

Data are presented as a mean ± standard error (SEM) unless otherwise noted. A two-factor ANOVA or student t-tests were performed using the Statview 5.0 statistical analysis package. When applicable, the Tukey-Kramer post-hoc test was performed as part of the ANOVA analysis. A value of $p<0.05$ was considered significant unless otherwise noted.

4.3 Results

4.3.1 Effect of Mechanical Stimulation on Myoblast Morphology

It has been well documented that spontaneous differentiation occurs in C2C12 myoblasts by switching high serum growth media to a low adult serum differentiation media [187]. In conjunction with the preliminary studies outlined in Chapter 3, various other frequencies and magnitudes of strains were examined with early passage cells to observe any downstream effects on microRNA expression. Results suggest that a stretch regimen consisting of a 5% strain (at 0.25Hz or 0.5Hz) does not have a noticeable effect on miRNA levels, particularly with miR-1, 133a, and 206. The ratios of miRNA expression of stretched versus unstretched samples with a regimen of 0.25Hz, 5% strain for 1 hour with 5 hours rest were 1.11 for miR-1, 1.05 for miR-133a, and 1.13 for miR-206. Similarly, the ratios of miRNA expression of stretched versus unstretched samples with a regimen of 0.5Hz, 5% strain for 1 hour with 5 hours rest were 1.08 for miR-1, 0.85 for miR-133a, and 0.95 for miR-206. Therefore, based on previous studies, we chose a cyclic strain regimen of 0.5Hz, 10% strain for 1 hour with a 5-hour rest period, which is shown to promote differentiation [192], for the remainder of the studies. Similarly, a 1.0Hz, 17% strain for 1 hour with a 23-hour rest period, which is shown to promote proliferation [79], was chosen to highlight differential responses of the myoblasts.

To evaluate the effect of stretch regimen on differentiation, we stretched differentiating C2C12 myoblasts using a 'moderate strain' regimen with parameters of 0.5Hz, 10% stretch for 1 hour followed by 5 hours rest in the presence of low serum media [192]. The 'high strain' regimen was based on conditions identified by Kumar *et al*. [79] and consisted of 17% strain at 1Hz applied for 1 hour with 23 hours of rest. Figure 4.1 shows global morphology with F-actin staining of unstretched and stretched myoblasts that were subjected to either a moderate strain (0.5Hz, 10% strain for 1 hour followed by 5 hours rest) or high strain (1Hz, 17% strain for 1 hour followed by 23 hours rest) regimen for 4 days post-differentiation (shift day 4). Multinucleated myotubes and striations were still apparent in the unstretched control, but were not as clearly organized as those in the stretched condition.

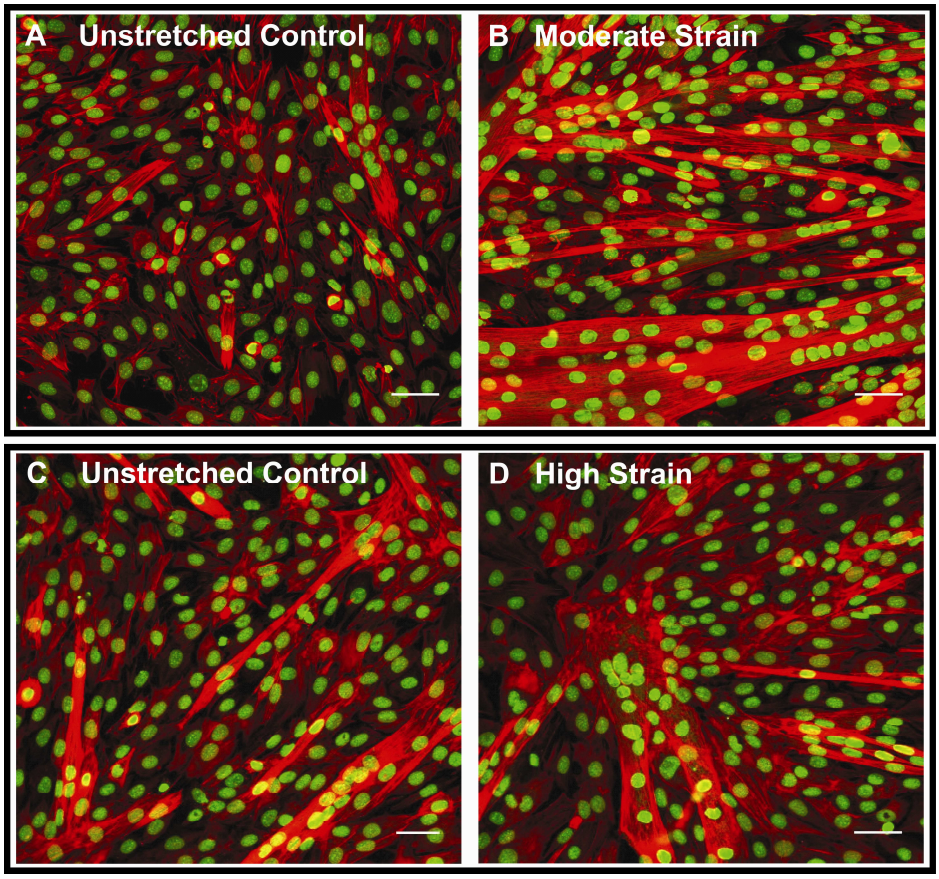

Figure 4.1 Rhodamine phalloidin stain for F-actin and Sytox green nuclear stain of differentiating myoblasts subjected to equibiaxial stretch (B) with a moderate strain regimen for 4 days, where fusion and multinucleation were more prominent in stretched samples versus (A) the unstretched control. Myoblasts subjected to a (D) high strain regimen for 4 days showed no major differences in fusion and multinucleation were observed in stretched samples compared to (C) the unstretched control. The images were captured at 20X, scale bar is 50μm.

Furthermore, immunostaining with alpha-actinin at various time points in the differentiation process showed that there was a differential response in myoblast morphology with the two stretch regimens. Figure 4.2 shows alpha-actinin immunostaining with a Sytox Green nuclei counterstain of differentiating myoblasts subjected to a moderate strain (10%) regimen from shift day 0 to shift day 6.

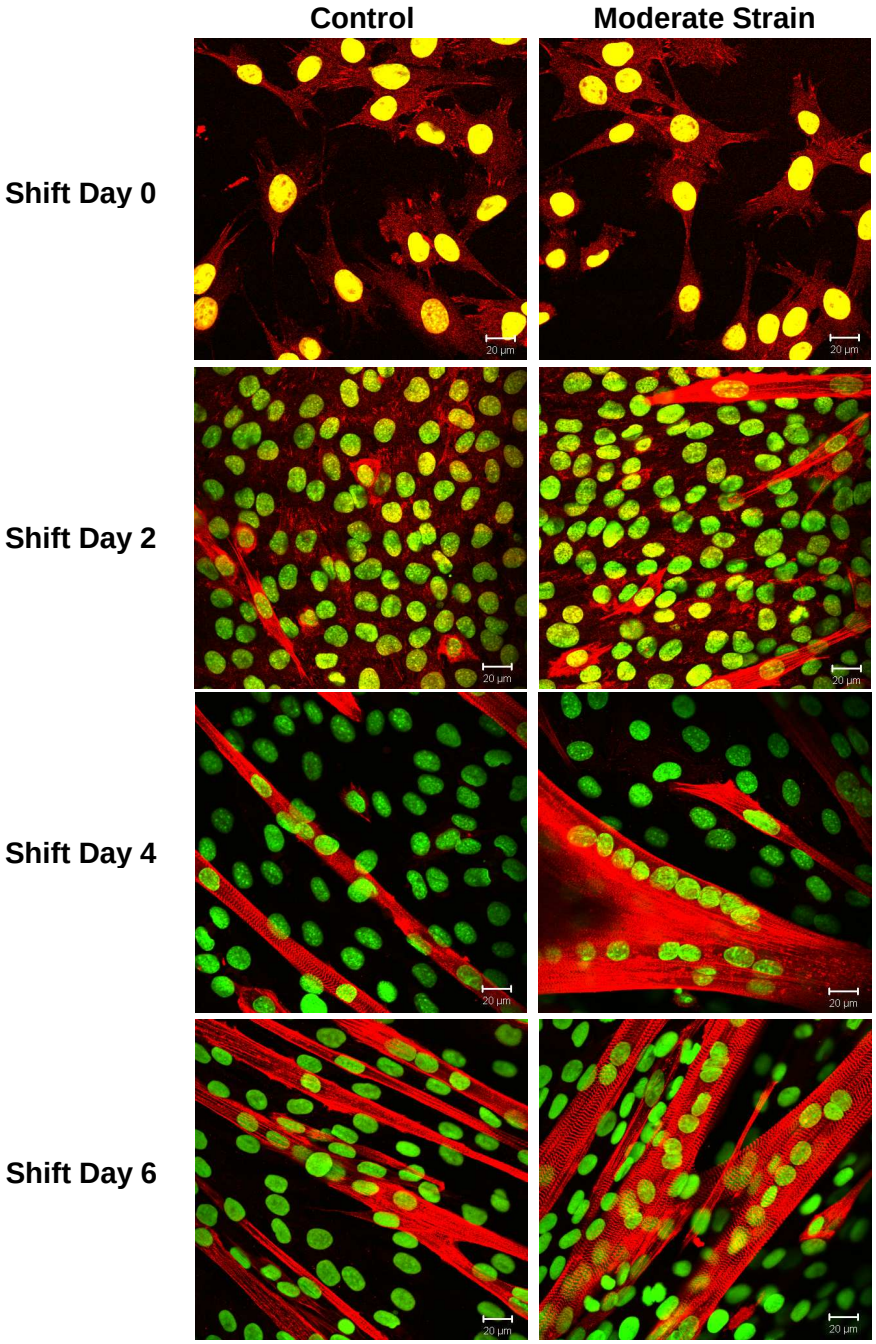

Figure 4.2 Alpha-actinin immunostaining with a Sytox Green nuclei counterstain of differentiating myoblasts subjected to a moderate strain (10%) regimen from shift day 0 to 6. By shift day 4, the effect of stretch becomes apparent with the appearance of more multinucleation and fiber formation. At shift day 6, striations are clearly visible in the stretched samples.

Between shift day 0 and shift day 2, the myoblasts have not all exited the cell cycle and continue to proliferate. The nuclei staining showed a notable increase in cell number by shift day 2, compared to shift day 0. By shift day 4, the effect of stretch became apparent with the appearance of more multinucleation and fiber formation. Myotubes often formed on top of a confluent layer of myoblasts, which explains the seemingly lower number of nuclei from shift day 2 to shift day 4 as it is attributed to the method of imaging. At shift day 6, striations were clearly visible in the stretched samples. On the other hand, Figure 4.3 shows alpha-actinin immunostaining of differentiating myoblasts subjected to a high strain (17%) regimen from shift day 0 to 6. There was less multinucleation and fiber formation in the myoblasts subjected to this regimen compared to its unstretched control.

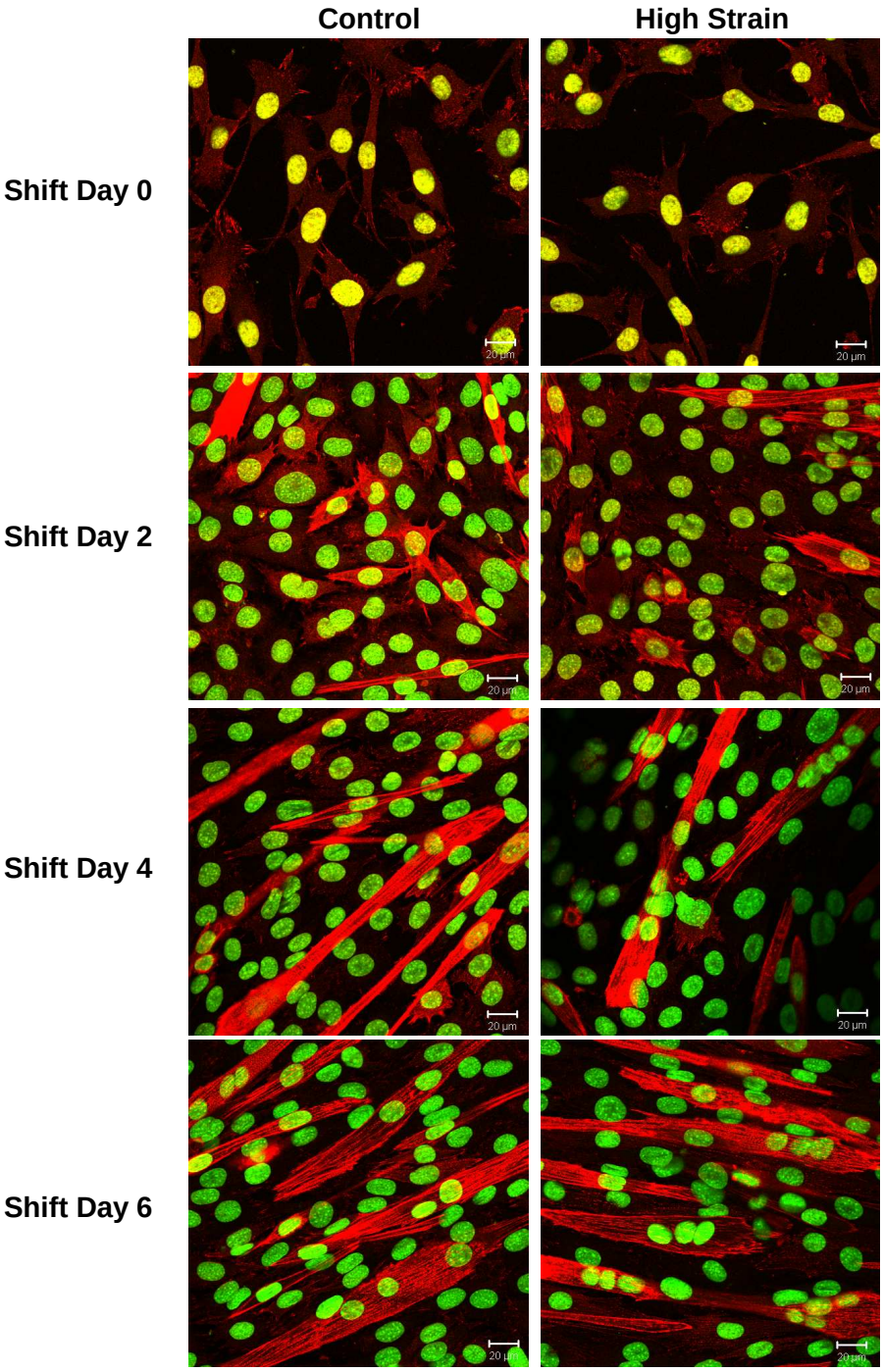

Figure 4.3 Alpha-actinin immunostaining with a Sytox Green nuclei counterstain of differentiating myoblasts subjected to a high strain (17%) regimen from shift day 0 to 6. There was less multinucleation and fiber formation in the myoblasts subjected to this regimen compared to its unstretched control.

A quantitative approach to determining myoblast differentiation was completed by assessing the myogenic fusion index as the percentage of nuclei in striated, or more organized, fibers. As listed in Table 4.1, a myogenic switch occurred approximately 4 days after shifting the media, at shift day 4, which corresponds with myoblast morphology (see Figure 4.2) confirming a marked increase in myotube formation at this time point.

Table 4.1 Myogenic fusion index, presented as the percentage of nuclei in striated myotubes

	Moderate Strain (n=7)		**High Strain (n=5)**	
	Control (%± SEM)	*Stretch (%± SEM)*	*Control (%± SEM)*	*Stretch (%± SEM)*
Shift Day 0	0.0±0.0		0.0±0.0	
Shift Day 2	0.5±0.3	0.9±0.5	0.7±0.2	1.3±0.4
Shift Day 4	30.8±1.6*	42.7±4.3*	28.7±4.5	31.2±4.6
Shift Day 6	47.9±3.0	52.1±3.8#	47.5±3.8	39.0±5.3#

*Indicates $p<0.05$, Control vs. Stretch
#Indicates $p<0.05$, Moderate Strain vs. High Strain

As shown in Figures 4.2 and 4.3, and quantified in Table 4.1, myoblasts continued to proliferate up until shift day 2 and did not show much fusion until after shift day 2. It is important to note that fusion increased with time, even without stretch, from the effect of the reducing growth factors in the media (shifting from GM to DM). An ANOVA for fusion index with each regimen showed a significant effect of time ($p<0.001$); however, only the moderate strain regimen produced a significant effect of

stretch ($p<0.02$). A significant difference in the myogenic fusion index was evident with the moderate strain regimen at shift day 4, but there was no difference by shift day 6. Conversely, there was no difference in fusion index between unstretched and stretched samples at any time point when subjected to a high strain regimen. There was a significant difference in fusion index of myoblasts subjected to the moderate strain regimen compared to the high strain regimen by shift day 6 where an ANOVA with all data combined from each regimen showed a significant effect of stretch (moderate or high strain) regimen ($p<0.02$).

4.3.2 Effect of Cyclic Stretch on MicroRNA Expression

The effect of cyclic stretch on three key, muscle-specific miRNAs (miR-1, miR-133a, miR-206) was assessed at various time points by quantitative RT-PCR (qRT-PCR). First, the baseline expression levels of miR-1, 133a, and 206 were assessed over time. Figure 4.4 shows a marked increase in all three miRNAs relative to shift day 0, demonstrating a significant temporal response as myoblasts differentiate *in vitro*. All three miRNAs were in low abundance (near zero levels compared to normal mouse embryo tissue) at shift day 0. Levels of miR-1 and miR-133 increased on a similar scale while miR-206 was regulated at significantly lower levels comparatively.

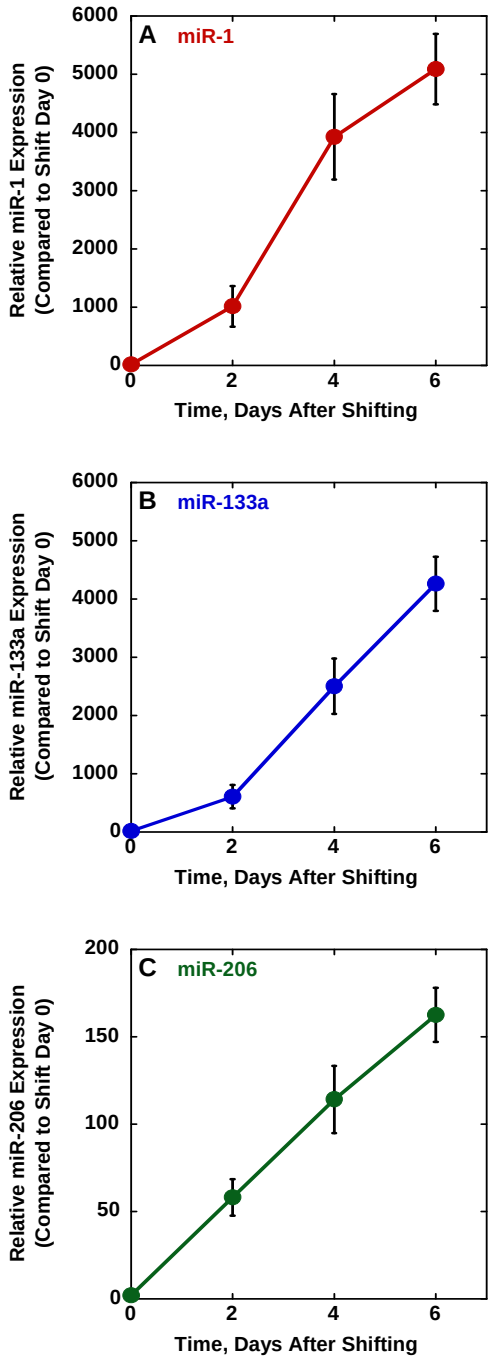

Figure 4.4 Temporal regulation of muscle specific miRNAs demonstrates a marked increase as muscle differentiation proceeds. Although on different scales for each of the miRNAs: (A) miR-1, (B) 133a, and (C) 206, all three exhibit this significant up-regulation with shifting media from GM to DM *in vitro*. Mean ± SEM, n=8.

To assess the effect of stretch, expression levels of miR-1, 133a, and 206 from both unstretched and stretched samples were fit to a linear regression over 6 days after shifting to a reduced growth factor serum media (Figure 4.5). Figure 4.5 shows two panels showing the effect of cyclic stretch, at both moderate and high strains, on miR-1, 133a, and 206 levels. The moderate strain (10%) regimen produced a significant increase in slope where miR-1 and 133a levels were up-regulated with stretch at an earlier time point than miR-206 (shift day 3 vs. shift day 4) (dashed vertical lines). There were no significant differences between stretched and unstretched cells with the high strain (17%) regimen.

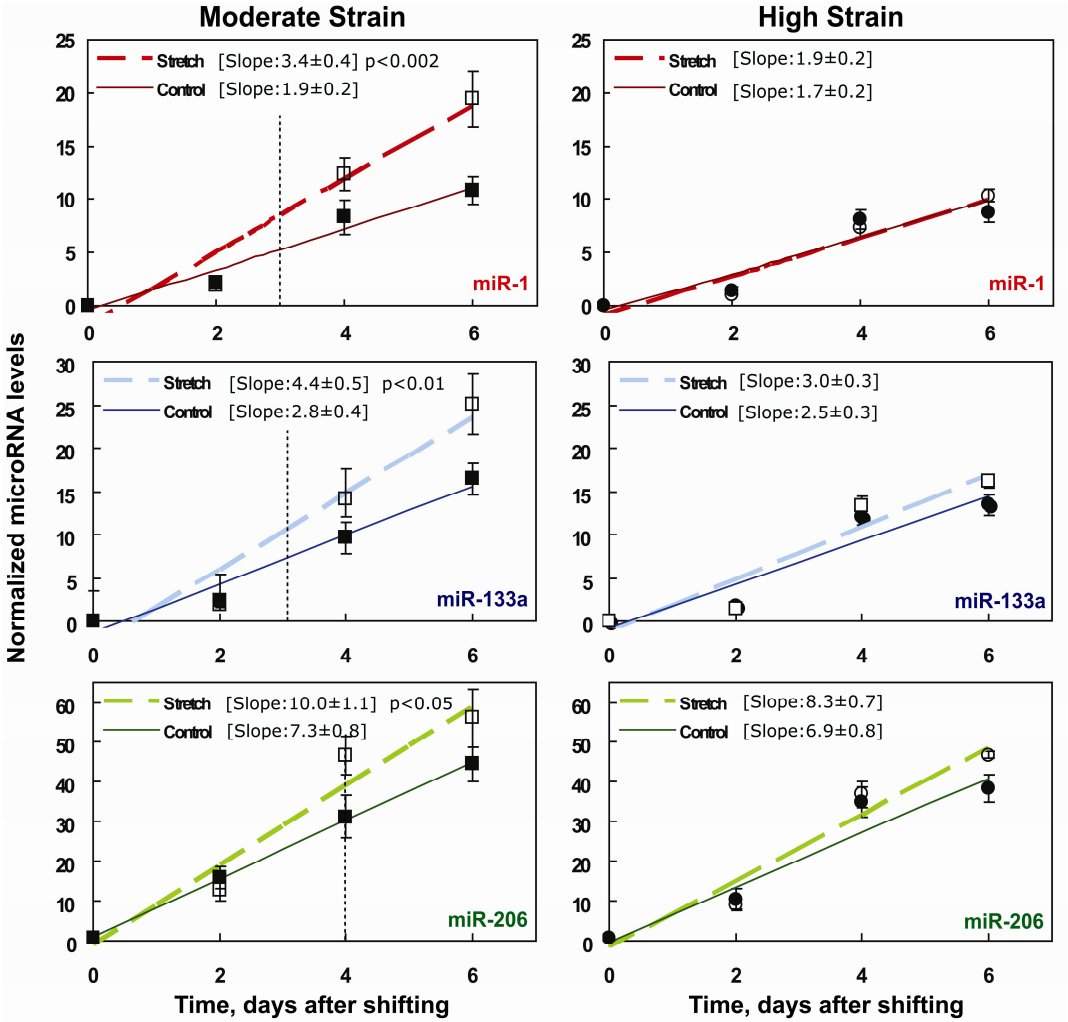

Figure 4.5 Effect of cyclic stretch on miRNA levels (miR-1, miR-133a, miR-206) at various time points measured by quantitative RT-PCR (qRT-PCR). Levels of miR-1, 133a, and 206 all increase linearly over 6 days after shifting to a reduced growth factor serum media. A moderate strain (10%) regimen produced a significant increase in slope and miR-1 and 133a levels were up-regulated with stretch at an earlier time point than miR-206 (SD3 vs. SD4) (dashed vertical lines). There were no significant differences between stretched and unstretched cells with the high strain (17%) regimen. Mean ± SEM, n = 8 for myoblasts exposed to moderate strains and n = 5 for high strain regimen.

Similarly, the ratio of miR-133 to miR-1 was also examined for each of the two regimens. Since miR-133 drives a proliferative response while miR-1 drives differentiation, the ratio of the two (miR-133 : miR-1) describes the interplay between the two miRNAs and the degree to which the proliferative effect may dominate myoblast differentiation. As presented in Figure 4.6a, the ratio of miR-133 to miR-1 for the myoblasts subjected to the moderate strain regimen remains fairly close to 1, with an increase by shift day 6 in the unstretched controls. While the decrease of the miR-133 : miR-1 ratios in the stretched samples at shift day 6 align with the more differentiated response, there was no statistically significant difference. In contrast, the ratio of miR-133 to miR-1 in myoblasts subjected to the high strain regimen peaked in the stretched cells at shift day 4 (Figure 4.6b). Both the unstretched control and the stretched samples were elevated at this time point, but the response is different compared to the myoblasts stretched with a moderate strain regimen. While the trend shows that a more proliferative response is observed in myoblasts stretched at high strains at shift day 4, a statistically significant difference was not observed. When the ratios were compared to 1, which signifies equal levels of miR-1 and miR-133 expression, there was statistical significance. For the moderate strain regimen, the ratios were significantly above 1 at shift day 6 while for the high strain regimen, the

miR-133 : miR-1 ratios were above 1 at shift day 4 and 6, regardless of stretch in both cases. It was also interesting to note that this ratio was continually above 1, even at later time points when one would expect the ratio to drop below 1.

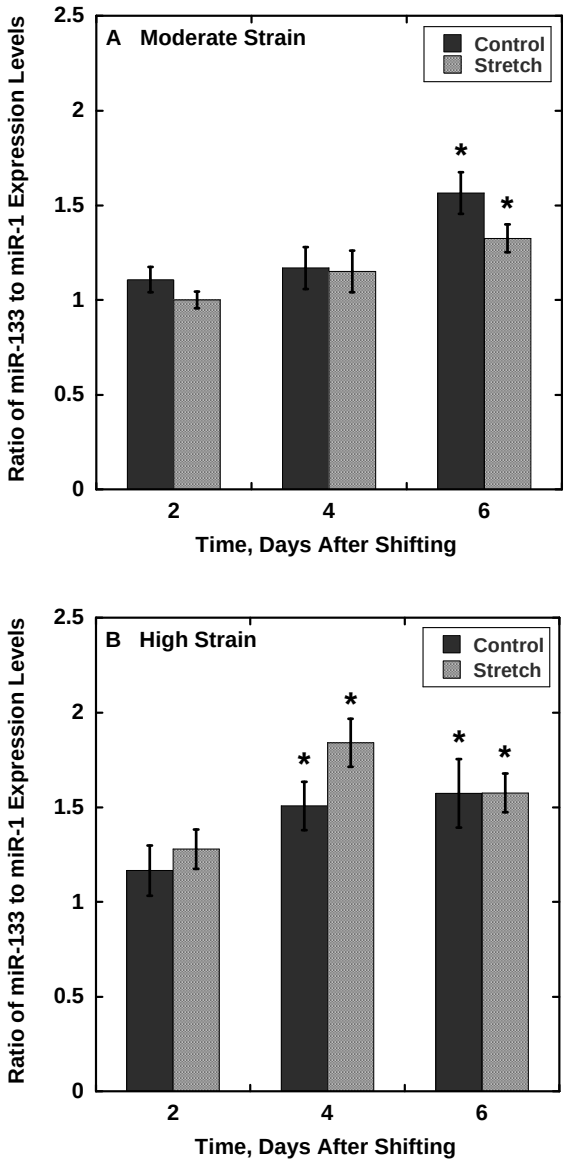

Figure 4.6 Ratio of miR-133 to miR-1 expression levels, presented in myoblasts subjected to the (A) moderate strain regimen and a (B) high strain regimen. A ratio greater than 1 suggests a more proliferative response, and is observed with myoblasts stretched with the high strain regimen versus the unstretched control at shift day 4. Similarly, a decrease in this ratio is observed with myoblasts stretched with the moderate strain regimen at shift day 6; however, the trends were not statistically significant. Mean ± SEM, n = 8 for myoblasts exposed to moderate strains and n = 5 for high strain regimen, *p<0.05, ratio compared to 1.

Because miRNAs are known to target specific mRNA targets, we also examined baseline changes in several muscle-specific genes, which included key regulators such as MyoD, myogenin, and Mef2c. The gene expression of validated targets of miR-1 (HDAC4) and miR-133 (SRF) was also examined to assess whether the changes in miRNA levels induced by stretch were linked to changes in the levels of these genes. Samples were pooled for comparison. Interestingly, neither the moderate nor high strain regimens significantly affected MyoD (Figure 4.7a) as a global ANOVA showed no effect of time or stretch regimen. Meanwhile, there was both a significant effect of time ($p<0.0002$) and regimen ($p<0.02$) on myogenin gene expression. A Tukey-Kramer post hoc test found significance between the two regimens (moderate and high strains), but at a given time point, no significance was established (Figures 4.7b). Similarly, there was also an effect of time ($p<0.0001$) and regimen ($p<0.02$) on HDAC4 gene expression, but the Tukey-Kramer post hoc test did not find significance ($p<0.05$) between control and high strain regimen samples at any given time point (Figure 4.7c). SRF gene expression was unchanged with time or regimen (Figure 4.7d).

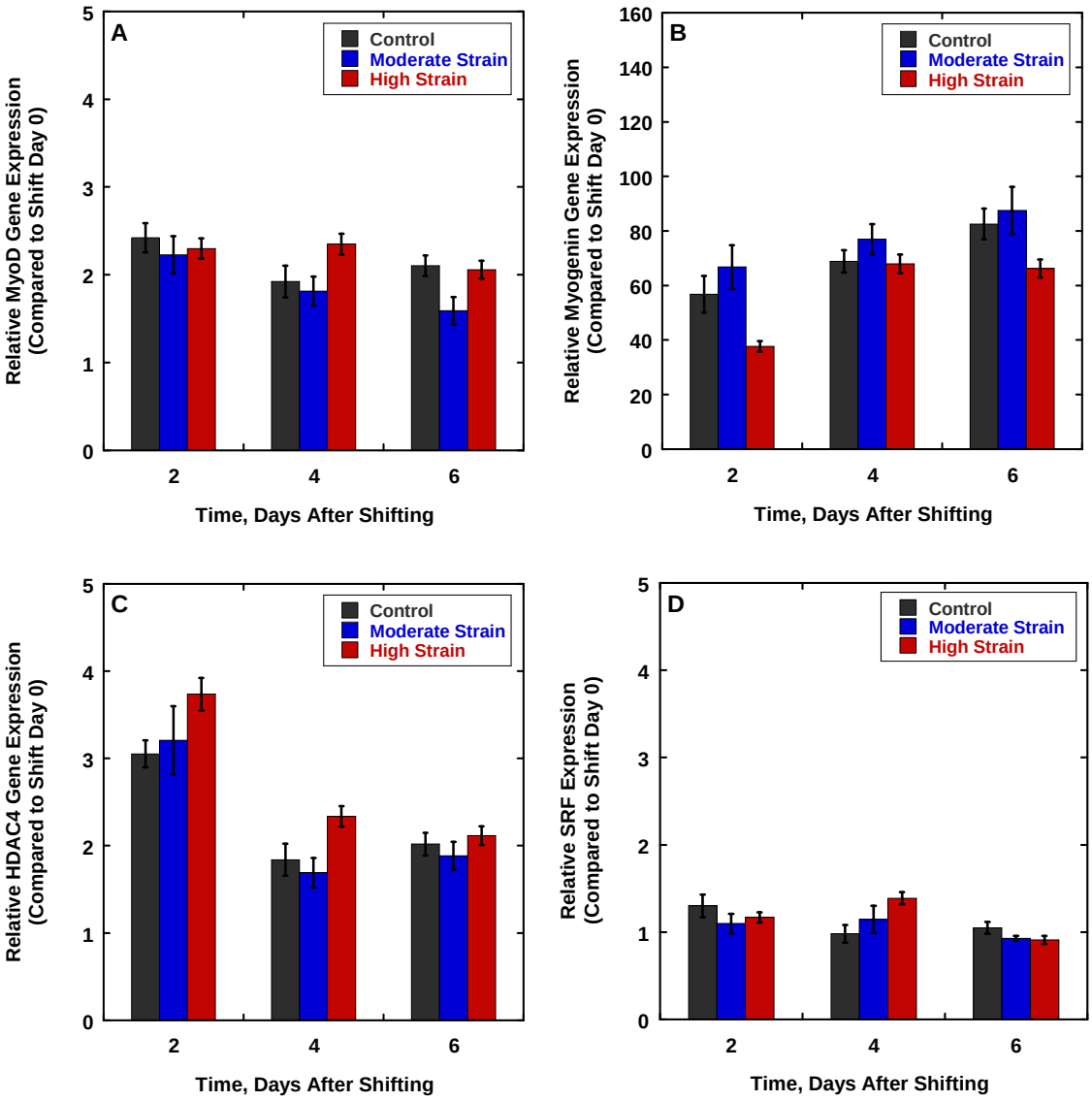

Figure 4.7 Gene expression analysis in myoblasts subjected to moderate and high strain regimens via quantitative RT-PCR for (A) MyoD, (B) Myogenin, (C) HDAC4, and (D) SRF. There was no major effect of time or stretch regimen on MyoD, Myogenin, HDAC4, or SRF. Data are presented as mean ± SEM, and control samples were pooled for n=12–13, n=6–7 for the moderate strain regimen, and n=4–5 for the high strain regimen.

Contrastingly, we found that levels of Mef2c mRNA were greater in myoblasts subjected to the moderate strain regimens by shift day 6 (Figure 4.8). Mef2c levels were unchanged in myoblasts stretched at high strains. Data were pooled for the unstretched controls, and a two-factor ANOVA verified a significant effect of time ($p<0.001$) and regimen (control vs. moderate vs. high strain) ($p<0.01$). A Tukey-Kramer post hoc test showed significance between Mef2c expression in unstretched controls and the moderate strain samples as well as between the moderate and high strain samples. There was no significance between the unstretched controls and the high strain samples over the entire temporal profile. Figure 4.8 shows this relationship as Mef2c expression is upregulated by shift day 4 and 6 in myoblasts subjected to the moderate strain regimen while there is only a significant difference with the high strain regimen at shift day 6, where it is significantly downregulated compared to the unstretched control and the moderate strain samples.

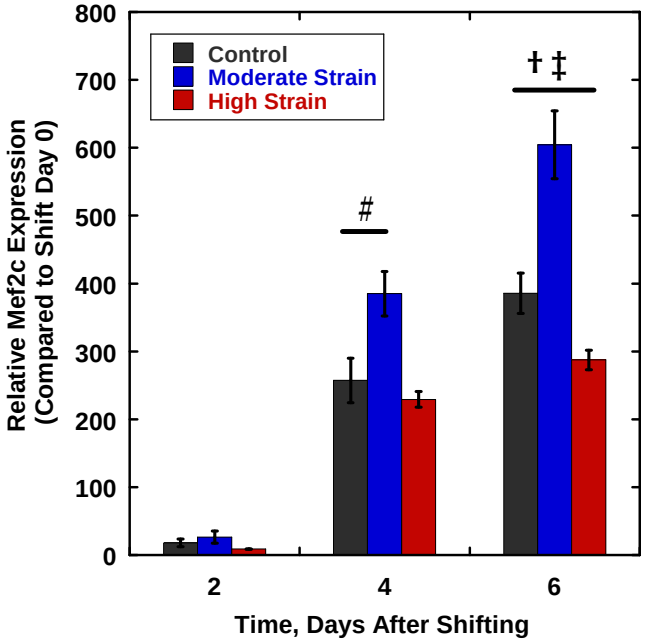

Figure 4.8 Gene expression analysis via quantitative RT-PCR for Mef2c. The effect of stretch is noted in the upregulation of Mef2c expression by shift day 6. Data are presented as mean ± SEM, and control samples were pooled for n=12, n=7 for the moderate strain regimen, and n=5 for the high strain regimen, #p<0.01 (control vs. moderate strain at shift day 4), †p<0.01 (control vs. moderate strain at shift day 6), ‡p<0.001 (moderate strain vs. high strain at shift day 6).

These gene expression results suggest that observed changes in the three muscle-specific miRNAs were not large enough to affect several critical mRNA levels. However, since miRNAs are translational regulators, we chose to examine the protein levels of miRNA targets. In this study, we focused on HDAC4, which is a downstream target of miR-1 to further elucidate the mechanism by which stretch may affect miRNA expression. Western blot analysis indicated a decreasing trend in HDAC4 protein expression in myoblasts exposed to a moderate strain cyclic stretch regimen (Figure 4.9).

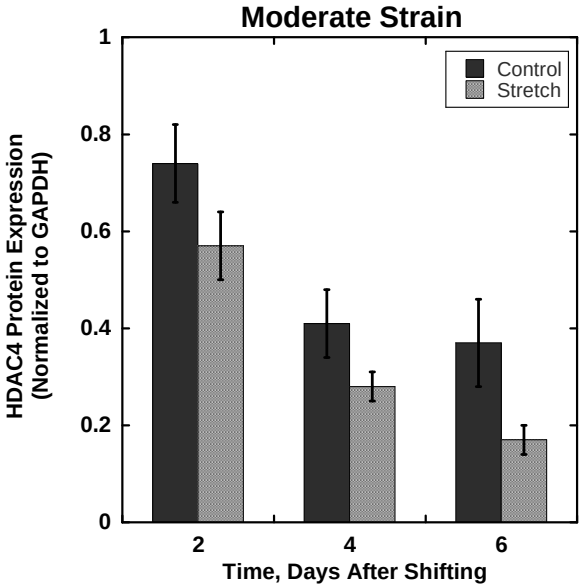

Figure 4.9 Western blot analysis for HDAC4 showing a decreasing trend in HDAC4 protein expression in myoblasts exposed to a moderate strain regimen. Although there were no major differences with stretch on the transcriptional level, this change on the translational level suggests that as miR-1 levels are upregulated by stretch post-SD4, and the downstream effect of suppressing HDAC4 protein levels is apparent at later time points. Mean ± SEM, n=6 or 7.

A two-factor ANOVA found significant effects of time ($p<0.0005$) and stretch ($p<0.02$), but no interaction between the two. There was no effect of stretch on HDAC4 protein levels with the high strain regimen. Although there were no major differences in HDAC4 levels with stretch (moderate or high strain) on the transcriptional level, this change on the translational level with the moderate strain regimen suggested that as miR-1 levels are upregulated by stretch four days after shifting to DM, the downstream effect of suppressing HDAC4 protein levels was apparent or more pronounced at later time points.

4.3.3 Effect of Cyclic Stretch on miRNA Levels with Over-expression and Inhibition of miR-1

The effect of stretch was also examined in conjunction with the over-expression of one of the myogenic miRNAs, miR-1, which is known to promote myoblast differentiation. Results shown in Figure 4.10 indicated that miR-1 levels were indeed over-expressed via transient transfection with Pre-miR-1 precursor molecules (Ambion), As assessed by qRT-PCR, there was an increase in miR-1 levels nearly five orders of magnitude one day after transfection, or at shift day 0, but these levels were drastically reduced by shift day 2. Levels of miR-1 were nearly equal to those of the negative control by shift day 4.

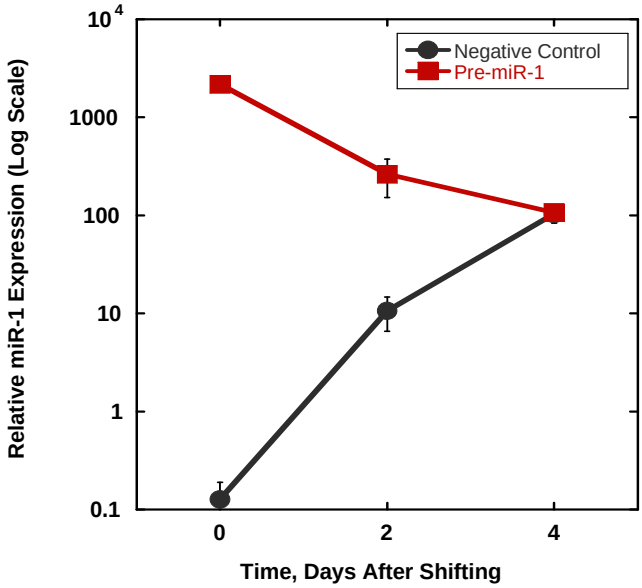

Figure 4.10 Average temporal effect of miR-1 over-expression demonstrating a marked increase in mature miR-1 expression in the transiently transfected myoblasts over the negative controls. Over-expression of miR-1 had no effect on baseline levels of miR-133a and miR-206. Mean ± SEM, n=4.

In order to assess whether the effects of stretching myoblasts are further enhanced by miRNA over-expression, we examined changes in miRNA levels with miR-1 over-expression combined with stretch (Figure 4.11). At shift day 2, qRT-PCR showed that there was a small, but significant down-regulation of miR-1 levels when stretch was combined with miR-1 over-expression, suggesting that a regulatory mechanism is in place to compensate for gross deviations in baseline levels of miRNAs. The overall effect of stretch was also diminished with the use of a transfection agent as the myoblasts without any transfection agent showed a greater stretch-induced effect

(similar to the response seen in Figure 4.5); however, for this comparison, we used an inert negative control nucleic acid sequence that was transiently delivered in the same manner as the pre-miR-1 oligonucleotides (for miR-1 over-expression). The change in levels of miR-133a and miR-206 with miR-1 over-expression and stretch were not different from their negative controls, verifying that over-expression of one miRNA did not have major effects on the others.

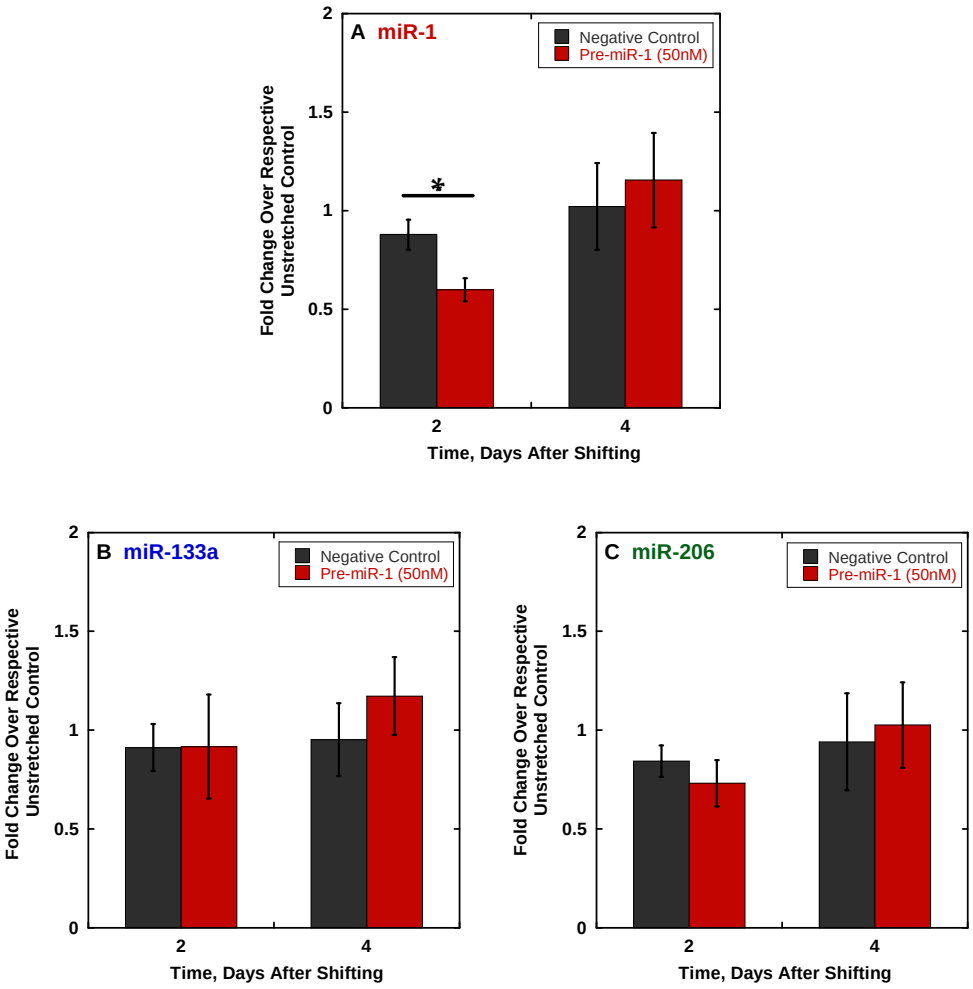

Figure 4.11 The effect of cyclic stretch with a moderate strain regimen combined with miR-1 over-expression. qRT-PCR shows (A) a down-regulation of miR-1 levels when stretch is combined with miR-1 over-expression, suggesting that a regulatory mechanism is in place to compensate for large deviations in baseline levels of miRNAs. (B, C) The change in levels of miR-133a and miR-206 with miR-1 over-expression and stretch were not different from their negative controls. Mean ± SEM, n=4, *p<0.05.

Studies have shown that blocking key muscle-specific miRNAs (particularly miR-1) is detrimental to promoting myoblast differentiation [34]; however, we aimed to observe if any compensatory mechanisms were induced by stretch with miR-1 inhibition (anti-miR-1). We hypothesized that stretch might have allowed the system to overcome the transient knockdown of miR-1, but the results show that miR-1 may be critical for a stretch-mediated effect to occur.

Since anti-miR-1 oligonucleotides do not degrade the mature miR-1 sequence, qRT-PCR could not be used to assess the degree of inhibition. Therefore, the effect of inhibiting miR-1 was assessed by HDAC4 protein expression because it is a direct target for miR-1. HDAC4 levels increased, as expected, in anti-miR-1 myoblasts. As shown in Figure 4.12, the effect of miR-1 inhibition was most apparent at shift day 2 with ratios of anti-miR-1 to negative control HDAC4 levels greater than 1 ($p<0.05$) in both unstretched and stretched samples. By shift day 4, HDAC4 levels between anti-miR-1 and negative control myoblasts were nearly the same (ratio ~1), suggesting that miR-1 inhibition was removed by this time. This time scale was similar to that observed with miR-1 over-expression (Figure 4.10).

There was no significant difference in response between unstretched and stretched myoblasts to transient miR-1 inhibition, which suggests that the stretch-mediated effect may be miRNA-dependent. With the current information combined, we

note that there is a complex interplay of the effect of mechanical stimulation on downstream regulation of muscle-specific genes and miRNAs.

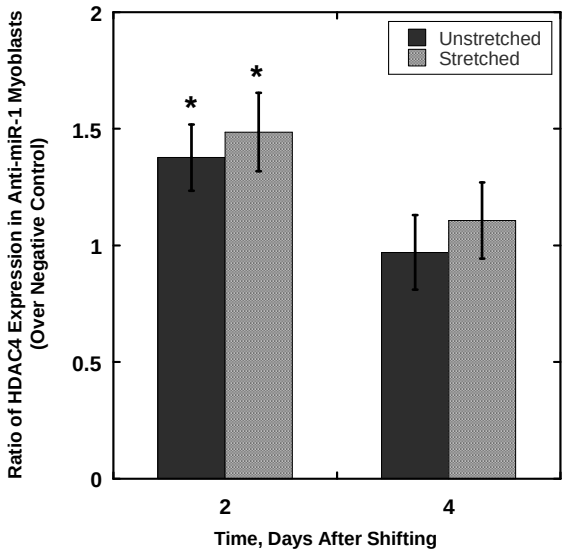

Figure 4.12 Western blot analysis of HDAC4 showing effect of cyclic stretch with a moderate strain regimen and miR-1 inhibition. At 2 and 4 days after shifting, stretch was unable to overcome the effect of inhibiting miR-1, as shown by the increased levels of HDAC4. Mean ± SEM, n=6, *p<0.05 compared to a ratio of 1.

4.4 Discussion

Much research has addressed the effect of mechanical stimulation on cellular processes. Data from our lab ([192] and S. Zhang, PhD dissertation, 2007) and from other published results show that applied stretch, whether cyclic or static, can have distinct effects on myoblast differentiation and proliferation. While other studies have examined one major set of mechanical stimulation conditions, this study examined two different regimens and showed differential responses to each. Previous studies suggest that using a stretch regimen of 0.5Hz, 10% strain for 1 hour followed by a 5 hour rest period promotes C2C12 myoblast differentiation in a 2-D system [192]. This was evidenced by increases in F-actin content and MHC protein levels while BrdU incorporation decreased with stretch, which corroborate our results showing that myoblast differentiation, as assessed by staining for F-actin and alpha-actinin (Figures 4.1a and 4.2) and fusion index (Table 4.1), is indeed enhanced using this moderate strain regimen.

The opposing effects were seen with the high strain regimen, suggesting that the differentiation cascade was not promoted in these myoblasts [79]. Particularly, Figure 4.3 and Table 4.1 showed that the stretch at high strains inhibited myoblasts from maturing beyond fusion when compared to their unstretched controls. These results correlate with previous studies, which showed increases in proliferation and reduced differentiation. For example, when primary myoblasts from Balb/c mice were

stretched 25% at 0.5Hz for 5 h over a total duration of 24-48 hours in a uniaxial stretch device, BrdU incorporation increased about 30% after 24 h and cell number increased 40% after 48 h, relative to unstretched controls. Stretch also decreased myogenin [118]. Although not a direct comparison, exposure of primary rat hind limb cultured satellite cells to 25% equibiaxial stretch at 12-s intervals for 12 to 36 hours led to increased BrdU incorporation after 12 hours [150]. Our system did not show these marked increases in proliferation, but this could be attributed to the use of a C2C12 cell line, variations in strains, rest periods, and myoblast confluence at the start of stretch, which can create significantly different responses in cellular behavior.

Prior to onset of differentiation, miR-1, miR-133a and miR-206 levels were very low in myoblasts. There was a significant increase in the levels of these miRNAs with the onset of differentiation in both stretched and unstretched samples, which continued to increase as differentiation proceeded (Figure 4.4). These results were consistent with previous time course studies [34, 69], and differences in miR-1 and miR-206 levels have been reported among different muscles [105]. Both miR-1 and miR-133a had parallel responses which were consistent with the similar regulation of these two miRNAs [34], [130], [52]. Muscle differentiation has been further enhanced by miR-206, and blocking it hindered withdrawal from the cell cycle and subsequent fusion and differentiation [69]. Marked increases in miR-206 levels with myoblast differentiation were observed with our system, which correlated with others observations [69]. Temporal changes in all

three miRNAs were similar to other studies as there was a significant effect of time with these key muscle-specific miRNAs ($p<0.001$) [34, 69, 130].

To our knowledge, this is the first study linking regulation of the three muscle-specific miRNAs – miR-1, 133, and 206 – with cyclic stretch. As Figure 4.5 presents, miRNA expression is dependent on the parameters of cyclic stretch, demonstrating a differential response to moderate and high strains. miR-1, miR-133a, and miR-206 expression was elevated with cyclic stretch, under the moderate strain regimen, while there was no different response with the high strain regimen. This suggests that mechanical stimulation is an effector of miRNA expression in differentiating myoblasts.

In our studies, we also found that the ratio between miR-133 and miR-1 varied over time and with stretch regimen (Figure 4.6). Although miR-133 promotes proliferation while miR-1 promotes differentiation [34], both increased dramatically over time, and the relationship between the two has not been explored much previously. With the moderate strain regimen, stretch depressed the miR-133 : miR-1 ratio at shift day 6, although not with statistical significance. In the high strain regimen, the miR-133: miR-1 ratio showed an increasing trend with stretch at shift day 4. Both follow the expected response where the moderate strain regimen promotes differentiation with miR-1 dominating, where the ratio is closer to one. The high strain promotes proliferation, and the ratio is higher with a slight tendency to favor miR-133. A significant difference was also found in this ratio in miRNA isolated from normal mice

(strain C57BL/10) compared to mdx muscle at 1 year, but otherwise the ratios remained close to one [189].

Even though the dynamic changes in miRNA regulation have not been widely explored, the levels of miRNA in diseased or stressed states have been studied. Most studies have focused on miRNA dysregulation in cardiac hypertrophy [27], [159], [140], [158]. In skeletal muscle, the effects of hypertrophy on miR-1, miR-133a, and miR-206 regulation were examined by *in vivo* injury to rat soleus and plantaris muscles. The level of miR-1 and miR-133 decreased following 7 days of functional overload, and levels of miR-206 did not change [104]. These studies further bolster the results we have seen here, suggesting a mechanical link to miRNA regulation.

Previous studies of miRNA expression in skeletal muscle focused on identifying targets and did not quantify the relationship between miRNA levels and their targets; hence, the levels of change in miRNAs needed to produce a functional effect have not been established. A 2.8 fold increase in miR-1 was observed in human hearts with coronary artery disease and could produce conduction abnormalities by reducing expression of connexin 43 and a potassium channel [185]. Similar changes in miR-1 and miR-133 levels in a cardiac hypertrophy model caused changes in the targets [27]. Since the change in miRNA levels induced by stretch were comparable to levels reported to induce functional effects *in vivo*, we postulated that observable functional changes could be attributable to mechanical stimulation.

It is unlikely that mechanical stimulation has a direct effect on miRNA expression since they seem to be regulated by a variety of different factors; however, the exact mechanism is unclear. Studies have found that Mef2 transcriptional control can affect miR-1 and miR-133 regulation [97]. Although some have postulated that miR-1 and miR-133 follow two independent pathways [34], as both Chen *et al*. and Rao *et al*. found that MyoD regulates the expression of miR-1 and miR-133 [34, 130]. Rao *et al*. also showed that MyoD and myogenin can bind to regions near the miR-1 and miR-133 chromosomal loci [130].

Alternatively, our studies found that MyoD gene expression was unchanged with cyclic stretch, regardless of the regimen used (Figures 4.7a), but there was a significant effect of time ($p<0.0002$) and regimen ($p<0.022$) on myogenin expression. A Tukey-Kramer post hoc test showed significance between the moderate and high strain regimens; however, subsequent tests at each time point did not show significance between specific groups (Figure 4.7b). The trend at shift day 2 for myogenin suggests that at early time points, a high strain stretch regimen could inhibit the myogenic pathway, partly by depressing myogenin gene expression. Similar gene expression studies of validated targets of miR-1 (HDAC4) and miR-133 (SRF) showed no change with stretch, with either the moderate or high strain regimens (Figures 4.7c and d). We postulate that since miR-1 and miR-133 are transcribed together, the factors that regulate one or the other oftentimes modulate the balance between the two.

From mRNA to miRNA expression, myoblasts subjected to the high strain regimen has not shown much change in any of the pro-myogenic factors examined here. We do know these higher levels of strain (greater than 15%) are towards the upper limit of strains encountered physiologically [23] and may induce an injury response involving the release of growth factors [154], and TNF- α at high strains may explain the shift in response to stretch. Low levels of TNF-α stimulate p38 production, but high levels inhibit differentiation [35]. Another study confirmed these results by showing that a low frequency, low strain cyclic stretch regimen (0.05Hz, 3% strain for up to 72h) was able to inhibit the anti-myogenic activity of TNF-α [31].

Higher strains, up to 18%, up-regulated proinflammatory genes, such as Nos2, which is induced by TNF-α, but application of a moderate strain cyclic stretch abrogated the effect of these proinflammatory cytokines [31]. Similarly, static stretch at strains of 8-9% induced p38 MAPK signaling which promotes myogenesis by Mef2c, myogenin, p21, and myosin heavy chain (MHC) [190]. Comparable results were observed with Mef2c in our system, where Mef2c gene expression was increased with stretch (Figure 4.8) with a moderate strain regimen and unchanged with a high strain regimen.

Although HDAC4 was not transcriptionally regulated with mechanical stimulation, downstream protein expression was altered with a moderate strain regimen, suggesting an indirect signaling pathway (Figure 4.9). HDAC4, as a known repressor of Mef2 [30, 123], may also be affected by Mef2 expression via a feedback

mechanism involving miR-1. In our studies, we found an upregulation of Mef2c gene expression levels with a moderate strain regimen (Figure 4.8) and corresponding increases in three myogenic miRNA levels (miR-1, 133a, and 206). In particular, Mef2 and SRF gene expression can activate expression of miR-1 and miR-133 in both skeletal and cardiac muscle [97, 130, 194]. Mef2 is thought to cooperate with MyoD to regulate an intragenic enhancer of these miRNAs [97]. Based on our results, mechanical stimulation with a moderate strain regimen did not produce a change in MyoD gene expression, as some have reported [97], but instead upregulated Mef2c mRNA levels. It is possible that increases in Mef2c mRNA may have directly increased miRNA levels, specifically miR-1 expression; however, further titrated, knockdown studies need to be completed before a concrete pathway can be determined. It is important to note that increases in Mef2c and miR-1 levels resulted in corresponding decreases in HDAC4 protein levels.

The combinatorial effect of modulating miRNAs and applying mechanical stimulation on myoblast differentiation has not been explored to a great degree, but may provide a method by which higher degrees of differentiation are achieved. How this regulation actually occurs will depend on the amount of miRNA target protein bound, and in essence, point to the fact that the potential regulatory loops are complex and not fully understood. Transient transfection methods were chosen over stable transfections in planning future *in vivo* studies to show the effect of miRNA over-expression in the

short term, where it may have a beneficial effect of promoting differentiation whereas viral over-expression may have deleterious effects if prolonged. By limiting expression, we expected to promote differentiation while limiting any adverse effects that may arise from continuous over-expression.

In the over-expression studies, we assessed the effect of stretch with a moderate strain regimen combined with miR-1 over-expression. The ratio of miRNA levels in stretched versus unstretched myoblasts corresponded closely to those found without transfection (see Figure 4.5). Without over-expression, at earlier time points (i.e. shift day 2), there was no significant effect of stretch on any of the three miRNAs investigated. However, by shift day 3 and shift day 4, the effect became more pronounced (Figure 4.5). At shift day 2, we observed a decreased effect of stretch when combined with miR-1 over-expression. Although used in a mild dosage, the transfection agent may have added to the suppression of a stretch-induced effect through some cellular stress since negative control levels were lower than those observed in the non-transfected cells; however, no gross damage was visible morphologically. At the earlier time point, shift day 2, a significant decrease in the stretch-induced effect, compared to the negative control, was observed (Figure 4.11) and may be a control mechanism to keep miRNA levels in balance to prevent gross or permanent inhibition of its targets, as noted by others as well [162].

In the opposite experiment, we observed that stretch alone was not able to overcome the effect of drastically inhibiting miR-1 (anti-miR-1), particularly at shift day 2 by measuring HDAC4 protein expression (Figure 4.12). The ratio of HDAC4 expression in the anti-miR-1 myoblasts to the negative control were significantly greater than 1 at shift day 2, but were diluted sufficiently by shift day 4, to a degree where no external effect of miR-1 inhibition was observed. However, there was no difference between the unstretched and stretched samples at shift day 2 or 4. These results were expected as miR-1 levels were not affected by stretch until later time points, suggesting that there is a set point at which miRNAs are able to respond to such a mechanical stimulus, or perhaps this stimulus is only translated to nuclear signals when cytoskeletal and ultrastructural elements are more developed (in myotubes vs. myoblasts). These results also could imply that the stretch-mediated effect is miR-1 dependent and without a nominal level present, may inhibit other factors that are mechanically linked.

Not surprisingly, our results show that mechanical stimulation is not a lone effector of miRNA regulation. Based on both studies involving the over-expression and inhibition of miR-1, we observed that stretch-mediated effects were often limited when baseline levels (miRNA levels arising from serum starvation alone as shown by the controls in Figure 4.5) were grossly altered, suggesting that miRNAs serve to maintain a balance of various transcription factors in the skeletal muscle differentiation process. A schematic below (Figure 4.13) depicts various links between mechanical stimulation and

miRNA regulation. A direct link between mechanical stimulation and miRNAs cannot be made at this time, but future studies using other knockdown models may shed light on this complex interplay of signal transduction. However, an indirect link through Mef2c is a viable possibility by which mechanical stimulation affects miRNA expression from our current set of results. If this were to be the case, the upregulation of Mef2c observed with a moderate strain regimen would directly affect transcription or processing of miR-1/133 clusters and downstream HDAC4 protein downregulation. A differential response to a high strain regimen (no change in Mef2c gene expression, miRNA levels, or HDAC4 protein expression) also solidifies how cellular responses can vary due to different stimuli.

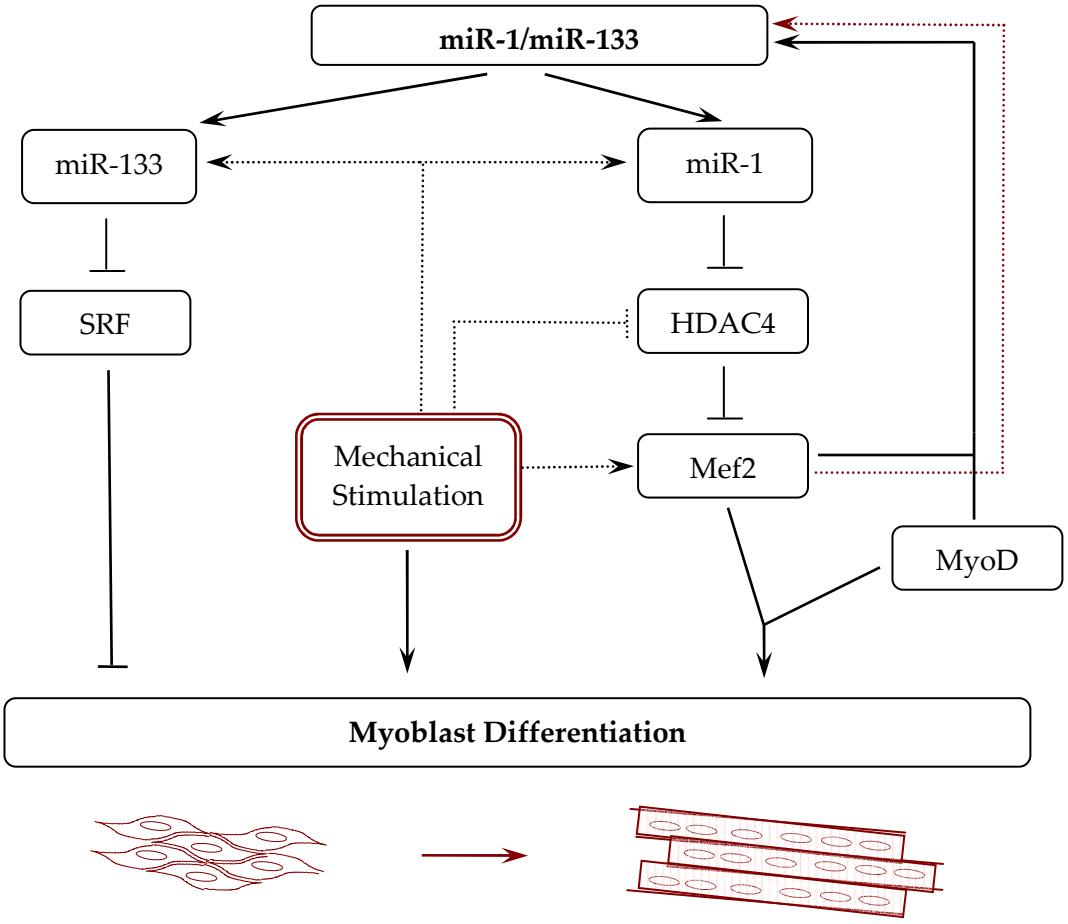

Figure 4.13 Schematic of miRNA regulation through mechanical stimulation. In conjunction with previous results [34], there are several possible modes of action, which include direct targeting of miRNA expression by mechanical stimulation and indirect targeting via different transcription factors (i.e. Mef2c). The black solid lines indicate validated mechanisms, whereas the black dotted lines show the results of this study and the red dotted lines shown possible mechanism to be explored in the future. Additionally, the effect of mechanical stimulation can vary depending on miRNA levels, suggesting that a strong balancing mechanism is in place to abrogate deleterious effects of gross over-expression or inhibition.

We can postulate that pro-myogenic factors aid in a feedback mechanism involving miRNA regulation. Perhaps sequestering these factors block miRNA targets for subsequent regulation, but further experiments must be directed to answer these questions. These results do, however, present the possible links between mechanical stretch and miRNA regulation and demonstrates the cells' ability to diversify its cellular response to varying parameters of stimulation. More so, we elucidate the complexity in translating mechanical signals outside the cell to biological cues inside the nucleus in the hopes of understanding the mechanism behind critical cellular processes.

4.5 Conclusions

This study proposes a link between mechanical signals outside the cell membrane and biological responses inside the nucleus, subsequently affecting a new class of non-coding RNA, known as miRNAs. Our system demonstrated a differential response of skeletal myoblasts to moderate and high strain cyclic strain regimens. Myoblast maturation was enhanced with a moderate strain regimen, as assessed morphologically and quantitatively with a higher myogenic fusion index. While neither strain regimen had significant effects on muscle-specific genes, such as MyoD and myogenin, only the moderate strain regimen saw an increase in Mef2c gene expression by 6 days post-differentiation. Corresponding to these results, HDAC4 protein expression, a direct target of miR-1 and repressor of Mef2, was decreased with the

moderate strain regimen, most pronounced by 6 days post-differentiation. While the high strain regimen showed no difference in miR-1, 133a, and 206 expression with stretch, a significant effect of stretch ($p<0.05$) was seen after 3 or 4 days, post-differentiation, with the moderate strain regimen. To further elucidate the relationship between cyclic stretch and miRNA expression, miR-1 was both over-expressed and inhibited in conjunction with the moderate strain regimen. Over-expression of miR-1 abrogated the effect of stretch at shift day 2 compared to its negative control and did not seem to accelerate the effect of a stretch-mediated response in altering miRNA levels. Inhibition of miR-1 similarly diminished the stretch-mediated response. The current results suggest that the balance of miRNAs and various transcription factors are crucial in promoting a response to stretch; however, there is a complex interplay of the effect of mechanical stimulation on downstream regulation of muscle-specific genes and miRNAs that will need more attention in the near future.

4.6 Acknowledgements

The authors would like to thank Cindy Cheng and Stephen Morton for their assistance, and Dr. H.S. Kim from the UNC Department of Cell Biology for oligonucleotide synthesis. We would also like to acknowledge funding from the National Institutes of Health (NIH) grant EB2408 and the McChesney Foundation.

Chapter 5. MicroRNA Delivery to Mediate Bioartificial Muscle Function

5.1 Introduction

With the prospect of reversing complex disease states, scientists and entrepreneurs have been exploring the idea of mediating small RNAs to modify downstream protein synthesis. In recent years, new ventures have been started to assess the commercial aspects of using miRNAs in particular to target various ailments [102]. For example, since miR-21 is an anti-apoptotic factor in certain brain tumors; thereby, inhibition of this miRNA could be used for cancer therapies [29, 102]. Similarly, inhibition of miR-122 lowered cholesterol in mice [37, 51, 75], leading both the scientific and entrepreneurial communities to believe that miRNAs are promising candidates for targeting various disease states or serving as drug targets themselves.

Similar to these ventures, miR-1 and miR-133 have been the subject of potential therapeutic applications, particularly in cardiac ailments. Care *et al*. found that both miR-1 and miR-133 were downregulated in cardiac hypertrophy models, and that by over-expressing one or the other, a hypertrophic response was inhibited [27]. In terms of cardiac function, miR-1 was found to repress two genes, KCNJ2 and GJA1, which encode for proteins, Kir2.1 and connexin 43, respectively, involved in regulating and maintaining arrhythmogenic potential; hence, miR-1 inhibition suppresses arrhythmias

in infarcted hearts of rats [186]. miR-133 also affected QT prolongation in rabbit diabetic hearts by repressing the ether-a-go-go (ERG) gene and its over-expression in this disease state was found to be detrimental [181]. Another pacing-related gene, HCN2, was a target of miR-133 and upregulated in the hypertrophic state associated with depressed miR-133 [100]. This brings to light the critical role of miR-1 and miR-133 in cardiac function.

While much of the current research has focused on cardiac tissue, less is known about the role of microRNAs on skeletal muscle function. A tissue engineering model of the skeletal muscle system has been one way to study myoblast differentiation and maturation *in vitro*. As outlined in Chapter 2, we found that a collagen gel-based skeletal muscle system was successfully able to form differentiated muscle in a 3D model. However, as is the case with all tissue engineered organ systems, there are limitations in replicating a native muscle *in vitro*, both in structure and function. Perhaps the biggest hurdle facing muscle tissue engineering is achieving force outputs like those *in vivo*; therefore, the objective of the current study was to assess if modulating miRNAs in a tissue-engineered model could affect functional output.

In Chapter 4, we showed that mechanical stretch upregulated three-muscle specific miRNAs – miR-1, miR-133, and miR-206 – in a 2D culture system, but found that modulating miRNAs in conjunction with stretch did not enhance overall miRNA expression. Hence, we chose to assess miRNA modulation alone on skeletal muscle

function in a 3D system using transient transfection of miRNA-specific molecules (for over-expression or inhibition). For future *in vivo* studies, a transient transfection would be preferable to stable transfections with viral vectors, which may lead to deleterious effects with continuous expression or inhibition of a miRNA in addition to uncontrolled viral delivery. This is the first study showing miRNA mediation in a tissue engineered skeletal muscle model and importantly, showing downstream changes in function by force response to different electrical stimulation frequencies.

5.2 Methods and Materials

5.2.1 Cell Culture & Transient Transfection

Murine C2C12 myoblasts (ATCC, Rockville, MD), a subclone derived from a cell line that originated from normal adult C3H mouse leg muscle [17], were cultured on standard tissue culture flasks, at passages 3 to 5 [182]. The cells were fed daily with growth medium (GM) containing high glucose Dulbecco's modified Eagles' medium (DMEM; Gibco/Invitrogen, Carlsbad, CA), 8% new born calf serum (HyClone Laboratories, Logan, UT), 8% fetal bovine serum (HyClone), 0.5% chicken embryo extract (Accurate Chemicals, Westbury, NY), and 0.1% gentamicin (Gibco/Invitrogen) at 37 ºC and 5% CO_2. To promote differentiation of myoblasts to fuse into myotubes, the growth medium was shifted to differentiation medium (DM), consisting of DMEM supplemented with 8% horse serum (HyClone) and 0.1% gentamicin (Gibco/Invitrogen).

For the over-expression studies, Pre-miR precursor molecules specific for the mature miR-1 sequence (Ambion) were transfected with siPORT NeoFX transfection agent (Ambion) into myoblasts per manufacturer instructions. Briefly, the transfection agent was diluted in Opti-MEM I (Gibco) and mixed with 50nM of the pre-miR-1 precursors (double-stranded miRNA mimic) or with the same concentration of the pre-miR negative control (or a random, inert nucleic acid sequence). After incubating for 10 minutes at room temperature, the mixture was then dispensed into appropriate tissue

culture flasks. A cell suspension, at sub-confluent densities, were added to each flask and cultured in normal conditions for 24 hours, with antibiotic-free GM. For inhibition of miR-1, the same transfection procedures outlined above were used with anti-miR-133, single-stranded RNA antisense molecules (Ambion) and the corresponding anti-miR negative control (Ambion). For fluorescent tracking of the transfection, Cy-3 labeled negative controls for both the precursors and anti-miRs were used in the same manner as described above and viewed using confocal microscopy.

5.2.2 Bioartificial Muscle (BAM) Assembly

After 24 hours, and before full confluence was reached, the myoblast cultures (non-transfected control, negative control, and miRNA-modified myoblasts) were trypsinized in a 0.05% trypsin/EDTA solution (Gibco, Grand Island, NY) and centrifuged at 1000 rpm for 5 minutes. Each cell pellet was then resuspended in a Matrigel solution (BD Biosciences, Bedford, MA) and added to a chilled solution of GM yielding final concentrations of 1.4mg/ml type I rat tail collagen (BD Biosciences, Bedford, MA) and 3mM NaOH to a final 3:1 ratio of collagen to Matrigel. Two million cells were suspended within this collagen gel mixture to give each BAM a total volume of 0.4ml.

As previously described [124, 165], BAM troughs were made using silicone tubing (Nalgene, Rochester, NY), split longitudinally with tiny sections of silicone sheets

(Nalgene, Rochester, NY) and glued to the open ends of the tubing with RTV silicone adhesive (GE, Waterford, NY). Small stainless steel minutien pins (Fine Science Tools, Foster City, CA) held Velcro tabs at the ends of the mold to act as attachment sites for the collagen/matrigel construct, and over time, to maintain passive tension. The assembled molds were glued onto the bottom of a standard tissue culture dish and gas sterilized with EtO.

After 1 hour at 37°C, warm GM was added to the dishes over the gelled Matrigel construct. The BAMs were cultured for 2 days in GM and then the media was shifted to promote differentiation. This differentiation media (DM) consisted of high glucose DMEM (Gibco, Grand Island, NY), 8-20% horse serum (HS, Hyclone Laboratories, Logan, UT), and 0.1% gentamicin (Gibco, Grand Island, NY). Cultures remained in SM for 6 to 12 days (shift day, SD 6 to 12).

5.2.3 Histology

The BAMs were fixed for 2 hours in a 3.7% paraformaldehyde solution at 4°C, then rinsed and stored in phosphate buffered solution (PBS) for histochemistry. All histochemistry procedures were performed in the Pathology Laboratory, Duke Medical Center. Briefly, the samples were dehydrated in a graded series of ethanol solutions and embedded in paraffin for sectioning. Specimens were cut into 5μm sections in both the

longitudinal and cross-sectional directions and stained using hematoxylin and eosin (H&E).

5.2.4 Immunostaining & Fiber Diameter Measurements

The BAMs were fixed for 2 hours in a 3.7% paraformaldehyde solution at 4°C, rinsed in PBS, then permeabilized with 0.05% Triton-X for 2 hours at 37°C. Afterwards, the samples were thoroughly rinsed and stored in PBS. The permeabilized BAMs were incubated for 1 hour with rhodamine-phalloidin (Molecular Probes, Eugene, OR), 25U/ml, to stain for F-actin filaments, and an additional 30 minutes with Sytox Green, (Molecular Probes, Eugene, OR), 1μM, was used for nuclei staining.

For immunohistochemical staining, the samples were fixed and permeabilized in the same manner as described above. Primary antibodies, alpha-actinin (Sigma, St. Louis, MO) and myosin MF20 (Developmental Studies Hybridoma Bank, Iowa City, IA), were diluted 1:500 and 1:50, respectively, in a 1% BSA solution and incubated with the BAMs overnight at 4°C. After thorough rinsing with PBS, the construct was incubated at room temperature with a secondary Alexa Fluor-488 or -546 goat anti-mouse antibody (Invitrogen, Carlsbad, CA) for 2 hours. In most cases, a nuclear stain, such as Sytox Green (Invitrogen) was added and incubated at room temperature for 1 hour. Samples were then viewed via confocal microscopy.

Using several sets of confocal images, fiber diameter measurements were

completed for clearly visible fibers within a given field of view. At least five independent sets of BAMs were analyzed with an average of 5-10 measurements per image using Image J (NIH, Bethesda, MD). The averages from all images linked to a given BAM set were then gathered for statistical analysis.

5.2.5 Functional Force Testing

BAM force measurements were gathered using a custom apparatus from Aurora Scientific (Aurora, Ontario, Canada) comprised of a force transducer (Aurora, Model 403A) with an upper limit specification of 5mN and a benchtop unit (Aurora, Model 801B). An image of the setup is shown below in Figure 5.1. Controlled with a Labview software program package, electrical stimulation was applied at frequencies in a range of 0 to 40Hz at 40V, 10ms duration, 0.03ms delay. Data was gathered as a text file and analyzed using a custom Matlab program (The Mathworks, Inc., Natick MA), which is included in Appendix B. Stress measurements were based on the force output of the machine and BAM cross-sectional area measurements taken from histology slides. Cross-sectional areas were determined using ImageJ (NIH).

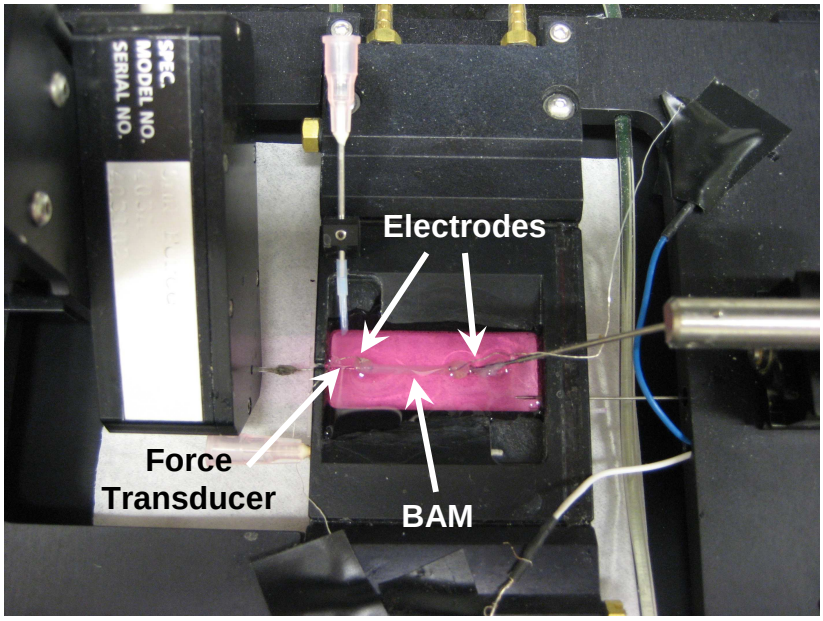

Figure 5.1 Functional force transducer setup, showing BAM held in suspension by two hooks, one of which is the transducer. Electrical stimulation was applied through two electrodes that were pierced into the construct.

5.2.6 Statistical Analysis

Data are presented as a mean ± standard error (SEM) unless otherwise noted. A two-factor ANOVA or student t-tests were performed using the Statview 5.0 statistical analysis package. When applicable, the Tukey-Kramer post-hoc test was performed as part of the ANOVA analysis. A value of $p<0.05$ was considered significant.

5.3 Results

5.3.1 Function Force Response in Non-Transfected BAMs

One of the most definitive tests for tissue-engineered constructs is its downstream function. For skeletal muscle constructs, spontaneous twitching and excitability, or responsive contractions to electrical stimulation, are two ways to determine function *in vitro*. BAMs cultured with non-transfected myoblasts were used as a baseline to assess overall construct health. Although the direct effect of miRNA mediation on BAM function was compared to the negative control (inert nucleic acid sequence), we first examined the non-transfected BAMs to verify that there were no functional differences by using a transfection agent.

Figure 5.2 plots the excitability of non-transfected BAMs to electrical stimulation frequencies ranging from 0Hz to 5Hz. Constructs displayed consistent peaks in force in response to a given frequency of stimulation, which was applied for 500ms from a time of 1s to 1.5s. However, no tetanus was achieved with these BAMs, and responses degraded when stimulation frequencies were greater than 20Hz. The average peak forces for non-transfected BAMs, cultured from shift day 6 to 8, were 0.88mN ± 0.18mN at a 1Hz stimulation frequency, 1.03mN ± 0.21mN at a 5Hz frequency, 1.02mN ± 0.18mN at a 10Hz frequency, and 1.11mN ± 0.21mN at a 20Hz frequency, showing that there was a slight increase in average peak force with increasing stimulation frequency from 1 to 5Hz. However, the peak forces were fairly consistent at frequencies greater than 5Hz.

There was no statistical difference in peak force values with different frequencies of stimulation. Five independent experiments were completed.

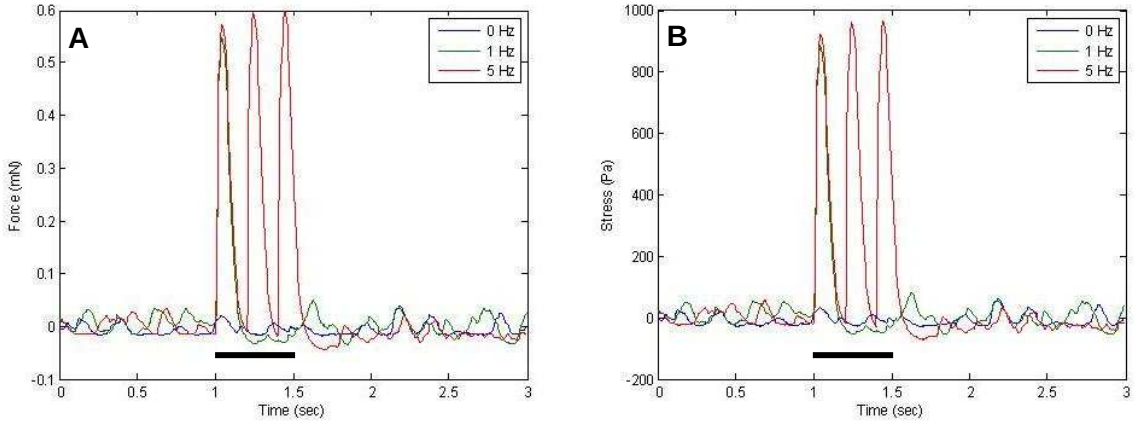

Figure 5.2 Representative functional force measurements showing peaks at various frequencies (0Hz – 5 Hz) for BAMs cultured with non-transfected myoblasts. Data is presented as (A) force output, mN and (B) stress output, Pa where cross-sectional area was considered. The bold black line segment signifies the time period of electrical stimulation (1s – 1.5s).

5.3.2 Transient Transfection in BAMs

The time scale by which the chemically modified miRNA pre-miRs (for over-expression) and anti-miRs (for inhibition) remained within the cell in the BAMs correlated somewhat to the 2D results in Chapter 4. For example, following miR-1 over-expression in C2C12 cells in 2D culture, mature miR-1 levels equaled the levels in the negative control cells by shift day 4 (Figure 4.11), or 5 days after transfection. Cy3-labeling of the pre-miR and anti-miR negative control (for tracking purposes) in Figure

5.3 shows the transfection of differentiating myoblasts 24 hours after transfection (still in the tissue culture flasks) and at the point before cells are cast into the collagen gel.

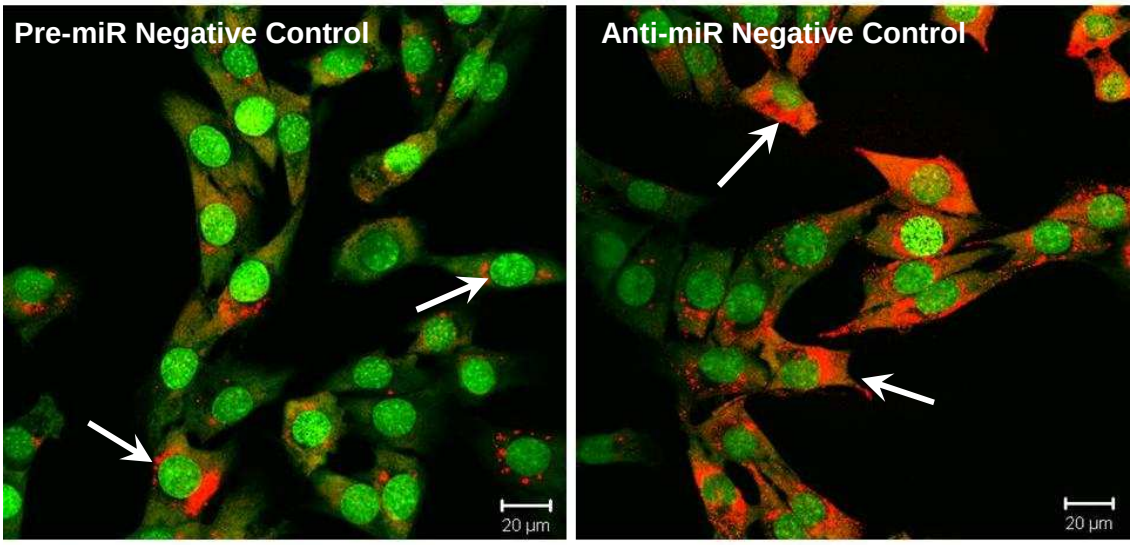

Figure 5.3 Transient transfection of Cy-3 labeled pre-miR and anti-miR negative controls in differentiating myoblasts 24 hours after transfection. Transfection was less efficient with the pre-miR miRNA precursors, as evident by the fluorescent tracking of the transfected molecules (see arrows).

There was a slight difference in transfection efficiencies of cells labeled with either pre-miR-1 or anti-miR-1, and this difference is likely due to the different configurations of each of these molecules. Whereas pre-miRs are double-stranded miRNA mimics, anti-miRs are single-stranded inhibitors. The effects of these differences are seen in the transfection efficiencies 24 hours after transfection (pre-miRs: ~35% efficiency versus anti-miRs: ~90% efficiency). In the 3D system, the miRNA molecules were nearly out of the cells at shift day 0, or 3 days after transfection (Figure 5.4). In the 2D studies, qRT-

PCR quantified miRNA transfection whereas in these 3D studies, visual examination was utilized and could explain the 1 or 2 days difference in retention of the exogenous miRNAs.

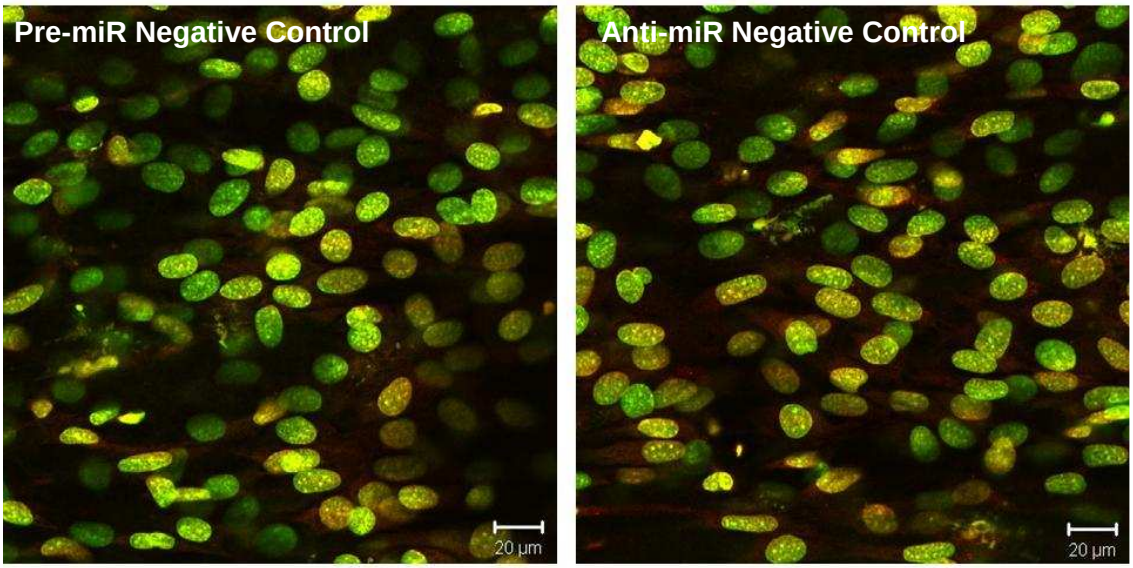

Figure 5.4 Transient transfection of Cy3-labeled pre-miR and anti-miR negative controls in BAMs 36 hours after transfection (shift day 0). By this time, nearly all added exogenous miRNAs were not detected by the Cy3-labeled probes.

Regardless of slight variations in the time scale by which the exogenous miRNAs are effective, we know that by the time force output is assessed, the presence of these miRNAs has diminished; hence, this experimental setup was considered a transient transfection.

5.3.3 Over-Expression of miR-1 in BAMs

We hypothesized that miR-1, a differentiation-promoting element, upon over-expression, would enhance myoblast differentiation and increase force production. The initial histological and immunostaining analyses showed no major differences between BAMs cultured with myoblasts transfected with the negative control or miR-1 precursors (pre-miR-1). Figure 5.5 shows that after 6 days in DM, myoblasts have fused in the outer periphery while mononuclear cells still remain dispersed throughout the collagen gel matrix.

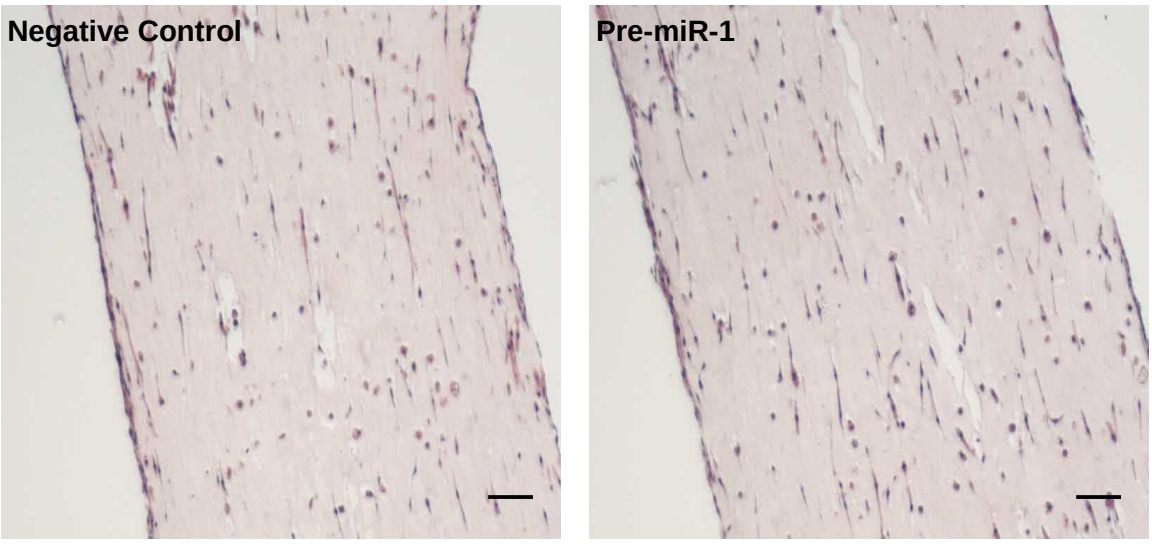

Figure 5.5 Representative H&E staining of longitudinal sections of negative control and pre-miR-1 BAMs, showing similar distribution of cells within the collagen gel matrix. BAMs were cultured for 2 days in GM and 6 days in DM. Image was taken at 4X, scale bars are 100μm.

Immunostaining for alpha-actinin in BAMs (negative control and pre-miR-1) showed striations in both sets at shift day 6 as myofiber and cytoskeletal protein organization was similar to its corresponding negative control as shown in Figure 5.6. There were no observations of major morphologic differences, such as fiber diameter and organization.

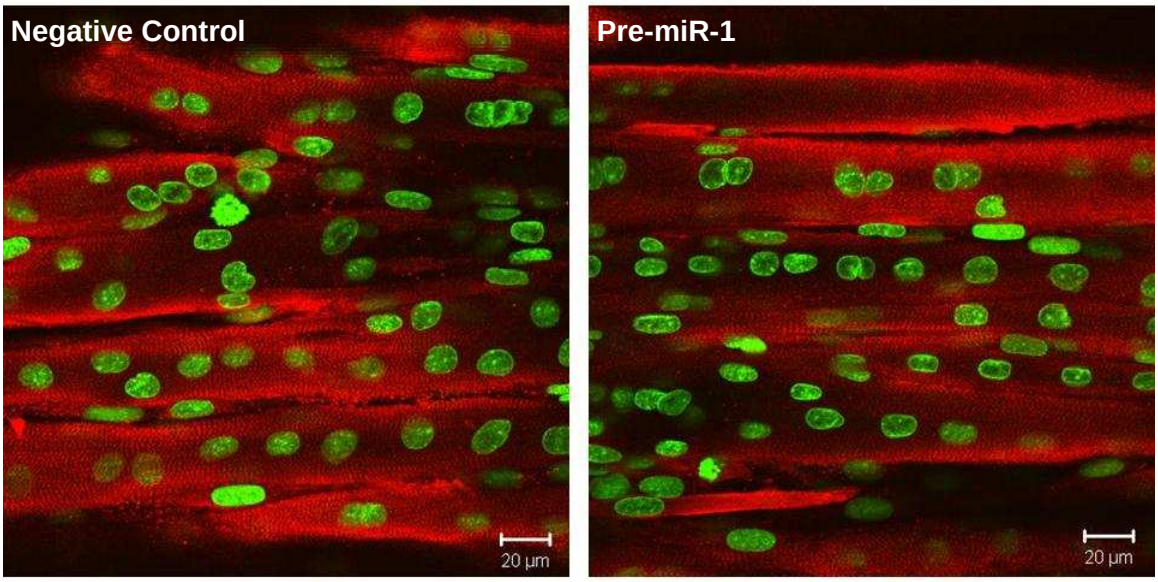

Figure 5.6 Immunostaining for alpha-actinin for negative control and pre-miR-1 BAMs, showed there was no major difference between negative control and pre-miR-1 BAMs at shift day 6.

In general, over-expression of miR-1 (pre-miR-1) created an increase in functional force output, and one set of force outputs from negative control and pre-miR-1 BAMs are shown below in Figure 5.7. As mentioned in section 5.2, negative controls for anti-miR-133 and pre-miR-1 were different according to the inhibition and over-expression mechanisms of action. However, over several independent cultures, statistical

significance (compared to a ratio of 1 for miRNA-mediated forces over negative control forces) was not achieved because of the ratio of force in pre-miR-1 BAMs over the negative control varied between 1 and 1.2.

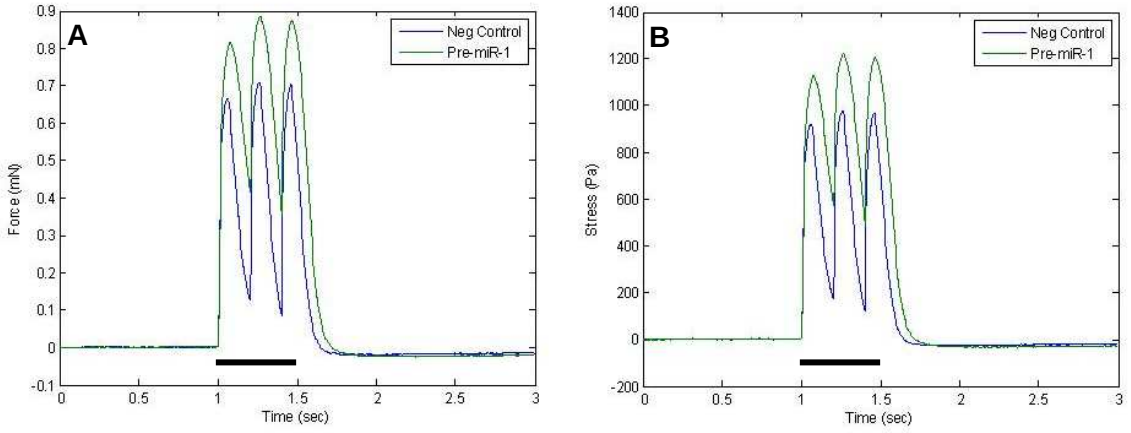

Figure 5.7 Functional force measurements at a stimulation frequency of 5 Hz for BAMs cultured with negative control and pre-miR-1 myoblasts. Data are presented as (A) force output, mN, and (B) stress output, Pa, where cross-sectional area was considered. The bold black line segment signifies the time period of electrical stimulation.

5.3.3 Inhibition of miR-133 in BAMs

In a similar theory to over-expressing miR-1, a differentiation-promoting element, miR-133, a proliferation-promoting element, was inhibited to observe if myoblast proliferation could be halted and the differentiation process could be expedited. Since miR-133 is associated with myoblast proliferation, we postulated that

inhibiting miR-133 may suppress proliferation, and thereby accelerate the differentiation process.

Histological analysis via hematoxylin and eosin (H&E) staining and immunostaining for various muscle-specific proteins showed organizational differences between negative control and anti-miR-133 BAMs. Longitudinal cross-sections of the BAMs showed morphologic differences in BAMs with and without miR-133 inhibition, as shown in Figure 5.8. Areas of thick myofiber densities were more apparent in the anti-miR-133 BAMs, although, striations were visible in both sets of BAMs showing that the structural proteins are organizing, regardless of miRNA modulation. Similar to the findings in Chapter 2, myotubes were concentrated on the outer 100μm of the BAM periphery.

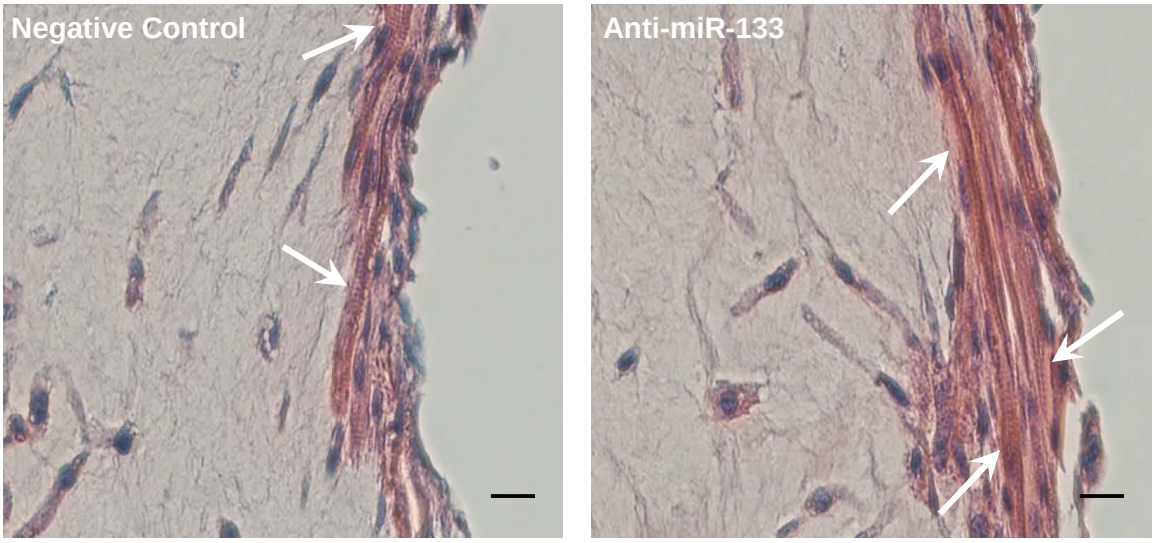

Figure 5.8 Representative H&E staining of negative control and anti-miR-133 BAMs, showing thicker area of myofiber density in BAMs with miR-133 inhibition. BAMs were cultured for 2 days in GM and 8 days in DM. Arrows point to striations observed in both sets of BAMs. Image was taken at 20X, scale bars are 20μm.

Previous work has shown that inhibiting miR-133 increased myogenin and myosin heavy chain protein expression [34]; therefore, we chose to examine myofiber formation and striations with myosin and alpha-actinin antibodies. Immunostaining for myosin in BAMs cultured for 8 days in DM (shift day 8) showed more pronounced striations in anti-miR-133 BAMs compared to the negative control (Figure 5.9). In addition to the striations, there were also more distinct areas of larger myofiber diameters in the anti-miR-133 BAMs as well. These conditions were consistent in nearly all sets of miRNA-mediated BAMs.

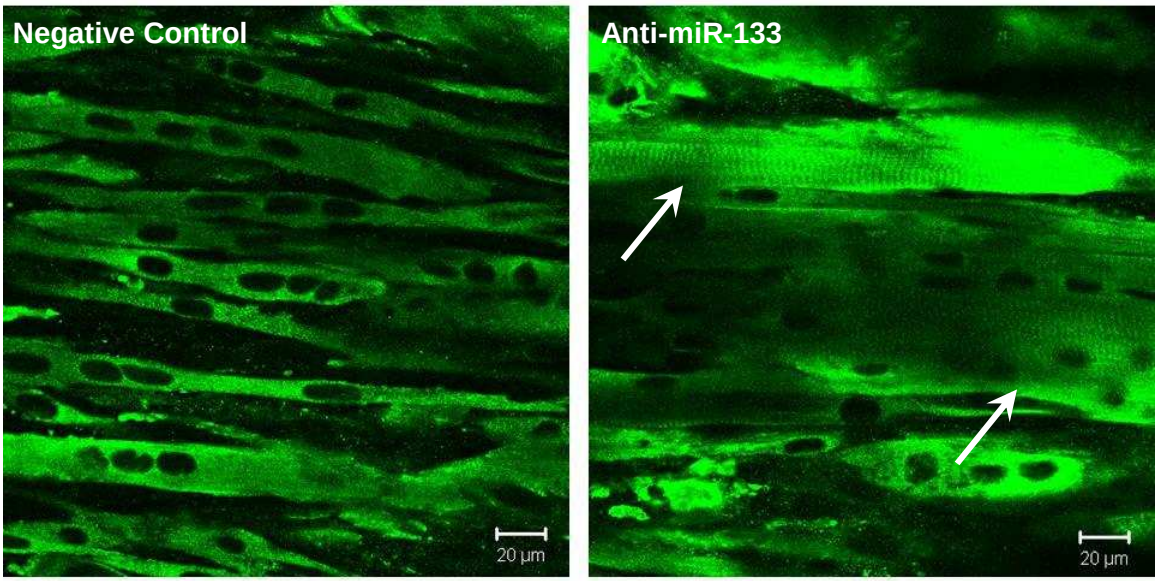

Figure 5.9 Immunostaining for myosin (MF20) in BAMs containing myoblasts transfected with either control sequence or anti-miR-133 and cultured for 8 days in DM. Distinct striations were more visible when miR-133 was transiently inhibited (see arrows). Additionally, myofiber size appeared to be larger in anti-miR-133 constructs.

Another myosin staining with a nuclear counterstain showed that BAMs cultured until shift day 6 showed the same phenomenon as constructs that were fixed at shift day 8. Figure 5.10 highlights the large fiber diameters and striations visible in the anti-miR-133 BAMs. Fusion and some organization was apparent in both the negative control and anti-miR-133 BAMs, but were more pronounced in those with miRNA mediation. In these set of images, it appears that myofiber density is higher in the negative control; however, this was a product of the z-stack image chosen to show optimum fiber clarity. The myofiber densities were similar in both negative control and anti-miR-133 BAMs.

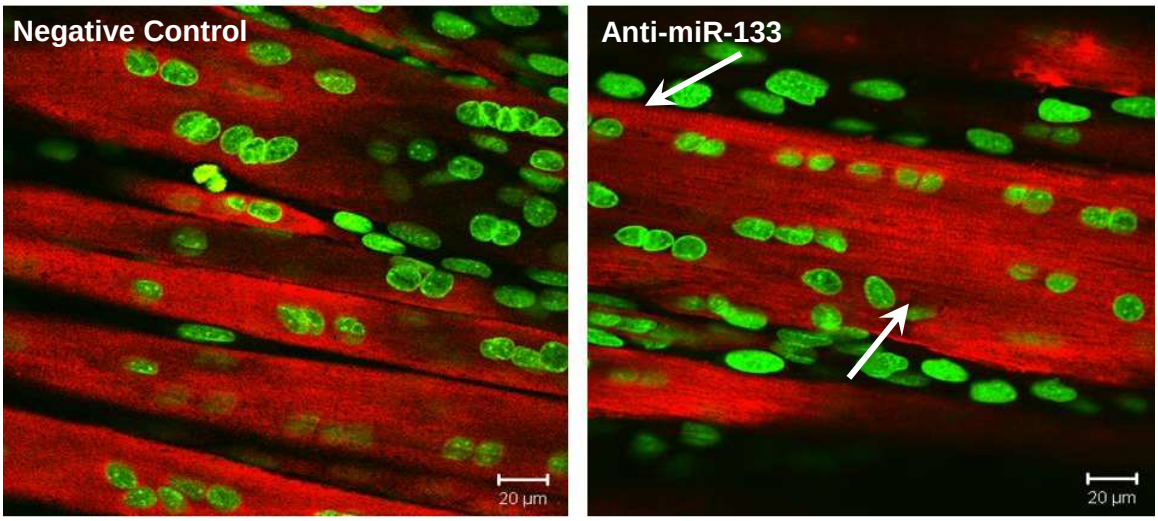

Figure 5.10 Immunostaining for myosin (MF20) in BAMs cultured with negative control-transfected or anti-miR-133 myoblasts for 6 days in DM, with a Sytox green nuclear counterstain. Distinct striations were more visible when miR-133 was transiently inhibited (see arrows). Additionally, myofiber size appeared to be larger in anti-miR-133 constructs.

Similarly, immunostaining with alpha-actinin in BAMs at shift day 6 showed visible striations in both negative control and anti-miR-133 BAMs. It was difficult to assess if there was a difference in the actual degree of striation (Figure 5.11) with this structural protein. However, in many cases, over independent samples, the instances of larger myofiber diameter were more pronounced in the anti-miR-133 BAMs, in both immunostaining with myosin and alpha-actinin.

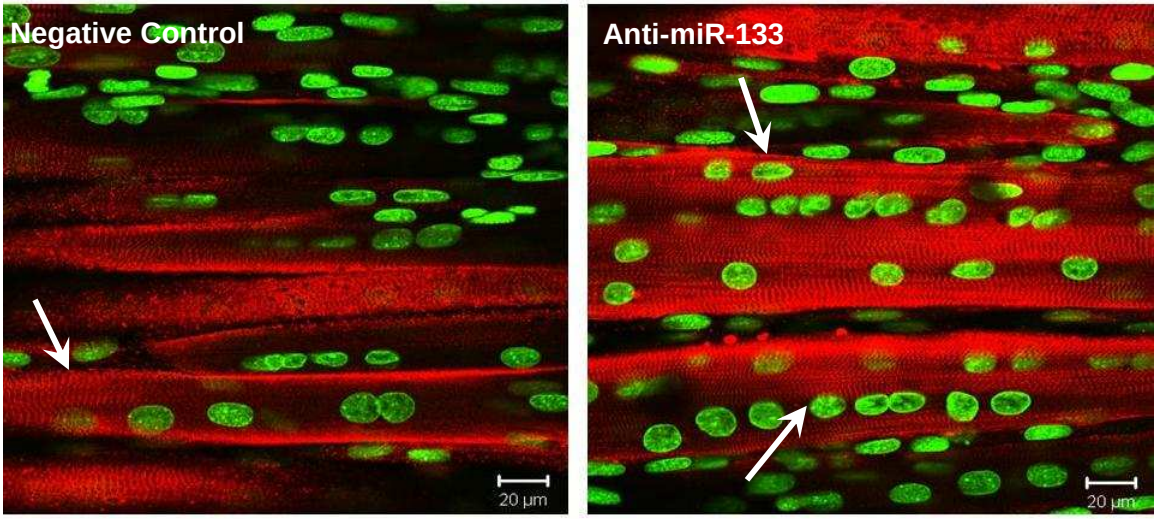

Figure 5.11 Immunostaining for alpha-actinin in BAMs cultured with negative control-transfected or anti-miR-133 myoblasts for 6 days in DM. Distinct striations were visible in both constructs; however, myofiber diameter appeared to be larger in the anti-miR-133 BAMs.

To assess the differences in fiber diameter, measurements of five independent sets of BAMs (from shift day 6 to 8) were completed. Depending on the z-stack image, each clearly visible fiber diameter was measured, and the results are shown below in Figure 5.12. The average fiber diameter of BAMs cultured with miR-133 inhibition had, on average, a significantly higher fiber diameter. While there was no significant difference in fiber diameter in the non-transfected and negative control BAMs (27.2µm ± 2.7µm versus 23.9µm ± 2.6µm), both of these sets were significantly different than the anti-miR-133 BAMs, which had an average fiber diameter of 41.1µm ± 2.7µm.

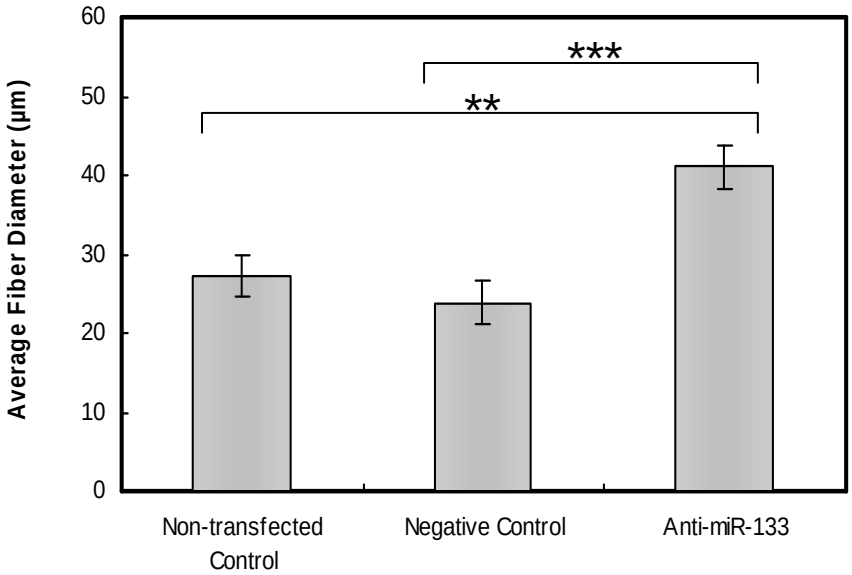

Figure 5.12 Average fiber diameter of non-transfected, negative control, and anti-miR-133 BAMs. BAMs cultured with miR-133-inhibited myoblasts cultured for 6 or 8 days had, on average, a large fiber diameter than either the corresponding non-transfected control or the negative control. Mean ± SEM, n=5, and **p<0.005 compared to non-transfected control, ***p<0.001 compared to negative control BAMs.

BAMs cultured with myoblasts that were transiently transfected with a miR-133a inhibitor (anti-miR-133) exhibited maximum forces that were on average 20% greater in magnitude than those cultured with the negative control cells. The response to electrical stimulation in BAMs cultured with transfected (both negative control and anti-miR-133a) myoblasts was similar to that observed with the non-transfected constructs (see Figure 5.2 above). A comparative set of peaks at a 5Hz stimulation frequency (applied stimulation at 1s to 1.5s) is shown below in Figure 5.13. In this particular example, the spontaneous twitch force of the anti-miR-133 BAMs was markedly higher than the

negative control constructs. The overall spontaneous twitch force (with no electrical stimulation) varied greatly between independent runs with an average ± SEM for the non-transfected BAMs (0.33mN ± 0.12mN), negative control BAMs (0.49mN ± 0.20mN), and anti-miR-133 BAMs (0.57mN ± 0.19mN). There was no significant difference in the passive forces between any of the sets of BAMs.

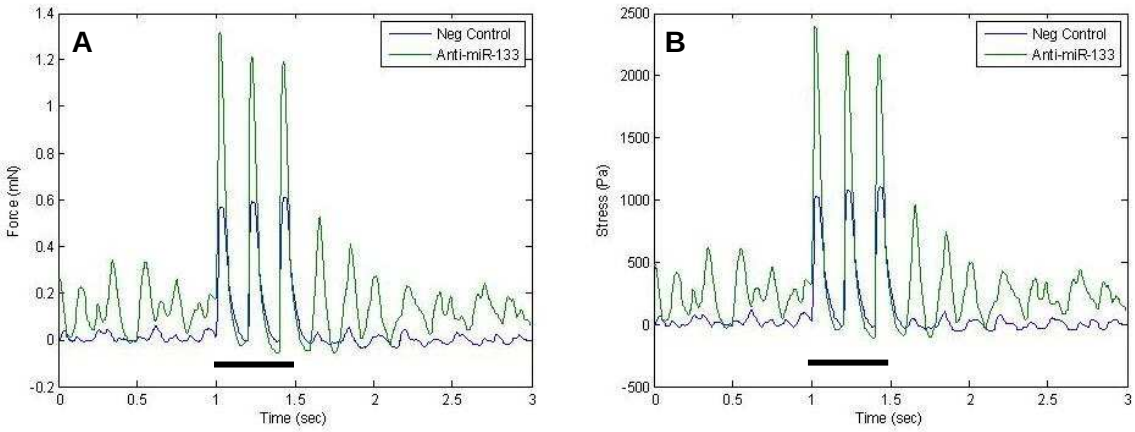

Figure 5.13 Functional force measurements at a stimulation frequency of 5 Hz for BAMs cultured with negative control and anti-miR-133a myoblasts. Data is presented as (A) force output, mN and (B) stress output, Pa, where cross-sectional area was considered. The bold black line segment signifies the time period of electrical stimulation.

For statistical verification, independent BAM forces were measured, and the ratio of peak force output over its corresponding negative control BAM forces were analyzed. Figure 5.14 shows that this ratio is statistically different than a ratio of 1 with forces and stresses generated by electrical stimulation at frequencies below 10Hz. While the ratio

of peak force output of miRNA-mediated BAMs at a stimulation frequency of 20Hz was generally greater than 1, the ratio was not statistically significant.

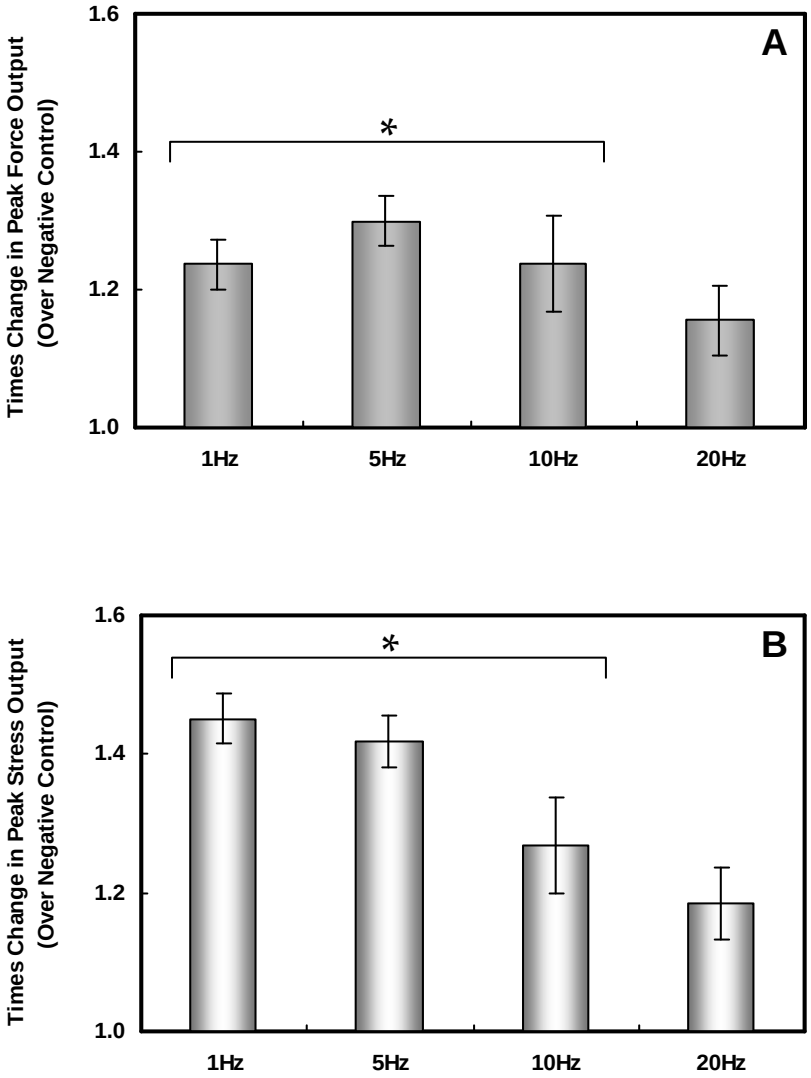

Figure 5.14 Bar graph showing ratio of peak (A) force and (B) stress of anti-miR-133 BAMs over negative control BAMs cultured for 6-8 days in DM. At stimulation frequencies of 1Hz, 5Hz, and 10Hz, the peak force and stress ratios were significantly greater than a ratio of 1 (no difference). Mean ± SEM, n=5, *p<0.05.

Although the ratio of stress is higher than the ratio of forces, there was no trend in cross-sectional area of the BAMs, but the differences are attributed to some difference in these areas over independent experiments.

Over-expression of miR-1 did not provide consistent results with our current model while inhibition of miR-133 led to increased forces and stresses exhibited by BAMs in response to electrical stimulation. These two approaches may shed light on using inhibition versus over-expression in a clinical setting. The results do show that transient miRNA mediation may be one way to exogenously affect myoblast differentiation at early stages of muscle maturation, even after presence of the added miRNA molecules has diminished.

5.4 Discussion

In this study we tested the hypothesis that transient transfection of miRNA precursors (over-expression) or inhibitors (knockdown) in a bioartificial muscle (BAM) system, would modulate muscle function. miR-1, which promotes differentiation in skeletal muscle, was over-expressed using chemically modified precursor molecules (pre-miR-1). miR-1 overepxression did not affect cell morphology. Although force output was higher in pre-miR-1 BAMs over its corresponding negative control BAMs at times, statistical significance was not reached because of inconsistent results.

On the other hand, BAMs were also cultured with myoblasts that had been transiently transfected with miR-133 inhibitors (anti-miR-133). The anti-miR-133 BAMs produced more organized fibers, as assessed by H&E histological stains as well as myosin and alpha-actinin immunostaining. Fiber diameters were also larger in anti-miR-133 BAMs compared to the negative control. The presence of the exogenous miRNAs (precursors or antimiRs) were diminished by shift day 0, but interestingly, the peak force output of the anti-miR-133 BAMs was, on average, 20% higher than its negative control.

Our results with over-expressing miR-1 in tissue engineered skeletal muscle constructs were not as clear as with the miR-133 inhibition. Not surprisingly, there was more variability in controlling the degree of over-expression, which was also observed in the 2D system and may be due to lower transfection efficiencies. In addition, the

over-expression of miR-1, which theoretically should further enhance differentiation, does not keep proliferation at bay. These results may have been due to the nature of the miRNA mimics, which are chemically modified, double-stranded nucleic acids whereas the anti-miRs used for the inhibition studies were single-stranded. The former is larger, and hence, has lower transfection efficiencies and also must go through further processing within the cell to function as a mature miRNA. Further tuning of the over-expression protocol may lead to more stable results, but these studies also show that miRNA mediation with anti- or antagomirs may be the more relevant approach to take.

The forces observed in our BAM constructs were on the same order of magnitude as others have reported for primary cells [63, 64, 124], as there were no direct comparisons using a pure myoblast cell line. Constructs cultured with primary human myoblasts in a collagen gel had passive forces (without electrical stimulation) in the 0.5mN range [124], which were slightly higher than our passive forces. Engineered skeletal muscle, cultured from slow soleus rat and fast tibialis anterior rat myoblasts up to 28 days, displayed forces on the average of 0.3mN [64], and rat myoblasts cast into a fibrin gel produced constructs that exhibited maximum twitch on the order of 0.3mN [63], which was in the same range as our passive forces.

Importantly, our results are the first to show that transient inhibition of miR-133a produced higher functional force outputs. Since miR-1 and miR-133 are highly involved in the developmental process of skeletal muscle maturation, continuous alterations or

gross deviations from baseline levels may lead to detrimental results. In our system, transient transfection was used one day before BAMs were cast into their collagen gels, and this appeared to provide sufficient time to allow for proliferation to be halted when it otherwise would have continued. With this, differentiation and subsequent myoblast fusion and myofiber maturation were able to commence earlier in the anti-miR-133 BAMs. Continuous injection of anti-miR-133a in mice inhibited miR-133 and led to cardiac hypertrophy [27]. Consistent with these results, we found that a transient block on miR-133 expression was enough to produce a hypertrophic response as larger fiber diameters were observed (Figure 5.12). However, whereas the previous study used continuous injection of antagomirs, in our study, the levels of anti-miR-133 nucleic acids were very low by shift day 0 or soon after. As shown by our experiments in chapter 4 and by others [34], miR-133 increases dramatically over time as the cell differentiates in tandem with miR-1, even though its main purpose is to promote proliferation. By inhibiting it in the early stages, we expected that the higher ratio of miR-1 to 133a would promote the differentiation cascade. This suggests that using anti-miRs in the early stages of muscle development may lead to a more differentiated construct, even without constant perfusion of nucleic acid moieties. Similar to this, others have suggested that single injections of a given antagomiR are sufficient to have an effect on its downstream target [163, 164]. This suggests that miR-133a acts at an early stage in the process of differentiation. Whereas a transient inhibition of miR-133 in the beginning stages of

myoblast fusion and maturation may enhance the differentiation process, continuous inhibition may lead to deleterious effects as shown by the Care *et al.* study. Therefore, the approach of using nonviral and transient delivery of oligonucleotides may be a better treatment option for miRNA-dependent disease states.

In addition to functional changes, some morphological differences were noted as well. When miR-133 was inhibited, fiber diameter increased compared to the negative control. In a cardiac mouse model, hypertrophy occurred when miR-133 was inhibited continuously for a period of 1 month [27]. But, unlike cardiac tissue, skeletal muscle has satellite cells that have regenerative properties and can ultimately repopulate a damaged area. Therefore, hyperplasia cannot be excluded at this point, even though our reasonable assumption is that a small degree of hypertrophy is occurring with an initial inhibition of miR-133 since proliferation is somewhat suppressed.

To examine excitability, the functional force outputs of the BAM constructs were measured with varying stimulation frequencies, and the values obtained corresponded with previous studies (Figure 5.2). Several different approaches have been utilized in attaining a more native muscle structure in vitro and include using combinations of cells and matrices, mechanical and electrical stimulation over time, and changes to surface morphology [40, 63, 64, 82, 124, 183]. Passive forces in myooids cultured with C2C12 myoblasts and $10T_{1/2}$ fibroblasts were found to be 0.37mN ± 0.05mN, neonatal rat constructs had forces 0.31mN ± 0.03mN, and adult rat soleus myooids forces were lower

at 0.12mN ± 0.03mN [40]. Engineered skeletal muscle, cultured from slow soleus rat and fast tibialis anterior rat myoblasts up to 28 days with 14 days of electrical stimulation (5 electrical pulses every 4s at 20Hz), produced higher forces in soleus muscle (0.55mN versus 0.3mN for no electrical stimulation) [64], which was in the same range as our results (see Figures 5.2, 5.7, 5.13). Rat myoblasts cast into a fibrin gel produced constructs that exhibited maximum twitch and tetanic forces on the order of 0.3mN and 0.8mN, respectively [63]. When grown on an aligned collagen gel matrix, engineered skeletal muscle strips produce similar forces, but had a lower maximal tetanic force at 0.5mN with a 100Hz stimulation frequency [183]. Differences were also observed between unaligned and aligned matrices (0.14 ± 0.05mN versus 0.31 ± 0.09mN average tetanic forces) [82]. In terms of stress, myooids grown up to 40 days with fetal and adult rat myoblasts exhibited stresses of 1-4 kPa [74], and similar stresses were observed with those cultured with a mixture of C2C12 myoblasts and $10T_{1/2}$ fibroblasts [40]. The stresses seen with our constructs are on the same order of magnitude.

However, compared to native muscle, there still is much progress that needs to be made. At its maximum contraction, native muscle exhibits forces on the order of 300-400kPa [71], but it is also critical to note that nearly all engineered skeletal muscle contain 'voids' of matrix or remnant gel which detract from the overall force output. In our case and others, we were unable to attain consistent tetanus with a pure C2C12 myoblast population, as the constructs were unable to maintain constant forces when

stimulation frequencies were above 20Hz. To date, the tissue-engineered models which show tetanic forces have involved a myoblast cell line mixed with a fibroblast population or constructs cultured with primary myoblasts. Our results explain the absence of mature neuromuscular junctions, which allows myofibers to respond to an electrical impulse [87]. However, it is key to note that the forces of these constructs were measured at extremely early time points where maturation of muscle fibers is just beginning. Additionally, myotube formation remained isolated to the outer periphery of the BAM, thereby, making the effective cross-sectional area smaller than the entire cross-sectional area of the collagen gel. Myofiber organization was also not completely parallel and densely packed as in native muscle, and is a major issue to be addressed in subsequent studies and tissue engineering models. But, in spite of these shortcomings, exogenous and transient delivery of miRNAs may be a viable way to modulate skeletal muscle function.

5.5 Conclusions

This is the first study that demonstrates that miRNA mediation has a downstream functional effect on tissue-engineered constructs. While other studies have focused on continuous or stable transfections on various tissues, our results show that differentiation of skeletal myoblasts *in vitro* may be enhanced by transient transfections of miRNAs. Peak forces exhibited by anti-miR-133 BAMs were, on average, 20% higher

than its corresponding negative control to electrical stimulation (from 0Hz to 20H), and reponses to electrical stimulation in miRNA-mediated BAMs (along with negative controls) were similar to non-transfected controls. Immunostaining also showed more distinct striations and myofiber organization in BAMs with miR-133 inhibition over the negative control. Fiber diameters were also significantly larger in these BAMs over both the non-transfected and negative controls. While over-expression of miR-1 did produce higher forces, a significant difference was not elucidated as inconsistent responses were more common with over-expression of miRNAs than inhibition. This study highlights the possibilities of non-viral, miRNA transfection to change downstream function *in vitro*, and eventually *in vivo*.

5.6 Acknowledgements

The authors would like to thank I-Chien Liao and Dr. Kam Leong for use of their force testing machine along with Matt Brown for configuring the Labview code. We would also like to thank Nima Badie for his expertise in Matlab as well. The MF-20 mouse monoclonal antibody developed by Donald A. Fischman, M.D. was obtained from the Developmental Studies Hybridoma Bank developed under the auspices of the NICHD and maintained by The University of Iowa, Department of Biological Sciences, Iowa City, IA 52242. Funding was provided by the McChesney Foundation and NIH Grant R21-AR55195.

6. Conclusions and Future Work

6.1 Conclusions

The driving force behind this research was to address two of the many factors important in muscle cell proliferation and differentiation, toward developing mature bioartificial skeletal muscle (BAMs). Our work focused on understanding the individual effects of mechanical stimulation and microRNAs (miRNAs), as well as the synergistic relationship between the two factors. We hypothesized that (1) myoblast proliferation and differentiation is modulated by mechanical stimulation via temporally regulated miRNAs and that (2) modulating these miRNAs can enhance skeletal muscle function in a 3D tissue-engineered system.

In **Chapter 2**, we first established a tissue-engineered skeletal muscle system to promote myofiber formation and maturation in a 3D model using a pure mammalian C2C12 myoblast cell line. Fluorescence and immunostaining verified that mature, striated muscle fibers were formed from a stable mammalian cell line, as early as shift day six (or six days in differentiation media, DM). Viable and mature cultures, or BAMs were maintained for 6 to 36 days in DM. Transmission electron microscopy (EM) provided conclusive evidence that mature sarcomeres had formed as early as shift day 16, and the beginning stages of myotendinous junction formation and newly synthesized collagen I fibers were apparent by shift day 33. With this first study, we established a

3D BAM culture model that could be used to evaluate the effects of various mechanical, biochemical, and biological cues on muscle development and maturation.

In **Chapter 3**, we focused on addressing the first hypothesis and surveyed the possible effects of mechanical stimulation on miRNA expression. Using the commercially available Flexercell™ system, silastic-bottomed six-well plates were plated with differentiating myoblasts and cyclically stretched with a moderate strain regimen (0.5Hz, 10% strain for 1 hour with a 5-hour rest period). This regimen has been previously shown to promote myoblast differentiation in C2C12 skeletal myoblasts in our lab. Through microarrays printed with over 650 miRNA probes, we found several leading candidate miRNA that showed a 1.5 to 2-fold difference between stretched and unstretched samples. Not surprisingly, cell age affected the results, specifically in the correlation of microarray data to the qRT-PCR results. Initial miRNA microarray studies presented possible candidates for stretch-induced miRNAs, such as miR-125b, 422b, and 31. However, subsequent qRT-PCR studies failed to detect significant effects of stretch upon these miRNAs. A single experiment was done using an older lot of cells (passage 6), where expression of miR-206 was unchanged with stretch. Stretch did seem to elevate expression of miR-1 and miR-133 over time in the older, passage 6 cells, but there was no statistically significant difference. In contrast, the use of a newer lot of cells (passage 3) produced less variability with stretch and significant upregulation of miR-1, miR-133a, and miR-206 with a moderate strain regimen, with a notable difference in the

stretch-induced effect on miR-206 expression in the newer cells. We chose to first focus on the three key muscle-specific miRNAs to show a link between stretch and miRNA regulation and in the future, look toward pursuing novel, stretch-sensitive miRNAs.

In **Chapter 4**, a comprehensive study was launched to fully address the first hypothesis and characterize the temporal effect of mechanical stimulation on miRNA expression in differentiating myoblasts. Based on the preliminary results in Chapter 3 and published literature, we focused on three validated, muscle-specific miRNAs – miR-1, miR-133, and miR-206 – and various muscle-related genes, such as MyoD, myogenin, SRF, HDAC4, and Mef2c. Our system demonstrated a differential response of skeletal myoblasts to moderate and high strain cyclic stretch regimens. Myoblast maturation was enhanced only with the moderate strain regimen, as assessed morphologically and quantitatively with a higher myogenic fusion index. While neither strain regimen had significant effects on muscle-specific genes, such as MyoD and myogenin, only the moderate strain regimen saw a decrease in SRF gene expression at shift day 2 and an increase in Mef2c gene expression by shift day 6. Corresponding to these results, HDAC4 protein expression, a direct target of miR-1 and repressor of Mef2, was decreased with the moderate strain regimen, and the effect was most pronounced by shift day 6. The high strain regimen showed no difference in miR-1, 133a, and 206 expression with stretch, while there was a significant effect of stretch ($p<0.05$) after 3 or 4 days, post-differentiation, with the moderate strain regimen.

To further clarify the relationship between cyclic stretch and miRNA expression, miR-1 was both over-expressed and inhibited in myoblasts that were exposed to the moderate strain regimen. Over-expression of miR-1 abrogated the effect of stretch at shift day 2 compared to its negative control and did not accelerate the effect of a stretch-mediated response in altering miRNA levels. By shift day 4, the levels of miR-1 in both transfected sets (pre-miR-1 and negative control) had equilibrated to the same levels; therefore, transient transfection would have the biggest impact on the transcription factors involved in the early stages of muscle development, regardless of the application of stretch. In our case, there was an effect of stretch observed with SRF with the moderate strain regimen and also a notable increase in myogenin (in stretched and unstretched samples of both stretch regimens) at early time points.

Inhibition of miR-1 similarly diminished the stretch-mediated response. The current results suggest that the balance of miRNAs and various transcription factors are crucial in promoting a response to stretch. In contrast to the sometimes abrupt action of transcription factors (on-off switch), miRNAs may be acting by balancing the expression of their targets around a stable expression set point [92]. Assuming a steady state, our results correlate to the mathematical model described by Levine *et al* [91, 92]. The effect of miRNA expression is significant in the case where mRNA and/or protein degradation is low compared to its synthesis. While this situation is within a narrow range, miRNA can have a large effect on its downstream target protein levels.

As we modulated miR-1 levels, the threshold levels at which its target, HDAC4, was expressed were also changed in a way such that a stretch-induced effect was quenched. Because of this balancing effect to minimize external changes in the system, we chose to focus on using miRNA modulation alone in our last set of studies (Chapter 5) to promote differentiation in our 3D BAM system.

Finally, in **Chapter 5**, we addressed the second hypothesis by examining the functional effect of modulating miRNAs in the more complex tissue engineered skeletal muscle system developed in Chapter 2. This work was the first study to demonstrate that miRNA mediation has a downstream functional effect on tissue-engineered constructs. While other studies have focused on the effects of continuous or stable transfections on various differentiated tissues, our results show that differentiation of skeletal myoblasts *in vitro* may be enhanced by transient transfections of miRNAs. We targeted miR-133 inhibition and miR-1 over-expression as two methods by which differentiation could be accelerated or enhanced. On average, peak forces exhibited by anti-miR-133 BAMs were 20% higher than its corresponding negative control in response to electrical stimulation (from 0Hz to 10Hz). By shift day 6 to 8, immunostaining showed more distinct striations and myofiber organization in BAMs with miR-133 inhibition over the negative control, and fiber diameters were also significantly larger in these BAMs over both the non-transfected and negative controls. While over-expression of miR-1 did produce BAMs generating higher forces, a

significant difference was not elucidated, as variable responses were more common with over-expression than inhibition of miRNAs. This study highlighted the viability of using a non-viral, miRNA transfection to change downstream function *in vitro*.

6.2 Future Work

Through this work, we confirmed that mechanical signals outside the cell membrane can affect the expression of miRNAs inside the cell, and to date, only one other study has shown this link [78]. While we have demonstrated that three muscle-specific miRNAs (miR-1, miR-133, and miR-206) are expressed differently depending on the stretch regimen to which the myoblasts are exposed, the exact mechanism remains unclear. We proposed an indirect mechanism through Mef2c, but titrated, knockdown studies combined with stretch would need to be completed to definitively attribute changes in miRNA expression to changes in Mef2c which arise from mechanical stimulation. Additionally, a complex interplay among miRNAs, mRNAs, and other proteins exists, and there are many secondary messengers and signaling pathways that could be affected by mechanical stimulation, in turn affecting miRNA expression. Therefore, a DNA microarray study and subsequent pathway analysis might be useful to scan for gene profiles that change with stretch (both moderate and high strains).

Perhaps the most urgent future work, however, is switching from the C2C12 cell line to primary cells, preferably human or mouse myoblasts. While the C2C12

myoblasts have been an excellent and valid model to start this work, the future direction of miRNA therapies will rely on data gathered from primary cells and its ultimate effect in the *in vivo* environment. Special care will need to be taken to ensure these cells do not go through many population doublings, since cell age, even with an immortalized cell line, has a deleterious effect on miRNA expression.

Furthermore, our preliminary miRNA microarray studies showed some evidence of novel, stretch-induced miRNAs as well as miRNA that displayed a different temporal profile than other muscle-specific miRNAs (e.g. miR-31). A more extensive set of microRNA microarray studies using lower passage primary myoblasts should be completed and possibly correlated to some of the novel miRNAs found in the preliminary results, followed by qRT-PCR analysis.

While transient transfection is an attractive approach to modulating miRNAs *in vitro* and possibly *in vivo*, the effects are lost at early time points with the current system. It is possible that mediating miRNAs at different times, still in a transient manner, may enhance the desired effect (myoblast function in our work). Hence, an attempt to control the release of various exogenous miRNAs may have a similar effect and thus be worth the challenge. Taking novel approaches to establish the desired cellular effects, while keeping the balanced relationship between miRNAs and their targets in mind, may be the key to creating the next generation of *in vitro* constructs that more closely resemble native skeletal muscle.

Appendix A: Oxygen Diffusion through Bioartificial Muscle

Calculations estimating oxygen diffusion through the BAM were derived from Krogh's cylinder model. The constitutive equation is shown below:

$$\frac{D_{O_2}}{r}\frac{d}{dr}\left(r\frac{dC_{O_2}}{dr}\right) = R_{O_2} \qquad (1)$$

where D_{O_2} is the diffusion coefficient of oxygen, C_{O_2} is the oxygen concentration in the tissue, and R_{O_2} is the oxygen consumption per volume of cells. Boundary conditions were set by approximating zero flux at the center of the construct, estimating equivalent oxygen concentration in the tissue and the media at the outermost edge of the BAM, and approximating a negligible rate of oxygen consumption in the inner portion of the gel where little to no metabolically active cells reside. The resulting equation reduced from these conditions is:

$$\frac{1}{\phi^2} = -(\eta^2 - 1) + 2\eta^2 \ln\frac{1}{\eta} \qquad (2)$$

where $\eta = \frac{R_c}{R_o}$ and $\phi^2 = \frac{R_{O_2} R_o^2}{4 D_{O_2} C_B}$.

The maximum radial distance, R_o, in which cell survival would be maintained occurs when C_{O_2} = 0 at the center of the BAM (r = 0). General approximations were taken where the diffusion coefficient, D_{O_2}, in tissue and assumed for culture medium is 2.0 x 10^{-5} cm^2 s^{-1}, [13, 57] and the oxygen concentration at the BAM surface and in the surrounding media ($C_B = C_{O_2}$) is equivalent to oxygen concentration in blood plasma at 1.34 x 10^{-7} mol cm^{-3}. For the BAMs cultured in this study, η primarily ranged from 0.77 to 0.95, with an overall thickness ranging from 700-800μm. The oxygen consumption rate, R_{O_2}, was estimated to be in the 10^{-9} to 10^{-8} mol cm^{-3} s^{-1} range. Although lower than values obtained for skeletal muscle in vivo (10^{-7} mol cm^{-3} s^{-1}), the rate of oxygen consumption within this in vitro system is higher than those reported in other C_2C_{12} cell culture studies where in vitro consumption rates were in the range of 10^{-11} and 10^{-13} mol cm^{-3} s^{-1} using a maximum cell density approximation (10^7 cells ml^{-1}) [58, 108]. These generalized calculations suggest that oxygen is a limiting factor in the 3D culture of bioartificial muscle; however, further experimental data is needed to verify these theoretical results.

Appendix B: Primer Sequences for Quantitative Real Time RT-PCR

Gene of Interest	Forward Primer	Reverse Primer
18S	TCAACTTTCGATGGTAGTCGCCGT	TCCTTGGATGTGGTAGCCGTTTCT
MyoD	GTGCATTCCAACCCACAGAACCTT	TGCTGTCTCAAAGGAGCAGAGAGA
Myogenin	ACAATCTGCACTCCCTTACGTCCA	TCTCAGTTGGGCATGGTTTCGTCT
Mef2c	AGGATCACCGGAACGAATTCCACT	GCATGCGCTTGACTGAAGGACTTT
HDAC4	AACTTCTTCCCAGGAAGTGGAGCA	GGGCAAACTCATTTGCGATAGGCA
SRF	ACCTTTCTGGCCTTTCTCCTGGAA	AAGCACTTGGCCTGAATCACTTGC

Appendix C: MatLab Code for Force Measurements

BAMforce.m

```
% BAMforce.m
% General code for analyzing functional force measurement for BAMs

% Get list of Labview files (.txt files) from appropriate directory
dirname = uigetdir;
all_filenames = dir(dirname);
filelist=[];
filelist{1}=[];
cnt=1;
for f=3:length(all_filenames)
    filename = all_filenames(f).name;
    if (strcmp(filename(end-2:end),'txt'))
        filelist{cnt} = filename;
        cnt=cnt+1;
    end
end

% Create array for all repeated measures within a given frequency
num_files = length(filelist);
all_force = zeros(5000,num_files);

for f=1:num_files
    filename = filelist{f};

    % Load in header
    hdr = dlmread([dirname '\' filename],'\t',0,1);

    % Load in force measurements
    all_force(1:5000,f) = dlmread([dirname '\' filename],'\t',6,0);
    force = dlmread([dirname '\' filename],'\t',6,0);

end

% Load in each file & makes plots for each
for f=1:num_files
    filename = filelist{f};

    % Account for header
    hdr = dlmread([dirname '\' filename],'\t',0,1);
    run_time = hdr(1);
    samp_rate = hdr(2);
    duty_cycle = hdr(3);
    pulse_freq = hdr(4);
    pulse_delay = hdr(5);
```

```
    % Correct for drift in force measurements - works only when
spontaneous twitch minimized, check each plot before choosing this
filtering (all_force vs. all_F_corr)
    F_corr=force-mean(force(1:1000));
    all_F_corr=all_force-repmat(mean(all_force(1:100,:)),5000,1);

    % Define x-scale
    t = [0:(length(force)-1)]/samp_rate;

    % Peak Force
    F_peak=max(force);
    F_peak_corr=max(F_corr);

    % Average replicate plots of peak force
    F_peakavg=mean(F_peak)
    F_peakavg_corr=mean(F_peak_corr)

    % Plots
    figure('name',filename,'color','w','position',[0 100 1514 358])
    % Plot 1: Plot of Force vs. Time
    subplot(1,3,1)
    plot(t, all_force(:,f))
    xlabel('Time (sec)')
    ylabel('Force (mN)')
    title('BAM Force Output')

    % Plot 2: Plot of Corrected (Averaged) Force vs. Time
    subplot(1,3,2)
    plot(t, all_F_corr(:,f))
    xlabel('Time (sec)')
    ylabel('Corrected Force (mN)')
    title('BAM Corrected Force Output')

    area = 0.848;  % Cross-sectional area of the construct (mm^2)
    % stress = all_force/area*1000;
    stress_corr = all_F_corr/area*1000; %Switch if necessary


   % Plot 3a: Plot of Stress (Pa) vs. Time
    subplot (1,3,3)
    plot (t, stress_corr (:,f))
    xlabel('Time (sec)')
    ylabel('Stress (Pa)')
    title('BAM Stress Output')

    % Plot 3b: Plot of Corrected Stress (Pa) vs. Time
%     subplot (1,3,3)
%     plot (t, stress_corr (:,f))
%     xlabel('Time (sec)')
%     ylabel('Corrected Stress (Pa)')
%     title('BAM Corrected Stress Output'
```

BAMforce_freq.m

```
% BAMforce_freq.m
% Functional force measurement for BAMs
% Plotting force measurements (force & stress) of one construct in a
single plot, at varying frequencies

% Get list of Labview files (.txt files) from appropriate directory
dirname = uigetdir;
i = find(dirname=='\',1,'last');
construct_name = dirname(i+1:end);
dirs = [];

% Can modify based on which frequencies desired on plot, but the
dirs(n) has to be changed accordingly…start with dirs(1) always
dirs{1} = [dirname '\' construct_name '_0Hz'];
dirs[27] = [dirname '\' construct_name '_1Hz'];
dirs{3} = [dirname '\' construct_name '_5Hz'];
dirs{4} = [dirname '\' construct_name '_10Hz'];
dirs{5} = [dirname '\' construct_name '_20Hz'];
area = dlmread([dirname '\area.txt'],'\t',0,0);

mean_force = zeros(5000,length(dirs));
for freq=1:length(dirs)    % For each stimulation frequency

 % Get all files associated with given frequency
    all_filenames = dir(dirs{freq});
    filelist=[];
    filelist{1}=[];
    cnt=1;
    for f=3:length(all_filenames)
        filename = all_filenames(f).name;
        if (strcmp(filename(end-2:end),'txt'))
            filelist{cnt} = filename;
            cnt=cnt+1;
        end
    end

    % Extract data from all files for given frequency
    num_files = length(filelist);
    all_force = zeros(5000,num_files);
    for f=1:num_files
        filename = filelist{f};

% disp([dirs{freq} '\' filename]) %Returns program path for targeted
      debugging

        hdr = dlmread([dirs{freq} '\' filename],'\t',0,1);
        run_time = hdr(1);
        samp_rate = hdr(2);
        duty_cycle = hdr(3);
```

```
        pulse_freq = hdr(4);
        pulse_delay = hdr(5);
        all_force(:,f) = dlmread([dirs{freq} '\' filename],'\t',6,0);
    end

    % Correct baseline (first check with BAMforce.m)
    all_force_corrected = zeros(size(all_force));
%     F_corr=force-mean(force(1:100));  Alternative methods of
            correcting baseline
%     all_F_corr=all_force-repmat(mean(all_force(1:100,:)),5000,1);

for f=1:num_files
        force_uncorrected = all_force(:,f);
        sorted_force_uncorrected = sort(force_uncorrected(1:100));
        min_value = median(sorted_force_uncorrected(1:100));
        force_corrected = force_uncorrected - min_value;
       % figure,plot(diff(force_corrected))
        all_force_corrected(:,f) = force_corrected;
    end

    % Average each time point
    % Each column shows forces for a given frequency (0,1,5,10,20)
    mean_force(:,freq) = mean(all_force_corrected,2);

    % Output Peak Force
    disp(['Peak force = ' num2str(max(mean_force(1000:1500,freq)))]);
end


% Plot #1: Force
t_end = 3000;   % end sample point to plot
t = [0:t_end-1]/samp_rate; % Define x-scale
figure('color','w');
plot(t,mean_force(1:t_end,:));
xlabel('Time (sec)')
ylabel('Force (mN)')
title('BAM Force Output')
% Change accordingly
legend('0 Hz','1 Hz','5 Hz','10 Hz', '20Hz');

% Plot #2: Stress
mean_stress = 1000*mean_force/area;
figure('color','w');
plot(t,mean_stress(1:t_end,:))
xlabel('Time (sec)')
ylabel('Stress (Pa)')
title('BAM Stress Output')
% Change accordingly
legend('0 Hz','1 Hz','5 Hz','10 Hz', '20Hz');
```

```
% Plot #3: Single Plot with two y-axes (Force & Stress)
figure('color', 'w');
[ax,h1,h2] = plotyy(t,mean_force(1:t_end,:),t,mean_stress(1:t_end,:))
set(get(ax(1),'xlabel'),'string','Time (sec)')
set(get(ax(1),'ylabel'),'string','Force (mN)')
set(get(ax(2),'ylabel'),'string','Stress (Pa)')
legend('0 Hz','1 Hz','5 Hz','10 Hz', '20Hz');
```

BAMforce_comp.m

```
%BAMforce_comp.m
%Functional force measurement for BAMs – comparing one BAM to another
(e.g. negative control to anti-miR-133)

% Get list of Labview files (.txt files) from appropriate directories
dirs_construct=[];
dirs_construct{1} = ‘Insert full file path for construct #1;
dirs_construct[27] = ‘Insert full file path for construct #2;
dirs_construct{3} = ‘Insert full file path for construct #3;

freq = '5Hz';

mean_force = zeros(5000,length(dirs_construct));
for c=1:length(dirs_construct)
    dirname = dirs_construct{c};
    i = find(dirname=='\',1,'last');
    construct_name = dirname(i+1:end);
    dirs = [dirname '\' construct_name '_' freq];
    area = dlmread([dirname '\area.txt'],'\t',0,0);

    % Get all files associated with given frequency
    all_filenames = dir(dirs);
    filelist=[];
    filelist{1}=[];
    cnt=1;
    for f=3:length(all_filenames)
        filename = all_filenames(f).name;
        if (strcmp(filename(end-2:end),'txt'))
            filelist{cnt} = filename;
            cnt=cnt+1;
        end
    end

Same remaining code as BAMforce_freq.m to filter and plot curves.
```

Appendix D: Copyright Releases

Wolters Kluwer
Health
530 Walnut Street
Philadelphia, PA 19106
215 521 8458 tel
www.LWW.com

06/05/09

INVOICE AND CONDITIONS

CAROLINE RHIM
DUKE UNIVERSITY
DEPT OF BIOMEDICAL ENGINEERING
PO BOX 90281
DURHAM, NC 27708-0281

Invoice # P55313166 Customer # 000162563769 FEE: 0.00
Re: LIEBER, SKELETAL MUSCLE STRUCTURE 2E
Spec Mat: Doctoral Dissertation, pg. 18-19; Figs 1-6&1-7 (matl must be orig to bk, no other source cited)

Permission is granted for your requested use. Please sign and date this form and return with payment (if applicable) in the enclosed envelope. Please retain a copy for your files. This permission is subject to the following conditions:

1) A credit line will be prominently placed and include: for books - the author(s), title of book, editor, copyright holder, year of publication; for journals - the author(s), title of article, title of journal, volume number, issue number and inclusive pages.

2) The requestor warrants that the material shall not be used in any manner which may be considered derogatory to the title, content, or authors of the material or to LWW.

3) Permission is granted for one time use only as specified in your correspondence. Rights herein do not apply to future reproductions, editions, revisions, or other derivative works.

4) Permission granted is non-exclusive, and is valid throughout the world in the English language only.

5) LWW cannot supply the requestor with the original artwork or a "clean copy."

6) The requestor agrees to secure written permission from the author (for book material only).

7) Permission is valid if the borrowed material is original to a LWW imprint (Lippincott-Raven Publishers, Williams & Wilkins, Lea & Febiger, Harwal, Igaku-Shoin, Rapid Science, Little Brown & Company, Harper & Row Medical, American Journal of Nursing Co, and Urban & Schwarzenberg - English Language).

8) Payment can be made via credit card (Amex, VISA, Discover and MC) or by check.

Card # N/A Exp Date: N/A

Signature: Caroline Rhim Date: 06/09/09

Johnson, Bradley - Hoboken

From: Caroline Rhim [caroline.rhim@duke.edu]
Sent: Sunday, May 31, 2009 11:15 PM
To: Johnson, Bradley - Hoboken
Subject: Re: FW: Question about using published material

Hi Brad, Attn: caroline

I just wanted to follow up with you since I have not yet received the fax. Our fax is: 919.684.4488 (attn: Caroline Rhim, Duke University, Department of Biomedical Engineering)

Thank you,
Caroline Rhim

On Tue 05/12/09 11:58 AM , "Johnson, Bradley - Hoboken" <bjohns@wiley.com> wrote:

> Caroline,
> What is the complete citation of our article in question? I will fax
> our approval and you will not be required to fill out our online form.
> Thanks.
> Brad Johnson, Permissions Assistant - John Wiley & Sons Inc. - 111
> River St. - Hoboken, NJ 07030 - Mail Stop 4.02 - Ph: 201.748.6786 -
> Fax: 201.748.6008 -
> Visit our website for permissions information ——Original
> Message——
> From: Krouser, Gale - Hoboken
> Sent: Tuesday, May 12, 2009 11:29 AM
> To: Johnson, Bradley - Hoboken
> Subject: FW: Question about using published material Help, see below.
> Thanks and best regards,
> Gale
> (Ms.) Gale Krouser
> Reprint Specialist
> John Wiley & Son, Inc.
> Reprint Department, MS 3-14
> 111 River Street
> Hoboken, NJ, 07030
> Phone 201 748-8789
> Fax 201 748-6326
> ——Original Message——
> From: caroline.rhim@duke.edu []
> Sent: Monday, May 11, 2009 9:51 AM
> To: Krouser, Gale - Hoboken
> Cc:
> Subject: Question about using published material Hi Gale, I had a
> quick question, but did not know if you were the person I should
> contact. I am a graduate student at Duke University and am planning
> on defending my dissertation in the near future. I published a
> manuscript in Muscle and Nerve in 2007 and would like to include some
> of that material in my dissertation. Since our thesis is publicly
> available, I need to know how to get approval. I also plan on putting
> an embargo on my thesis for 2 years (in order to publish other
> manuscripts), which means that the information will not be available
> online for another few years.
> I believe that I need to fill out a permission request form (which I
> do have), but I would appreciate your help directing me to the right
> place!

PERMISSION GRANTED 6/9/09
BY: _____
Global Rights Dept., John Wiley & Sons, Inc.

NOTE: No rights are granted to use content that appears in the work with credit to another source

References

1. Abraham, M.R., et al., *Antiarrhythmic engineering of skeletal myoblasts for cardiac transplantation.* Circ Res, 2005. **97**: p. 159-67.
2. Acker, M.A., et al., *Skeletal muscle as the potential power source for a cardiovascular pump: assessment in vivo.* Science, 1987. **236**: p. 324-327.
3. Ambros, V., *The functions of animal microRNAs.* Nature, 2004. **431**(7006): p. 350-5.
4. Aravin, A. and T. Tuschl, *Identification and characterization of small RNAs involved in RNA silencing.* FEBS Lett, 2005. **579**(26): p. 5830-40.
5. Baar, K., et al., *Adaptations of skeletal muscle to exercise: rapid increase in the transcriptional coactivator PGC-1.* Faseb J, 2002. **16**(14): p. 1879-86.
6. Bach, A.D., J.P. Beier, and G.B. Stark, *Expression of Trisk 51, Agrin and Nicotinic-Acetycholine Receptor e-subunit During Muscle Development in a Novel Three-Dimensional Muscle-Neuronal Co-culture System.* Cell Tissue Res, 2003. **314**: p. 263-274.
7. Bandres, E., et al., *Identification by Real-time PCR of 13 mature microRNAs differentially expressed in colorectal cancer and non-tumoral tissues.* Mol Cancer, 2006. **5**: p. 29.
8. Barani, A.E., et al., *Age-related changes in the mitotic and metabolic characteristics of muscle-derived cells.* J Appl Physiol, 2003. **95**(5): p. 2089-98.
9. Bartel, D.P., *MicroRNAs: genomics, biogenesis, mechanism, and function.* Cell, 2004. **116**(2): p. 281-97.
10. Bartel, D.P., *MicroRNAs: target recognition and regulatory functions.* Cell, 2009. **136**(2): p. 215-33.
11. Baskerville, S. and D.P. Bartel, *Microarray profiling of microRNAs reveals frequent coexpression with neighboring miRNAs and host genes.* Rna, 2005. **11**(3): p. 241-7.
12. Beach, R.L., et al., *Extracellular Matrix Synthesis by Skeletal Muscle in Culture.* J Biol Chem, 1982. **257**(19): p. 11437-11442.
13. Bentley, T.B., H. Meng, and R.N. Pittman, *Temperature dependence of oxygen diffusion and consumption in mammalian striated muscle.* Am J Physiol, 1993. **264**: p. H1825-30.
14. Bentwich, I., *Prediction and validation of microRNAs and their targets.* FEBS Lett, 2005. **579**(26): p. 5904-10.
15. Berezikov, E., E. Cuppen, and R.H. Plasterk, *Approaches to microRNA discovery.* Nat Genet, 2006. **38 Suppl**: p. S2-7.
16. Bian, W. and N. Bursac, *Engineered skeletal muscle tissue networks with controllable architecture.* Biomaterials, 2009. **30**(7): p. 1401-12.
17. Blau, H.M., et al., *Plasticity of the Differentiated State.* Science, 1985. **230**(4727): p. 758-766.

18. Borschel, G.H., R.G. Dennis, and J. William M. Kuzon, *Contractile skeletal muscle tissue-engineered on an acellular scaffold.* Plastic Reconstructive Surg, 2004. **113**: p. 595-602.
19. Boutz, P.L., et al., *MicroRNAs regulate the expression of the alternative splicing factor nPTB during muscle development.* Genes Dev, 2007. **21**(1): p. 71-84.
20. Brennecke, J., A. Stark, and S.M. Cohen, *Not miR-ly muscular: microRNAs and muscle development.* Genes Dev, 2005. **19**(19): p. 2261-4.
21. Brennecke, J., et al., *Principles of microRNA-target recognition.* PLoS Biol, 2005. **3**(3): p. e85.
22. Bruneau, B.G., *Developmental biology: tiny brakes for a growing heart.* Nature, 2005. **436**(7048): p. 181-2.
23. Burkholder, T.J. and R.L. Lieber, *Sarcomere length operating range of vertebrate muscles during movement.* J Exp Biol, 2001. **204**: p. 1529-1536.
24. Calin, G.A., et al., *Human microRNA genes are frequently located at fragile sites and genomic regions involved in cancers.* Proc Natl Acad Sci U S A, 2004. **101**(9): p. 2999-3004.
25. Calin, G.A. and C.M. Croce, *MicroRNA signatures in human cancers.* Nat Rev Cancer, 2006. **6**(11): p. 857-66.
26. Callis, T.E., et al., *Minireview: Muscling through the microRNA world.* Society for Experimental Biology and Medicine, 2008. **DOI: 10.3181/0709-MR-237**.
27. Care, A., et al., *MicroRNA-133 controls cardiac hypertrophy.* Nat Med, 2007. **13**(5): p. 613-8.
28. Carson, J.A. and L. Wei, *Integrin signaling's potential for mediating gene expression in hypertrophying skeletal muscle.* J Appl Physiol, 2000. **88**(1): p. 337-43.
29. Chan, J.A., A.M. Krichevsky, and K.S. Kosik, *MicroRNA-21 is an antiapoptotic factor in human glioblastoma cells.* Cancer Res, 2005. **65**(14): p. 6029-33.
30. Chan, J.K., et al., *Functional characterization of an amino-terminal region of HDAC4 that possesses MEF2 binding and transcriptional repressive activity.* J Biol Chem, 2003. **278**(26): p. 23515-21.
31. Chandran, R., et al., *Biomechanical signals upregulate myogenic gene induction in the presence or absence of inflammation.* Am J Physiol Cell Physiol, 2007. **293**(1): p. C267-76.
32. Charge, S.B. and M.A. Rudnicki, *Cellular and molecular regulation of muscle regeneration.* Physiol Rev, 2004. **84**(1): p. 209-38.
33. Chen, C.Z., et al., *MicroRNAs modulate hematopoietic lineage differentiation.* Science, 2004. **303**(5654): p. 83-6.
34. Chen, J.F., et al., *The role of microRNA-1 and microRNA-133 in skeletal muscle proliferation and differentiation.* Nat Genet, 2006. **38**(2): p. 228-33.

35. Chen, S.-E., B. Jin, and Y.-P. Li, *TNF-{alpha} regulates myogenesis and muscle regeneration by activating p38 MAPK.* Am J Physiol Cell Physiol, 2007. **292**(5): p. C1660-1671.
36. Cheng, A.M., et al., *Antisense inhibition of human miRNAs and idnciations for an involvement of miRNA in cell growth and apoptosis.* Nucleic Acid Res., 2005. **33**: p. 1290-1297.
37. Czech, M.P., *MicroRNAs as therapeutic targets.* N Engl J Med, 2006. **354**(11): p. 1194-5.
38. Delgado, I., et al., *Dynamic gene expression during the onset of myoblast differentiation in vitro.* Genomics, 2003. **82**(2): p. 109-21.
39. Dennis, R.G. and P.E. Kosnik, *Excitability and Isometric Contractile Properties of Mammalian Skeletal Muscle Constructs Engineered In Vitro.* In Vitro Cell Dev Biol, 2000. **36**: p. 327-335.
40. Dennis, R.G., et al., *Excitability and Contractility of Skeletal Muscle Engineered from Primary Cultures and Cell Lines.* Am J Physiol Cell Physiol, 2001. **280**: p. C288-C295.
41. Dennis, R.G. and D.E. Dow, *Excitability of skeletal muscle during development, denervation, and tissue culture.* Tissue Eng, 2007. **13**(10): p. 2395-404.
42. Dodou, E., S.M. Xu, and B.L. Black, *Mef2c is activated directly by myogenic basic helix-loop-helix proteins during skeletal muscle development in vivo.* Mech Dev, 2003. **120**(9): p. 1021-32.
43. Doench, J.G. and P.A. Sharp, *Specificity of microRNA target selection in translational repression.* Genes Dev, 2004. **18**(5): p. 504-11.
44. Drummond, M.J., et al., *Aging differentially affects human skeletal muscle microRNA expression at rest and after an anabolic stimulus of resistance exercise and essential amino acids.* Am J Physiol Endocrinol Metab, 2008. **295**(6): p. E1333-40.
45. Du, T. and P.D. Zamore, *microPrimer: the biogenesis and function of microRNA.* Development, 2005. **132**(21): p. 4645-52.
46. Dudley, S.C., Jr., *Beware of cells bearing gifts: cell replacement therapy and arrhythmic risk.* Circ Res, 2005. **97**: p. 99-101.
47. Edmondson, D.G., et al., *Mef2 gene expression marks the cardiac and skeletal muscle lineages during mouse embryogenesis.* Development, 1994. **120**(5): p. 1251-63.
48. Eisenberg, I., et al., *Distinctive patterns of microRNA expression in primary muscular disorders.* Proc Natl Acad Sci U S A, 2007. **104**(43): p. 17016-21.
49. Eisenberg, I., M.S. Alexander, and L.M. Kunkel, *miRNAS in normal and diseased skeletal muscle.* J Cell Mol Med, 2009. **13**(1): p. 2-11.
50. Engler, A.J., et al., *Myotubes Differentiate Optimally on Substrates With Tissue-Like Stiffness: Pathological Implications for Soft or Stiff Microenvironments.* J Cell Biol, 2004. **166**(6): p. 877-87.

51. Esau, C., et al., *miR-122 regulation of lipid metabolism revealed by in vivo antisense targeting.* Cell Metab, 2006. **3**(2): p. 87-98.
52. Farh, K.K., et al., *The widespread impact of mammalian MicroRNAs on mRNA repression and evolution.* Science, 2005. **310**(5755): p. 1817-21.
53. Filipowicz, W., et al., *Post-transcriptional gene silencing by siRNAs and miRNAs.* Curr Opin Struct Biol, 2005. **15**(3): p. 331-41.
54. Franzini-Armstrong, C. and D.A. Fischman, *Morphogenesis of Skeletal Muscle Fibers*, in *Myology Basic and Clinical*, A.G. Engel, Franzini-Armstrong, C., Editor. 1994, McGraw-Hill, Inc.: New York. p. 74-96.
55. Fujita, T., et al., *Glucosamine induces lipid accumulation and adipogenic change in C2C12 myoblasts.* Biochem Biophys Res Commun, 2005. **328**(2): p. 369-74.
56. Fux, C., et al., *Dual-regulated expression of C/EBP-alpha and BMP-2 enables differential differentiation of C2C12 cells into adipocytes and osteoblasts.* Nucleic Acids Res, 2004. **32**(1): p. e1.
57. Griffith, L.G. and M.A. Swartz, *Capturing complex 3D tissue physiology in vitro.* Nat Rev Mol Cell Biol, 2006. **7**: p. 211-24.
58. Guarino, R.D., et al., *Method for determining oxygen consumption rates of static cultures from microplate measurements of pericellular dissolved oxygen concentration.* Biotechnol Bioeng, 2004. **86**: p. 775-87.
59. Guglielmelli, P., et al., *MicroRNA expression profile in granulocytes from primary myelofibrosis patients.* Exp Hematol, 2007. **35**(11): p. 1708-18.
60. Hammond, S.M., *MicroRNA therapeutics: a new niche for antisense nucleic acids.* Trends Mol Med, 2006. **12**(3): p. 99-101.
61. Hawke, T.J. and D.J. Garry, *Myogenic satellite cells: physiology to molecular biology.* J Appl Physiol, 2001. **91**: p. 534-551.
62. Hidestrand, M., et al., *Sca-1-expressing nonmyogenic cells contribute to fibrosis in aged skeletal muscle.* J Gerontol A Biol Sci Med Sci, 2008. **63**(6): p. 566-79.
63. Huang, Y.-C., et al., *Rapid Formation of Functional Muscle in vitro Using Fibrin Gels.* J App Phys, 2005. **98**: p. 706-713.
64. Huang, Y.C., R.G. Dennis, and K. Baar, *Cultured slow vs. fast skeletal muscle cells differ in physiology and responsiveness to stimulation.* Am J Physiol Cell Physiol, 2006. **291**(1): p. C11-7.
65. Hutvagner, G., *Small RNA asymmetry in RNAi: function in RISC assembly and gene regulation.* FEBS Lett, 2005. **579**(26): p. 5850-7.
66. Kaushal, S., et al., *Activation of the myogenic lineage by MEF2A, a factor that induces and cooperates with MyoD.* Science, 1994. **266**(5188): p. 1236-40.
67. Kessler, P.D. and B.J. Byrne, *Myoblast cell grafting into heart muscle: cellular biology and potential applications.* Annu Rev Physiol, 1999. **61**: p. 219-242.
68. Khodabukus, A. and K. Baar, *Regulating Fibrinolysis to Engineer Skeletal Muscle from the C2C12 Cell Line.* Tissue Eng Part C Methods, 2009.

69. Kim, H.K., et al., *Muscle-specific microRNA miR-206 promotes muscle differentiation.* J Cell Biol, 2006. **174**(5): p. 677-87.
70. Kimmel, A.R. and B. Oliver, *DNA microarrays*. Methods in enzymology ; v. 410-411, etc. 2006, Amsterdam ; San Diego: Elsevier/Academic Press. v.
71. King, A.M., D.S. Loiselle, and P. Kohl, *Force generation for locomotion of vertebrates: skeletal muscle overview.* IEEE Journal of Oceanic Engineering, 2004. **29**(3): p. 684-691.
72. Kitzmann, M. and A. Fernandez, *Crosstalk between cell cycle regulators and the myogenic factor MyoD in skeletal myoblasts.* Cell Mol Life Sci, 2001. **58**(4): p. 571-9.
73. Kook, S.H., et al., *Cyclic Mechanical Stretch Stimulates the Proliferation of C2C12 Myoblasts and Inhibits Their Differentiation via Prolonged Activation of p38 MAPK.* Mol Cells, 2008. **25**(4).
74. Kosnik, P.E., J.A. Faulkner, and R.G. Dennis, *Functional development of engineered skeletal muscle from adult and neonatal rats.* Tissue Eng, 2001. **7**(5): p. 573-84.
75. Krutzfeldt, J., et al., *Silencing of microRNAs in vivo with 'antagomirs'.* Nature, 2005. **438**(7068): p. 685-9.
76. Krutzfeldt, J., M.N. Poy, and M. Stoffel, *Strategies to determine the biological function of microRNAs.* Nat Genet, 2006. **38 Suppl**: p. S14-9.
77. Krutzfeldt, J., et al., *Specificity, duplex degradation and subcellular localization of antagomirs.* Nucleic Acids Res, 2007. **35**(9): p. 2885-92.
78. Kuang, W., et al., *Cyclic stretch induced miR-146a upregulation delays C2C12 myogenic differentiation through inhibition of Numb.* Biochem Biophys Res Commun, 2009. **378**(2): p. 259-63.
79. Kumar, A., et al., *Cyclic mechanical strain inhibits skeletal myogenesis through activation of focal adhesion kinase, Rac-1, GTPase, and NF-kB transcription factor.* FASEB J., 2004. **18**: p. 1524-1535.
80. Kwon, C., et al., *MicroRNA1 influences cardiac differentiation in Drosophila and regulates Notch signaling.* Proc Natl Acad Sci U S A, 2005. **102**(52): p. 18986-91.
81. Lagos-Quintana, M., et al., *Identification of tissue-specific microRNAs from mouse.* Curr Biol, 2002. **12**(9): p. 735-9.
82. Lam, M.T., et al., *Microfeature guided skeletal muscle tissue engineering for highly organized 3-dimensional free-standing constructs.* Biomaterials, 2009. **30**(6): p. 1150-5.
83. Landgraf, P., et al., *A mammalian microRNA expression atlas based on small RNA library sequencing.* Cell, 2007. **129**(7): p. 1401-14.
84. Landgraf, P., et al., *A mammalian microRNA expression atlas bBased on small RNA library sequencing.* Cell, 2007. **129**: p. 1401-1414.
85. Lao, K., et al., *Multiplexing RT-PCR for the detection of multiple miRNA species in small samples.* Biochem Biophys Res Commun, 2006. **343**(1): p. 85-9.
86. Larkin, L.M., et al., *Structure and Functional Evaluation of Tendon-Skeletal Muscle Constructs Engineered in Vitro.* Tissue Eng, 2006.

87. Larkin, L.M., et al., *Functional evaluation of nerve-skeletal muscle constructs engineered in vitro.* In Vitro Cell Dev Biol Anim, 2006. **42**(3-4): p. 75-82.
88. Lee, E.J., et al., *Systematic evaluation of microRNA processing patterns in tissues, cell lines, and tumors.* Rna, 2008. **14**(1): p. 35-42.
89. Lee, R.C., R.L. Feinbaum, and V. Ambros, *The C. elegans heterochronic gene lin-4 encodes small RNAs with antisense complementarity to lin-14.* Cell, 1993. **75**(5): p. 843-54.
90. Levenberg, S., et al., *Engineering vascularized skeletal muscle tissue.* Nat Biotechnol, 2005. **23**: p. 879-84.
91. Levine, E., et al., *Quantitative characteristics of gene regulation by small RNA.* PLoS Biol, 2007. **5**(9): p. e229.
92. Levine, E. and T. Hwa, *Small RNAs establish gene expression thresholds.* Curr Opin Microbiol, 2008. **11**(6): p. 574-9.
93. Lewis, B.P., C.B. Burge, and D.P. Bartel, *Conserved seed pairing, often flanked by adenosines, indicates that thousands of human genes are microRNA targets.* Cell, 2005. **120**(1): p. 15-20.
94. Lieber, R.L., *Skeletal Muscle Structure, Function, & Plasticity: The Physiological Basis of Rehabilitation*. 2nd ed. 2002, Baltimore: Lippincott Williams & Wilkins.
95. Lim, L.P., et al., *Microarray analysis shows that some microRNAs downregulate large numbers of target mRNAs.* Nature, 2005. **433**(7027): p. 769-73.
96. Liu, C.G., et al., *An oligonucleotide microchip for genome-wide microRNA profiling in human and mouse tissues.* Proc Natl Acad Sci U S A, 2004. **101**(26): p. 9740-4.
97. Liu, N., et al., *An intragenic MEF2-dependent enhancer directs muscle-specific expression of microRNAs 1 and 133.* Proc Natl Acad Sci U S A, 2007. **104**(52): p. 20844-9.
98. Livak, K.J. and T.D. Schmittgen, *Analysis of relative gene expression data using real-time quantitative PCR and the 2(-Delta Delta C(T)) Method.* Methods, 2001. **25**(4): p. 402-8.
99. Lu, S., et al., *Novel and mechanical stress-responsive MicroRNAs in Populus trichocarpa that are absent from Arabidopsis.* Plant Cell, 2005. **17**(8): p. 2186-203.
100. Luo, X., et al., *Down-regulation of miR-1/miR-133 contributes to re-expression of pacemaker channel genes HCN2 and HCN4 in hypertrophic heart.* J Biol Chem, 2008. **283**(29): p. 20045-52.
101. Ma, K., et al., *Myocyte enhancer factor 2 acetylation by p300 enhances its DNA binding activity, transcriptional activity, and myogenic differentiation.* Mol Cell Biol, 2005. **25**(9): p. 3575-82.
102. Mack, G.S., *MicroRNA gets down to business.* Nat Biotechnol, 2007. **25**(6): p. 631-8.
103. Martin, G., et al., *Prediction and validation of microRNA targets in animal genomes.* J Biosci, 2007. **32**(6): p. 1049-52.

104. McCarthy, J.J. and K.A. Esser, *MicroRNA-1 and microRNA-133a expression are decreased during skeletal muscle hypertrophy.* J Appl Physiol, 2007. **102**(1): p. 306-13.
105. McCarthy, J.J., K.A. Esser, and F.H. Andrade, *MicroRNA-206 is overexpressed in the diaphragm but not the hindlimb muscle of mdx mouse.* Am J Physiol Cell Physiol, 2007. **293**(1): p. C451-457.
106. McCarthy, J.J., *MicroRNA-206: the skeletal muscle-specific myomiR.* Biochim Biophys Acta, 2008. **1779**(11): p. 682-91.
107. McKinsey, T.A., et al., *Signal-dependent nuclear export of a histone deacetylase regulates muscle differentiation.* Nature, 2000. **408**(6808): p. 106-11.
108. Minners, J., et al., *Ischemic and pharmacological preconditioning in Girardi cells and C2C12 myotubes induce mitochondrial uncoupling.* Circ Res, 2001. **89**: p. 787-92.
109. Miska, E.A., et al., *Differential localization of HDAC4 orchestrates muscle differentiation.* Nucleic Acids Res, 2001. **29**(16): p. 3439-47.
110. Molkentin, J.D., et al., *Cooperative activation of muscle gene expression by MEF2 and myogenic bHLH proteins.* Cell, 1995. **83**(7): p. 1125-36.
111. Morgan, J.E., et al., *Formation of skeletal muscle in vivo from the mouse C2 cell line.* J Cell Sci, 1992. **102 (Pt 4)**: p. 779-87.
112. Murry, C.E., et al., *Skeletal myoblast transplantation for repair of myocardial necrosis.* J Clin Invest, 1996. **98**: p. 2512-2523.
113. Naguibneva, I., et al., *The microRNA miR-181 targets the homeobox protein Hox-A11 during mammalian myoblast differentiation.* Nat Cell Biol, 2006. **8**(3): p. 278-84.
114. Nakajima, N., et al., *MicroRNA-1 facilitates skeletal myogenic differentiation without affecting osteoblastic and adipogenic differentiation.* Biochem Biophys Res Commun, 2006. **350**(4): p. 1006-12.
115. Obernosterer, G., et al., *Post-transcriptional regulation of microRNA expression.* Rna, 2006. **12**(7): p. 1161-7.
116. Okano, T. and T. Matsuda, *Hybrid Muscular Tissues: Preparation of Skeletal Muscle Cell-Incorporated Collagen Gels.* Cell Transplantation, 1997. **6**(2): p. 109-118.
117. Okano, T. and T. Matsuda, *Tissue Engineered Skeletal Muscle: Preparation of Highly Dense, Highly Oriented Hybrid Muscular Tissues.* Cell Transplantation, 1998. **7**(1): p. 71-82.
118. Otis, J.S., T.J. Burkholder, and G.K. Pavlath, *Stretch-induced myoblast proliferation is dependent on the COX2 pathway.* Exp Cell Res, 2005. **310**(2): p. 417-25.
119. Otis, J.S., T.J. Burkholder, and G.K. Pavlath, *Stretch-induced myoblast proliferation is dependent on the COX2 pathway.* Experimental Cell Research, 2005. **310**(2): p. 417-425.
120. Politz, J.C., F. Zhang, and T. Pederson, *MicroRNA-206 colocalizes with ribosome-rich regions in both the nucleolus and cytoplasm of rat myogenic cells.* Proc Natl Acad Sci U S A, 2006. **103**(50): p. 18957-62.

121. Pollock, R. and R. Treisman, *Human SRF-related proteins: DNA-binding properties and potential regulatory targets.* Genes Dev, 1991. **5**(12A): p. 2327-41.
122. Potthoff, M.J., et al., *Regulation of Skeletal Muscle Sarcomere Integrity and Postnatal Muscle Function by Mef2c.* Mol Cell Biol, 2007. **27**(23): p. 8143-8151.
123. Potthoff, M.J. and E.N. Olson, *MEF2: a central regulator of diverse developmental programs.* Development, 2007. **134**(23): p. 4131-40.
124. Powell, C.A., et al., *Mechanical Stimulation Improves Tissue-Engineered Human Skeletal Muscle.* Am J Physiol Cell Physiol, 2002. **283**: p. C1557-C1565.
125. Powell, C.A., et al., *Mechanical stimulation improves tissue-engineered human skeletal muscle.* Am J Physiol Cell Physiol, 2002. **283**(5): p. C1557-65.
126. Qu, Z., et al., *Development of Approaches to Improve Cell Survival in Myoblast Transfer Therapy.* J Cell Biol, 1998. **142**(5): p. 1257-1267.
127. Rajewsky, N., *microRNA target predictions in animals.* Nat Genet, 2006. **38 Suppl**: p. S8-13.
128. Ramanujan, S., et al., *Diffusion and Convection in Collagen Gels: Implications for Transport in the Tumor Interstitium.* Biophys J, 2002. **83**: p. 1650-1660.
129. Rao, J.S., R.L. Beach, and B.W. Festoff, *Extracellular Matrix (ECM) Synthesis in Muscle Cell Cultures: Quantitative and Qualitative Studies During Myogenesis.* Biochem Biophys Res Commun, 1985. **130**(1): p. 440-446.
130. Rao, P.K., et al., *Myogenic factors that regulate expression of muscle-specific microRNAs.* Proc Natl Acad Sci U S A, 2006. **103**(23): p. 8721-6.
131. Rauch, C. and P.T. Loughna, *Static stretch promotes MEF2A nuclear translocation and expression of neonatal myosin heavy chain in C2C12 myocytes in a calcineurin- and p38-dependent manner.* Am J Physiol Cell Physiol, 2005. **288**(3): p. C593-605.
132. Reedy, M.K. and M.C. Reedy, *Rigor Crossbridge Structure in Tilted Single Filament Layers and Flared-X Formations From Insect Flight Muscle.* J Mol Biol, 1985. **185**(1): p. 145-76.
133. Rhim, C., et al., *Morphology and ultrastructure of differentiating three-dimensional mammalian skeletal muscle in a collagen gel.* Muscle Nerve, 2007. **36**(1): p. 71-80.
134. Rhoades, M.W., et al., *Prediction of plant microRNA targets.* Cell, 2002. **110**(4): p. 513-20.
135. Rosenberg, M.I., et al., *MyoD inhibits Fstl1 and Utrn expression by inducing transcription of miR-206.* J Cell Biol, 2006. **175**(1): p. 77-85.
136. Ross, J.S., J.A. Carlson, and G. Brock, *miRNA: the new gene silencer.* Am J Clin Pathol, 2007. **128**(5): p. 830-6.
137. Ross, J.S., J.A. Carlson, and G. Brock, *miRNA: the new gene silencer.* Anatomic Pathology, 2007. **128**: p. 830-836.
138. Rudnicki, M.A., et al., *MyoD or Myf-5 is required for the formation of skeletal muscle.* Cell, 1993. **75**(7): p. 1351-9.

139. Safdar, A., et al., *miRNA in the regulation of skeletal muscle adaptation to acute endurance exercise in C57Bl/6J male mice.* PLoS ONE, 2009. **4**(5): p. e5610.
140. Sayed, D., et al., *MicroRNAs play an essential role in the development of cardiac hypertrophy.* Circ Res, 2007. **100**(3): p. 416-24.
141. Schulman, B.R.M., A. Esquela-Kerscher, and F.J. Slack, *Reciprocal expression of lin-41 and the microRNAs let-7 and mir-125 during mouse emrbyogenesis.* Dev. Dynamics, 2005. **234**: p. 1046-1054.
142. Schultz, E. and B.H. Lipton, *Skeletal muscle satellite cells: changes in proliferation potential as a function of age.* Mech Ageing Dev, 1982. **20**(4): p. 377-83.
143. Sempere, L.F., et al., *Expression profiling of mammalian microRNAs uncovers a subset of brain-expressed microRNAs with possible roles in murine and human neuronal differentiation.* Genome Biol, 2004. **5**(3): p. R13.
144. Slaby, O., et al., *Altered expression of miR-21, miR-31, miR-143 and miR-145 is related to clinicopathologic features of colorectal cancer.* Oncology, 2007. **72**(5-6): p. 397-402.
145. Soifer, H.S., J.J. Rossi, and P. Saetrom, *MicroRNAs in Disease and Potential Therapeutic Applications.* Mol Ther, 2007.
146. Stark, A., et al., *Animal MicroRNAs confer robustness to gene expression and have a significant impact on 3'UTR evolution.* Cell, 2005. **123**(6): p. 1133-46.
147. Sun, Q., et al., *Transforming growth factor-beta-regulated miR-24 promotes skeletal muscle differentiation.* Nucleic Acids Res, 2008. **36**(8): p. 2690-9.
148. Swasdison, S. and R. Mayne, *Formation of Highly Organized Skeletal Muscle Fibers in Vitro.* J Cell Sci, 1992. **102**: p. 643-652.
149. Sweetman, D., et al., *Specific requirements of MRFs for the expression of muscle specific microRNAs, miR-1, miR-206 and miR-133.* Dev Biol, 2008. **321**(2): p. 491-9.
150. Tatsumi, R., et al., *Mechanical stretch induces activation of skeletal muscle satellite cells in vitro.* Exp Cell Res, 2001. **267**: p. 107-114.
151. Taylor, D.A., et al., *Regenerating functional myocardium: improved performance after skeletal myoblast transplantation.* Nat Med, 1998. **4**: p. 929-933.
152. Thomson, J.M., et al., *A custom microarray platform for analysis of microRNA gene expression.* Nat Methods, 2004. **1**(1): p. 47-53.
153. Tidball, J.G., et al., *Mechanical loading regulates NOS expression and activity in developing and adult skeletal muscle.* Am J Physiol, 1998. **275**(1 Pt 1): p. C260-6.
154. Tidball, J.G., *Mechanical signal transduction in skeletal muscle growth and adaptation.* J Appl Physiol, 2005. **98**: p. 1900-1908.
155. Tuddenham, L., et al., *The cartilage specific microRNA-140 targets histone deacetylase 4 in mouse cells.* FEBS Lett, 2006. **580**(17): p. 4214-7.
156. Turner, C.E., et al., *Localization of paxillin, a focal adhesion protein, to smooth muscle dense plaques, and the myotendinous and neuromuscular junctions of skeletal muscle.* Exp Cell Res, 1991. **192**(2): p. 651-5.

157. Valencia-Sanchez, M.A., et al., *Control of translation and mRNA degradation by miRNAs and siRNAs.* Genes Dev, 2006. **20**(5): p. 515-24.
158. van Rooij, E., et al., *A signature pattern of stress-responsive microRNAs that can evoke cardiac hypertrophy and heart failure.* Proc Natl Acad Sci U S A, 2006. **103**(48): p. 18255-60.
159. van Rooij, E. and E.N. Olson, *MicroRNAs: powerful new regualtors of heart disease and provocative therapeutic targets.* J Clin Invest, 2007. **117**: p. 2369-2376.
160. Van Rooij, E. and E.N. Olson, *MicroRNAs Put their Signatures on the Heart.* Physiol Genomics, 2007.
161. van Rooij, E. and E.N. Olson, *MicroRNAs: powerful new regulators of heart disease and provocative therapeutic targets.* J Clin Invest, 2007. **117**(9): p. 2369-76.
162. van Rooij, E., N. Liu, and E.N. Olson, *MicroRNAs flex their muscles.* Trends Genet, 2008. **24**(4): p. 159-66.
163. van Rooij, E., W.S. Marshall, and E.N. Olson, *Toward microRNA-based therapeutics for heart disease: the sense in antisense.* Circ Res, 2008. **103**(9): p. 919-28.
164. van Rooij, E., et al., *Dysregulation of microRNAs after myocardial infarction reveals a role of miR-29 in cardiac fibrosis.* Proc Natl Acad Sci U S A, 2008. **105**(35): p. 13027-32.
165. Vandenburgh, H., et al., *Tissue Engineered Skeletal Muscle Organoids for Reversible Gene Therapy.* Hum Gene Ther, 1996. **7**: p. 2195-2200.
166. Vandenburgh, H.H., P. Karlisch, and L. Farr, *Maintenance of Highly Contractile Tissue-Cultured Avian Skeletal Myotubes in Collagen Gel.* In Vitro Cell Dev Biol, 1988. **24**(3, Part 1): p. 166-174.
167. Vandenburgh, H.H. and P. Karlisch, *Longitudinal growth of skeletal myotubes in vitro in a new horizontal mechanical cell stimulator.* In Vitro Cell and Dev Biol, 1989. **25**: p. 607-616.
168. Vandenburgh, H.H., *Mechanical forces and their second messengers in stimulating cell growth in vitro.* Am. J. Physiol., 1992. **262**: p. R350-R355.
169. Vandenburgh, H.H., *Functional assessment and tissue design of skeletal muscle.* Ann NY Acad Sci, 2002. **961**: p. 201-202.
170. Venuti, J.M., et al., *Myogenin is required for late but not early aspects of myogenesis during mouse development.* J Cell Biol, 1995. **128**(4): p. 563-76.
171. Vester, B. and J. Wengel, *LNA (locked nucleic acid): high-affinity targeting of complementary RNA and DNA.* Biochemistry, 2004. **43**(42): p. 13233-41.
172. Wang, D.Z., et al., *The Mef2c gene is a direct transcriptional target of myogenic bHLH and MEF2 proteins during skeletal muscle development.* Development, 2001. **128**(22): p. 4623-33.
173. Wang, D.Z., *Micro or mega: how important are MicroRNAs in muscle?* Cell Cycle, 2006. **5**(10): p. 1015-6.

174. Weintraub, H., et al., *Activation of muscle-specific genes in pigment, nerve, fat, liver, and fibroblast cell lines by forced expression of MyoD.* Proc Natl Acad Sci U S A, 1989. **86**(14): p. 5434-8.
175. Wengel, J., et al., *LNA and alpha-L-LNA: towards therapeutic applications.* Nucleosides Nucleotides Nucleic Acids, 2003. **22**(5-8): p. 601-4.
176. Wienholds, E. and R.H. Plasterk, *MicroRNA function in animal development.* FEBS Lett, 2005. **579**(26): p. 5911-22.
177. Wong, C.F. and R.L. Tellam, *MicroRNA-26a Targets the Histone Methyltransferase Enhancer of Zeste homolog 2 during Myogenesis.* J. Biol. Chem., 2008. **283**(15): p. 9836-9843.
178. Wong, C.F. and R.L. Tellam, *MicroRNA-26a targets the histone methyltransferase Enhancer of Zeste homolog 2 during myogenesis.* J Biol Chem, 2008. **283**(15): p. 9836-43.
179. Wozniak, A.C., et al., *Signaling satellite-cell activation in skeletal muscle: markers, models, stretch, and potential alternate pathways.* Muscle Nerve, 2005. **31**(3): p. 283-300.
180. Wu, H., et al., *Regulation of mitochondrial biogenesis in skeletal muscle by CaMK.* Science, 2002. **296**(5566): p. 349-52.
181. Xiao, J., et al., *MicroRNA miR-133 represses HERG K+ channel expression contributing to QT prolongation in diabetic hearts.* J Biol Chem, 2007. **282**(17): p. 12363-7.
182. Yaffe, D. and O. Saxel, *Serial Passaging and Differentiation of Myogenic Cells Isolated From Dystrophic Mouse Muscle.* Nature, 1977. **270**(5639): p. 725-7.
183. Yan, W., et al., *Tissue Engineering of Skeletal Muscle.* Microsc Microanal, 2005. **11 (Suppl 2)**: p. 1-2.
184. Yan, W., et al., *Tissue Engineering of Skeletal Muscle.* Tissue Eng, 2007.
185. Yang, B., et al., *The muscle-specific microRNA miR-1 regulates cardiac arrhythmogenic potential by targeting GJA1 and KCNJ2.* Nature Medicine, 2007. **13**(486-491).
186. Yang, B., et al., *The muscle-specific microRNA miR-1 regulates cardiac arrhythmogenic potential by targeting GJA1 and KCNJ2.* Nat Med, 2007. **13**(4): p. 486-91.
187. Yoshiko, Y., K. Hirao, and N. Maeda, *Differentiation in C2C12 myoblasts depends expression of endogenous IGFs and not serum depletion.* Am. J. Physiol., 2002. **283**: p. 1278-1286.
188. Yu, Y.T., et al., *Human myocyte-specific enhancer factor 2 comprises a group of tissue-restricted MADS box transcription factors.* Genes Dev, 1992. **6**(9): p. 1783-98.
189. Yuasa, K., et al., *MicroRNA-206 is highly expressed in newly formed muscle fibers: implications regarding potential for muscle regeneration and maturation in muscular dystrophy.* Cell Struct Funct, 2008. **33**(2): p. 163-9.
190. Zhan, M., et al., *TACE release of TNF-alpha mediates mechanotransduction-induced activation of p38 MAPK and myogenesis.* J Cell Sci, 2007. **120**(Pt 4): p. 692-701.

191. Zhang, C.L., T.A. McKinsey, and E.N. Olson, *Association of class II histone deacetylases with heterochromatin protein 1: potential role for histone methylation in control of muscle differentiation.* Mol Cell Biol, 2002. **22**(20): p. 7302-12.
192. Zhang, S.J., G.A. Truskey, and W.E. Kraus, *Effect of cyclic stretch on beta1D-integrin expression and activation of FAK and RhoA.* Am J Physiol Cell Physiol, 2007. **292**(6): p. C2057-69.
193. Zhao, X., et al., *The modular nature of histone deacetylase HDAC4 confers phosphorylation-dependent intracellular trafficking.* J Biol Chem, 2001. **276**(37): p. 35042-8.
194. Zhao, Y., E. Samal, and D. Srivastava, *Serum response factor regulates a muscle-specific microRNA that targets Hand2 during cardiogenesis.* Nature, 2005. **436**(7048): p. 214-20.
195. Zhou, X., et al., *Histone deacetylase 4 associates with extracellular signal-regulated kinases 1 and 2, and its cellular localization is regulated by oncogenic Ras.* Proc Natl Acad Sci U S A, 2000. **97**(26): p. 14329-33.

Biography

Caroline Rhim
Date of Birth: July 11, 1979
Place of Birth: Los Angeles, CA

Education:
Duke University, Pratt School of Engineering, Durham, NC
Ph.D. Candidate in Biomedical Engineering

Massachusetts Institute of Technology, School of Engineering, Cambridge, MA
S.M. in Materials Science and Engineering, June 2002

Massachusetts Institute of Technology, School of Engineering, Cambridge, MA
S.B. in Materials Science and Engineering, June 2001

Selected Publications:
Rhim C, Kraus WE, Truskey GA, "MicroRNA Delivery to Mediate Bioartificial Muscle Function", Manuscript in preparation.

Rhim C, Kraus WE, Truskey GA, "Biomechanical Effects on MicroRNA Expression in Skeletal Muscle Differentiation", Manuscript in preparation.

Carnell LS, Siochi EJ, Holloway NM, Stephens RM, **Rhim C**, Niklason LE, Clark RL, "Aligned Mats from Electrospun Single Fibers", Macromolecules, 41(14): 5345-5349, 2008.

Rhim C, Lowell DA, Reedy MC, Slentz DH, Zhang SJ, Kraus WE, Truskey GA, "Morphology and Ultrastructure of Differentiating Three-Dimensional Mammalian Skeletal Muscle in a Collagen Gel", Muscle and Nerve, 36:71-80, 2007.

Dahl SLM, **Rhim C**, Song YC, Niklason LE, "Mechanical Properties and Compositions of Tissue Engineered and Native Arteries", Annals of Biomedical Engineering, 35(3): 348-355, 2007.

Rhim C and Niklason LE, "Tissue Engineered Vessels: Cells to Telomeres", Progress in Pediatric Cardiology, 21: 185-191, 2006.

Patents:

Lisa A. Scott-Carnell, Ralph M. Stephens, Nancy M. Holloway, **Caroline Rhim**, Laura Niklason, Robert L. Clark, Emilie J. Siochi, 'Method and System for Aligning Fibers During Electrospinning', Patent Application PCT/US2008/065506, Publication date: 12/11/2008.

Awards & Honors:

Kewaunee Student Achievement Award (2009)
Sigma Xi Honor Society (Inducted 2008)
Senior Graduate Student Poster Award, Duke University Kewaunee Lecture (2008)
NIH Training Grant Fellowship, Center for Biomolecular & Tissue Engineering (2003-2005)
MIT Ida M. Green Graduate Fellowship (2001-2002)
ASM Foundation Scholarship (2000)
Tau Beta Pi Membership (Inducted 2000)
National Society of Collegiate Scholars (Inducted 1999)